

DM

**Development of HA-based hydrogels  
for biomedical applications  
using different crosslinkers**

MASTER DISSERTATION

**João Pedro Serradas Carreira**

MASTER IN APPLIED BIOCHEMISTRY



UNIVERSIDADE da MADEIRA

*A Nossa Universidade*

[www.uma.pt](http://www.uma.pt)

September | 2024

# **Development of HA-based hydrogels for biomedical applications using different crosslinkers**

MASTER DISSERTATION

**João Pedro Serradas Carreira**

MASTER IN APPLIED BIOCHEMISTRY

SUPERVISOR  
Rita Maria de Castro

CO-SUPERVISOR  
Helena Maria Pires Gaspar Tomás



# **Development of HA-based hydrogels for biomedical applications using different crosslinkers**

Dissertation submitted to the University of Madeira in fulfilment of the requirements for  
the degree of Master in Applied Biochemistry

By João Pedro Serradas Carreira

Work developed under the supervision of

Dr. Rita Maria de Castro and

Co-supervised by Professor Dr. Helena Tomás

Faculdade de Ciências Exatas e da Engenharia

Centro de Química da Madeira

Universidade da Madeira

Funchal – Portugal

2024



## **ORIGINALITY STATEMENT**

“Plagiarism consists of the presentation, as your own and even if there has been translation, of ideas, opinions, phrases/texts, results, or conclusions of others. The practice of plagiarism is a serious violation of academic ethics and may lead to failure or withdrawal of the degree, as well as civil, criminal, and disciplinary liability.”

I hereby declare on my honor that this dissertation is of my own exclusive authorship, it is original, and that I have referenced and quoted all sources used in it.

September | 2024

João Pedro Serradas Carreira



---



## Acknowledgments

Firstly, a sincere thank you to my supervisor Dr. Rita Maria de Castro. Your patience, advice, teachings, and support were crucial in this project and allowed me to gain and improve skills that made me grow professionally and that will be valuable in my future. Thank you for your readiness to help, for your comforting and motivating words, and for challenging me.

I also would like to thank Professor Helena Tomás for the opportunity to work on this project, and for all the support, assistance, and guidance given to me throughout its development.

Thank you to the laboratory technician Paula Andrade, for the patience, attention, and availability in providing me the necessary tools for developing this work.

I would like to thank the professors and colleagues from CQM, mainly Dr. Mara Gonçalves and Dr. Dina Maciel for their assistance, availability, advice, and contributions to this dissertation as well as their friendship throughout this year.

A special thanks to my dear friends, whose support was essential during this year: Jéni Monroy, Bárbara Pedra, and Emanuel Costa. For their help, patience, and support, for listening and for advising in times of need, and for celebrating when the opportunities came, for their valuable friendship and company throughout this year, and for making this journey far more enjoyable and memorable.

Finally, I would like to thank CQM for the tools and the support provided to me during the development of this Master's Dissertation. I would also like to thank all the funding institutions involved: *Fundação para a Ciência e a Tecnologia* (FCT) through the CQM Base Fund - UIDB/00674/2020 (DOI: 10.54499/UIDB/00674/2020), and through the CQM Programmatic Fund – UIDP/00674/2020 (DOI 10.54499/UIDP/00674/2020), and *Agência Regional para o Desenvolvimento da Investigação, Tecnologia e Inovação* (ARDITI), for financing CQM.



## Abstract

Hyaluronic acid (HA) is a biomolecule that has been widely used in the synthesis of hydrogels, receiving considerable attention due to its unique physiological properties and functions. HA-based hydrogels have been applied in the biomedical field, especially in drug delivery, wound healing, cosmetics, and tissue engineering. However, these hydrogels often face some challenges like their susceptibility to degradation by hyaluronidase, which limits their application to a certain extent. The objective of this thesis was to develop HA-based hydrogels using various crosslinkers, with the goal of creating materials that exhibit enhanced stability and cytocompatibility for potential biomedical applications. Studies were conducted using polyethylene glycol diglycidyl ether (PEGDE), ethylene glycol diglycidyl ether (EGDE), and genipin as crosslinkers, with glutaraldehyde included for comparison as a classical crosslinker. These hydrogels were not only successfully prepared and characterized (e.g., FTIR, SEM), but this thesis also represents the first study to explore hydrogels crosslinked simultaneously by PEGDE and genipin. The prepared hydrogels displayed high swelling capacity and stability in both water and PBS over time. The swelling behavior of the hydrogels was influenced by factors such as the formulation composition, degree of crosslinking, crosslinker length and swelling media. In this regard, greater swelling was observed in water compared to PBS. The *in vitro* stability and resistance of HA-based hydrogels to enzymatic degradation were influenced by the crosslinking density, with the highest degree of crosslinking producing the most stable and resilient hydrogels. Importantly, the hydrogel crosslinked by both PEGDE and genipin demonstrated particular high swellability and stability. Despite their high stability, the developed hydrogels exhibited significant cytotoxicity, particularly when cells were cultured in direct contact with them. In this context, further studies are needed to draw more definitive conclusions about the biocompatibility of these hydrogels and their potential applications in the biomedical domain.

**Keywords:** Hydrogel, Hyaluronic Acid, Crosslinking, Cytotoxicity.



## Resumo

O ácido hialurónico (HA) é uma biomolécula que tem sido amplamente utilizada na síntese de hidrogéis, recebendo uma atenção considerável devido às suas propriedades e funções fisiológicas únicas. Os hidrogéis à base de HA têm sido aplicados na área biomédica, especialmente na administração de fármacos, cicatrização de feridas, cosmética e engenharia de tecidos. No entanto, estes hidrogéis enfrentam constantemente certos desafios tais como a sua suscetibilidade à degradação pela hialuronidase, o que limita a sua aplicação até certo ponto. O objetivo desta tese foi desenvolver hidrogéis à base de HA, usando vários agentes de reticulação, com o intuito de criar materiais que exibissem uma melhor estabilidade e citocompatibilidade para potenciais aplicações biomédicas. Estudos foram realizados usando éter diglicidílico de polietilenoglicol (PEGDE), éter diglicidílico de etilenoglicol (EGDE) e genipina como agentes de reticulação, incluindo o glutaraldeído para comparação como clássico agente de reticulação. Estes hidrogéis não foram apenas preparados e caracterizados com sucesso (FTIR, SEM), mas esta tese também representa o primeiro estudo em explorar hidrogéis reticulados simultaneamente com PEGDE e genipina. Os hidrogéis sintetizados apresentaram uma elevada capacidade de hidratação e uma grande estabilidade tanto em água como em PBS ao longo do tempo. O comportamento de hidratação dos hidrogéis foi influenciado por fatores como a composição da formulação do gel, o grau de reticulação, o comprimento do agente de reticulação e o meio de hidratação. Tendo isto em conta, foi possível observar uma maior capacidade de hidratação em água em relação ao PBS. A estabilidade *in vitro* e a resistência dos hidrogéis à base de HA à degradação enzimática foram influenciadas pela densidade de reticulação, sendo que um maior grau de reticulação produziu os hidrogéis mais estáveis e resilientes. É importante referir que o hidrogel duplamente reticulado por PEGDE e genipina demonstrou particularmente uma elevada capacidade de hidratação e estabilidade. Apesar de apresentarem uma elevada estabilidade, os hidrogéis sintetizados mostraram uma citotoxicidade significativa, particularmente quando as células foram cultivadas em contacto direto com estes. Neste contexto, serão necessários mais estudos para obter conclusões mais definitivas sobre a biocompatibilidade destes hidrogéis e as suas potenciais aplicações no domínio da biomedicina.

**Palavras-Chave:** Hidrogel, Ácido hialurónico, Reticulação, Citotoxicidade.



# Contents

Acknowledgments .....	v
Abstract.....	vii
Keywords .....	vii
Resumo.....	ix
Palavras-Chave.....	ix
List of Figures.....	xiv
List of Tables .....	xvi
Abbreviations .....	xviii
1. INTRODUCTION.....	1
1.1. Hydrogels: nature and classification .....	1
1.2. Crosslinking .....	2
1.2.1. Physical crosslinking methods .....	3
1.2.2. Chemical crosslinking methods.....	4
1.2.3. Hydrogel properties.....	6
1.3. Hyaluronic acid hydrogels .....	8
1.3.1. HA hydrogels crosslinking .....	9
1.3.1.1. Glutaraldehyde as crosslinker.....	11
1.3.1.2. Polyethylene glycol as crosslinker.....	12
1.3.1.3. Genipin as crosslinker .....	14
1.3.2. HA hydrogel applications.....	15
1.3.2.1. Tissue engineering.....	15
1.3.2.2. Drug delivery.....	17
1.3.2.3. Wound healing.....	19
1.3.2.4. Cosmetics.....	20
1.4. Hydrogel Characterization.....	21
1.4.1. Instrumental tools for hydrogel characterization.....	21
1.4.1.1. Scanning electron microscopy (SEM).....	21
1.4.1.2. Atomic force microscopy (AFM).....	22
1.4.1.3. Nuclear magnetic resonance (NMR).....	23
1.4.1.4. Fourier transform infrared spectroscopy (FTIR).....	23
1.4.1.5. Absorption spectroscopy (UV-vis).....	24
1.4.2. Physical and chemical stability.....	25
1.4.3. Biocompatibility .....	27
1.5. OBJECTIVES OF THE THESIS .....	30

2. MATERIALS AND METHODS .....	31
2.1. Cells, materials, reagents, and general equipment.....	31
2.2. Preparation of HA-based hydrogels.....	31
2.2.1. HA-lysine functionalization.....	33
2.2.2. HAGA hydrogel .....	33
2.2.3. HA-PEGDE and HA-EGDE hydrogels .....	33
2.2.4. HA-Gen hydrogel.....	33
2.2.5. Gen – HA – PEGDE hydrogel .....	34
2.3. Swelling studies .....	34
2.4. Stability studies .....	35
2.5. Degradation studies using hyaluronidase.....	35
2.6. HA-based hydrogels characterization .....	34
2.6.1. NMR spectroscopy .....	34
2.6.2. Scanning Electron Microscopy (SEM).....	34
2.6.3. ATR-FTIR Spectroscopy.....	34
2.7. Cell culture .....	36
2.8. Metabolic activity .....	36
3. RESULTS AND DISCUSSION.....	38
3.1. HA-based hydrogels.....	38
3.1.1. HA-lysine functionalization.....	38
3.1.2. Hydrogel’s macroscopic features .....	39
3.1.3. Characterization by ATR-FTIR Spectroscopy .....	41
3.1.4. Characterization by Scanning Electron Microscopy (SEM) .....	45
3.1.5. Hydrogels’ swelling behavior .....	47
3.2. Stability and Degradation Studies.....	52
3.2.1. <i>In vitro</i> stability studies .....	52
3.2.2. <i>In vitro</i> degradation studies.....	55
3.3. <i>In vitro</i> Cytotoxicity Evaluation.....	57
4. CONCLUSIONS AND FUTURE PERSPECTIVES .....	63
5. BIBLIOGRAPHY.....	66
6. ANNEXES .....	80



## List of Figures

Figure 1 - Hydrogel's classification regarding its polymeric composition. ....	2
Figure 2 - Chemical composition of HA.....	8
Figure 3 - Chemical structures of typical HA derivatives obtained from HA with different modification methods. ....	10
Figure 4 - Origin and chemical structure of genipin. ....	14
Figure 5 - Reaction of genipin crosslinking with primary amine groups.....	15
Figure 6 - Use of HA hydrogels as a matrix in tissue engineering applications.....	17
Figure 7 - The role of HA as a platform for cell and drug delivery in the Intervertebral disc repair (IVD). ....	19
Figure 8 - Schematic illustration of HA hydrogel preparation through copper-free click chemistry, encapsulation of REG peptides, and its application in wound repair through activating cellular migration.....	20
Figure 9 - Use of Injectable HA-based hydrogels as a novel, biocompatible and nontoxic dermal filler. ....	21
Figure 10 - Schematic representation of the HA-based hydrogels formulation. ....	32
Figure 11 - <sup>1</sup> H NMR spectrum of HALys with lysine unit signals assigned. ....	38
Figure 12 - HA-based hydrogels. HALys was used for HAGA, HA-Gen and Gen-HA-PEGDE hydrogels formation, meanwhile native HA (0.6-1.0 million Da) was used for the formation of HA-PEGDE and HA-EGDE hydrogels.....	41
Figure 13 – ATR-FTIR spectra of A) HA-EGDE 20_1; B) HA-EGDE 20_5; C) HA-PEGDE 20_5; D) HA-PEGDE 20_10 and E) HA-PEGDE 10_10 hydrogels. ....	43
Figure 14 – ATR-FTIR spectrum of Gen20-HA10-PEGDE10 hydrogel. ....	44
Figure 15 - SEM images of lyophilized HA-based hydrogels after swelling in water and PBS (pH = 7.4) at different magnifications. ....	47
Figure 16 - Swelling behavior of HAGA hydrogels in water and 1x PBS as a function of time...	49
Figure 17 - Swelling behavior in water and PBS as a function of time. (A) HA-EGDE and (B) HA-PEGDE.....	50
Figure 18 - Swelling behavior in water and PBS as a function of time. (A) HA-Gen and (B) Gen-HA-PEGDE.....	52
Figure 19 - Stability studies, determined by weight loss (%) of prepared hydrogels. (A) swelled and lyophilized HA-EGDE in water, 37°C; (B) swelled and lyophilized HA-EGDE in PBS (pH=7.4), 37°C; (C) swelled and lyophilized HA-PEGDE in water, 37°C; and (D) swelled and lyophilized HA-PEGDE in PBS (pH=7.4), 37°C.....	54
Figure 20 - Stability studies, determined by weight loss (%) of prepared hydrogels. (A) swelled and lyophilized HAGA in water, 37°C and (B) swelled and lyophilized HAGA in PBS (pH=7.4), 37°C.....	54
Figure 21 - Stability studies, determined by weight loss (%) of prepared hydrogels. (A) swelled and lyophilized HA-Gen in water, 37°C and (B) swelled and lyophilized HA-Gen in PBS (pH=7.4), 37°C.....	55

Figure 22 - Stability studies, determined by weight loss (%) of Gen20-HA10-PEGDE10 hydrogel. ....	55
Figure 23 - Stability studies, determined by weight loss (%) in water and PBS at 37°C, of prepared hydrogels previously swelled and then lyophilized. (A) HA-EDGE and (B) HA-PEGDE. ....	55
Figure 24 - Hyaluronidase digestion of HA-based hydrogels.....	56
Figure 25 - Uronic acid vs HA in vitro degradation studies. ....	57
Figure 26 - Metabolic activity of embryo mouse fibroblasts (NIH 3T3) in direct contact with HA-PEGDE, HA-EGDE, and Gen-HA-PEGDE hydrogels as measured by the resazurin reduction assay. ....	58
Figure 27 - Optical microscopy images of cells control (a) and cells exposed directly with the HA-based hydrogels ((b-d) HA-PEGDE; (e-f) HA-EGDE and (g) Gen-HA-PEGDE hydrogels).....	59
Figure 28 - Metabolic activity of embryo mouse fibroblasts (NIH 3T3) in the presence of HA-PEGDE, HA-EGDE, and Gen-HA-PEGDE hydrogel extracts as measured by the resazurin reduction assay. ....	60
Figure 29 - Metabolic activity of embryo mouse fibroblasts (NIH 3T3) in direct contact with HA-Gen and HAGA hydrogels as measured by the resazurin reduction assay. ....	60
Figure 30 - Metabolic activity of embryo mouse fibroblasts (NIH 3T3) in the presence of Gen solutions of different concentrations (0.1 – 20mM) as measured by the resazurin reduction assay. ....	61
Figure 31 - Metabolic activity of embryo mouse fibroblasts (NIH 3T3) in the presence of HA1Gen2 hydrogel in transwell inserts as measured by the resazurin reduction assay. ....	62
Figure A1 - The proposed reversible ring-opening reactions of genipin in aqueous solution. (Reaction that makes Genipin-HA-PEGDE turns brown).....	80
Figure A3 – ATR-FTIR spectrum of Gen powder.....	81
Figure A3 – ATR-FTIR spectrum of EGDE standard.....	81
Figure A4 – ATR-FTIR spectrum of PEGDE powder.....	81
Figure A5 - ATR-FTIR spectrum of native HA (0.6-1.0 million Da).....	82
Figure A6 - ATR-FTIR spectrum of acidic Gen solution (pH = 6). ....	82
Figure A7 - ATR-FTIR spectrum of alkaline Gen solution (pH = 12). ....	82
Figure A8 - Metabolic activity of embryo mouse fibroblasts (NIH 3T3) in direct contact with HA-PEGDE, HA-EGDE, and Gen-HA-PEGDE hydrogels as measured by the resazurin reduction assay. ....	83

## List of Tables

Table 1 - Advantages and disadvantages of the hydrogels' chemical and physical crosslinking processes. ....	6
Table 2 - HA-based hydrogels and their applications in the biomedical domain.....	10
Table 3 - HA-based hydrogels and their crosslinking conditions. ....	32
Table A1 - FTIR peak table of Genipin, HA, PEGDE and EGDE standards. ....	80



## **Abbreviations**

**2D** Bidimensional

**3D** Tridimensional

**AA** Antibiotic-Antimycotic

**ADH** Adipic acid dihydrazide

**AFM** Atomic force microscopy

**ATR** Attenuated Total Reflectance

**BDDE** Butanediol diglycidyl ether

**BMP** Bone Morphogenetic Protein

**D<sub>2</sub>O** Deuterium Oxide

**D-MEM** Dulbecco's Modified Eagle Medium

**DVS** Divinyl sulfone

**ECM** Extracellular matrix

**EDC** 1-Ethyl-3-(3- Dimethylaminopropyl)Carbodiimide

**EDS** Energy dispersion spectroscopy

**EDTA** Ethylenediaminetetraacetic acid

**EGDE** Ethylene Glycol Diglycidyl Ether

**ELISA** Enzyme Linked Immunosorbent Assay

**EPR** Enhanced permeability and retention

**FBS** Fetal Bovine Serum

**FTIR** Fourier-transform infrared spectroscopy

**GA** Glutaraldehyde

**GAGs** Glycosaminoglycans

**Gen** Genipin

**HA** Hyaluronic Acid

**HAase** Hyaluronidase

**HARE** Hyaluronic acid receptor for endocytosis

**HMDI** Hexamethylene diisocyanate

**IPNs** Interpenetrating Polymer Networks

**IVD** Intervertebral disc repair

**LDH** Lactate dehydrogenase

**Lys** Lysine

**LYVE-1** Lymphatic vessel endothelial hyaluronan receptor 1  
**MSCs** Mesenchymal Stem Cells  
**MTT** 3-(4,5-Dimethylthiazol-2-yl)-2,5-Diphenyltetrazolium Bromide  
**MTX** Methotrexate  
**NGF** Nerve growth factor  
**NHS** N-Hydroxysuccinimide  
**NIH 3T3** Embryonic mouse fibroblasts  
**NMR** Nuclear Magnetic Resonance  
**PBS** Phosphate-Buffered Saline  
**PEG** Polyethylene glycol  
**PEGDE** Polyethylene glycol diglycidyl ether  
**PVA** Polyvinyl alcohol  
**SEM** Scanning Electron Microscopy  
**TGF-  $\beta$**  Transforming growth factor beta family  
**UV-Vis** Ultraviolet-visible

# 1. INTRODUCTION

## 1.1. Hydrogels: nature and classification

Hydrogels are tridimensional (3D) structures, usually made of polymers, formed through several chemical and/or physical crosslinking strategies. The components of hydrogels possess excellent hydrophilicity, being able to absorb high quantities of water, resulting in a “gel-like” material. These have been used for several purposes, especially in the biomedicine domain, since they have the ability to mimic natural tissues and present a mechanical strength similar to that of soft tissues <sup>1-3</sup>.

One possible way to classify hydrogels is based on the type of interactions that are established among the polymeric chains. In this regard, physical hydrogels are those formed by non-covalent, reversible interactions. These hydrogels usually lead to dynamic and responsive properties and present low mechanical strength. Chemical hydrogels are formed by covalent, irreversible bonds, resulting in stable and robust structures with higher mechanical strength <sup>4</sup>.

Hydrogels can also be classified based on the polymer source, that is, can be synthetic or natural <sup>5,6</sup>. Synthetic hydrogels are prepared from man-made polymers, such as polyethylene glycol, polyacrylate, polyacrylamide, and others. Meanwhile, due to their non-bioactive nature, difficulty in degradation, and potential cytotoxicity associated with the crosslinkers, synthetic hydrogels have limited biomedical applications <sup>7,8</sup>. Therefore, several researchers have progressively turned their focus to natural hydrogels, made from natural, low-cost, abundant, biocompatible, and easily degradable macromolecules, such as hyaluronic acid, chitosan, alginate, collagen, among others <sup>9-11</sup>.

In addition, hydrogels can be classified according to their polymeric composition (Figure 1). There are, therefore, homopolymeric <sup>12</sup>, co-polymeric <sup>13</sup>, and multipolymeric hydrogels <sup>14</sup>. Homopolymeric hydrogels are polymeric networks derived from only one monomer species <sup>12</sup>. The homopolymer skeletal structure depends on the monomer nature and the polymerization approach. Co-polymeric hydrogels derive from polymers constituted by two or more different species of monomers, with at least one hydrophilic component, arranged randomly, in block, or alternated configuration along their chain <sup>13</sup>. Multipolymeric hydrogels involve different polymers and the existence of crosslinking between them, which can be physical or chemical <sup>14</sup>. The interpenetrating polymer networks (IPNs) constitute a type of multipolymeric hydrogel <sup>15</sup>. IPNs correspond to an important hydrogel class, in which two or more polymeric networks coexist in the same space, but without chemical bonds between them (the networks are intertwined in such

a way that, to be separated, there would have to happen a breaking of chemical bonds, at least in one of them). In a semi-IPN hydrogel, one component is a crosslinked polymer and the other is a non-crosslinked polymer <sup>15</sup>.

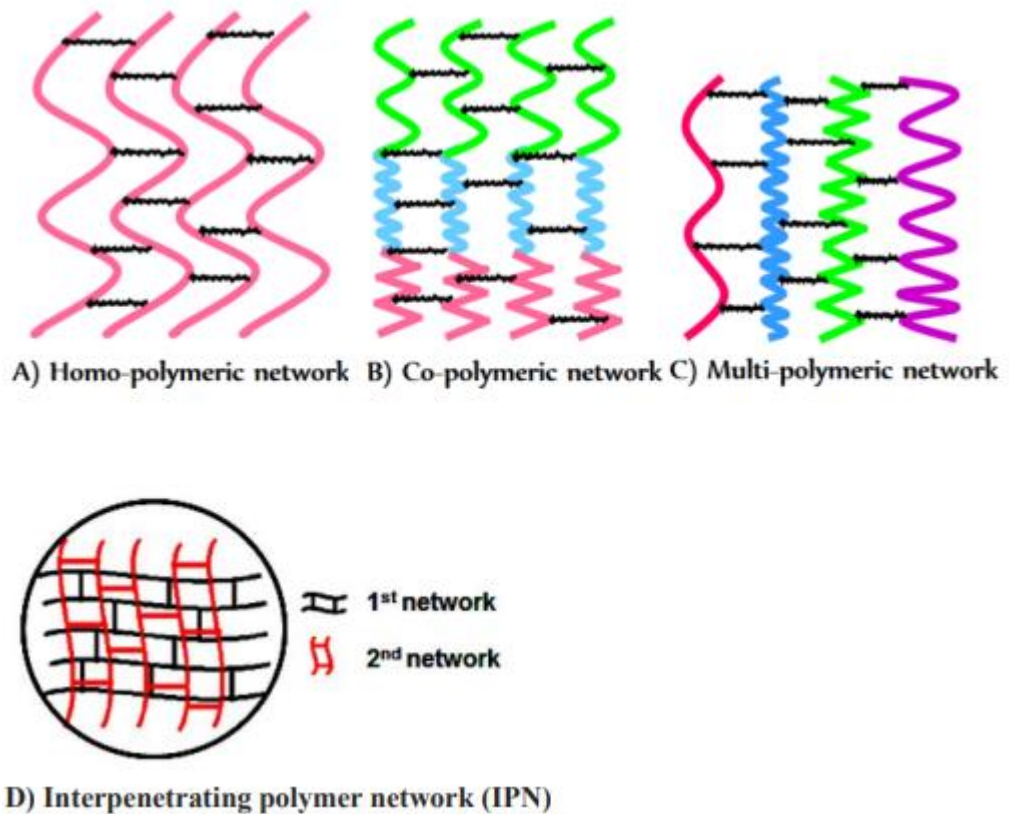


Figure 1- Hydrogel's classification regarding its polymeric composition <sup>16</sup>.

## 1.2. Crosslinking

The crosslinking processes to form a stable 3D network are divided into two major categories, namely physical and chemical crosslinking, that offer different advantages <sup>17</sup>. Physical crosslinking usually results in the establishment of physical interactions within the network structure, such as hydrogen bonding, ionic interactions, and hydrophobic interactions. However, covalent bonds may also be formed through physical crosslinking, as is the case when radiation is applied. On the other hand, chemical crosslinking always involves the establishment of covalent bonds and is commonly based on molecules (the crosslinkers) that contain two or more functional reactive groups at the extremities, such as primary amines, thiol groups, etc. <sup>17</sup>.

### 1.2.1. Physical crosslinking methods

Physical crosslinking is a way to obtain a hydrogel through physical methods, forming a 3D network. Several physical methods can be used to prepare hydrogels, such as those based on hydrogen (H) bonds<sup>18</sup>, hydrophobic interactions<sup>19</sup>, thermogelation<sup>20</sup>, polymer complexation<sup>21</sup>, and radiation<sup>22,23</sup>. Except in the last case, the type of crosslinking is reversible and can be broken by physical stress application, such as agitation and pH change (physical hydrogels are formed). Physical crosslinked hydrogels can be prepared at environmental conditions, without the use of crosslinkers that, many times, cause additional cytotoxicity to cells or may affect the activity of biological molecules incorporated into the hydrogel<sup>24</sup>.

Hydrogen bond crosslinking occurs when molecules that have hydrogen-donating functional groups (such as hydroxyl, carboxyl, or amide groups) and hydrogen-accepting functional groups (such as ester groups, for example) bind together via hydrogen bonds. These bonds form an inter or intramolecular network which forms the hydrogel. The H-bond formation is influenced by temperature<sup>25</sup>, pH<sup>26</sup>, and concentration<sup>27</sup> of the components involved in the process<sup>18</sup>. On the other hand, hydrophobic crosslinking occurs when a hydrophobic polymer is added to the aqueous medium that self-associates and ends up crosslinking the hydrogel. The addition of salts that reduce the hydrophobic polymer solubility may also promote crosslinking<sup>19</sup>.

Thermogelation is a crosslinking method that involves a reversible sol-gel transition in response to temperature changes. Hydrogels formed by thermogelation are (typically) liquid at room temperature and form a hydrogel when the solution is heated above the gelation critical temperature. This temperature can be adjusted by modifying the polymer hydrophobicity or the presence of specific groups, sensitive to temperature, in the polymer's structure. In thermogelation, the polymeric chains become more hydrophobic with the temperature increase, leading to an increase in the intermolecular interactions and the formation of a hydrogel's physical network. The gel formation is reversible, and the hydrogel can return to its liquid state by cooling below the critical gelling temperature<sup>20</sup>. This reversibility allows for the incorporation of cells or bioactive molecules in the hydrogel solution before gelation, which can be performed *in situ*. Nonetheless, it is important to note that this process is dependent on gelation temperature because the gelation temperature can affect the thermal stability and reversibility of the hydrogel. Thermogelated hydrogels have a variety of applications in the biomedical area, including drug delivery<sup>28</sup>, tissue engineering<sup>29</sup>, and wound healing<sup>30</sup>.

Polymer complexation crosslinking is a technique that involves the interaction between two different polymers that can form stable complexes by non-covalent interactions, such as H-bonds, *Van der Waals* forces, and electrostatic interactions. Polymer complexation can occur between different types of polymers (heterocomplexation) or between the same type of polymers (homocomplexation). Complexation can be used for hydrogel crosslinking, providing different mechanical and stability properties, depending on the polymers used. Besides that, this technique can be used to incorporate bioactive compounds, like proteins<sup>31</sup>, drugs<sup>32</sup>, as well as cells<sup>33</sup>, in the crosslinked hydrogel. Polymer complexation is a versatile and promising technique for hydrogel preparation with different applications in the biomedical domain<sup>21</sup>.

Radiation crosslinking is a process in which the radiation energy is used to induce covalent bonds between the polymers, forming a 3D network. It relies on the physical interaction between high-energy radiation and the polymer material to induce crosslinking. This process can be carried out by different types of ionizing radiation, such as gamma rays and UV light. In UV light radiation crosslinking, a crosslinker with double bonds is added to the monomers in solution. Upon exposure to UV radiation, the crosslinker becomes activated and generates free radicals. These free radicals then react with the double bonds of the monomers, forming covalent bonds and polymeric chains. The resulting polymeric chains crosslink, ultimately producing a hydrogel. The crosslinker quantity and the intensity of the energy source can be adjusted to control the crosslink network density and, therefore, the properties of the resulting hydrogel<sup>22</sup>. Radiation crosslinking is a fast and efficient hydrogel crosslinking method since, usually, it does not require the addition of crosslinking agents, as in the chemical crosslinking methods. In addition, this process can be performed at room temperature and does not present contamination risks, since additional chemical agents are not used. However, it could present limitations regarding the crosslinking process uniformity and the possibility of damaging any biological components that might be present in the hydrogel, so it is necessary to take special care with radiation exposure, which could also present risks to the user's health<sup>23</sup>.

### **1.2.2. Chemical crosslinking methods**

Chemical crosslinking refers to the intermolecular or intramolecular joining of two or more molecules by a covalent bond to form a 3D network. This is achieved through chemical reactions between reactive groups<sup>24</sup>. In general, chemically crosslinked hydrogels have better performance and stability than physically crosslinked hydrogels, due to a stronger binding energy and improved mechanical properties. Hydrogel-forming water-soluble polymers may have many functional groups such as hydroxyl groups (-OH), carboxylic

groups (-COOH), and amines (-NH<sub>2</sub>). The 3D network can be established by covalent bonding between these functional groups using, for example, glutaraldehyde. Nevertheless, crosslinker toxicity may limit their applications in tissue engineering. For example, small crosslinker molecules, like glutaraldehyde, have been reported as toxic and not recommended to fabricate hydrogels for biomedical applications. There are many methods to prepare chemically crosslinked hydrogels, such as the use of chemical agents <sup>34</sup>, oxidation reactions <sup>35</sup>, and click reactions <sup>36</sup>.

Crosslinking with chemical agents is a common technique for hydrogel preparation, in which one molecule, usually of low molecular weight, is added to the hydrogel's precursor mixture to induce covalent bonding formation between polymer chains. These agents can be bifunctional, which react with two functional groups in the polymers to form covalent bonds, or multifunctional, which bind to multiple functional groups in the polymers to create a stronger and more durable crosslinking. Chemical crosslinking is generally performed in controlled conditions of temperature, pH, and reaction time, among others, to ensure the bonds' appropriate formation and to avoid precursor's or resulting hydrogels excessive degradation <sup>34</sup>.

Oxidation is a chemical crosslinking method in which free radicals are generated through the oxidation of certain groups (such as unsaturated bonds or other reactive sites) in a polymer or other organic molecules. These free radicals can then react with other radicals or molecular species, leading to the formation of covalent bonds between different polymer chains, which results in crosslinking. Oxidation crosslinking can be useful to enhance hydrogel's mechanical properties and stability, as well as to control the drug delivery kinetic and other molecules incorporated in the hydrogel's matrix <sup>37</sup>.

Click reaction is a type of chemical crosslinking that involves a fast and efficient formation of covalent bonds between the monomers' reactive groups. This technique is very used in hydrogel preparation, due to its high efficiency and specificity. Some of the most used click reactions include the Alkyne-Azide reaction <sup>38</sup>, the Tetrazine-Click Reaction <sup>39</sup>, the Diels-Alder reaction <sup>40</sup>, and Michael's reaction <sup>41</sup>. In a general way, click-reaction crosslinking allows for the formation of hydrogels with highly controllable physical and mechanical properties, in addition to allowing for the incorporation of different functionalities in hydrogels, such as bioactive groups, proteins, or nanoparticles, which make them ideal for application in the biomedicine domain <sup>36</sup>.

Chemical crosslinking provides better stability, strength, and stiffness to the hydrogels, in comparison with physical crosslinking methods, corresponding also to a versatile process <sup>24</sup>. Considering the aforementioned, hydrogels crosslinked through

chemical or physical methods offer different advantages and disadvantages, which are described in Table 1.

Table 1- Advantages and disadvantages of the hydrogels' chemical and physical crosslinking processes <sup>4</sup>.

<b>Crosslinking methods</b>			
<b>Chemical</b>		<b>Physical</b>	
<b>Advantages</b>	<b>Disadvantages</b>	<b>Advantages</b>	<b>Disadvantages</b>
Increased stability of the hydrogel	May require complex manufacturing/specialized equipment	Simple manufacturing processes	Lower mechanical stability
Better control of the mechanical properties of the hydrogel	Modify the hydrogel's chemical properties, influencing cell and protein interactions	Absence of toxic chemical reagents	Hydrogels sensitive to environmental conditions (temperature, pH, ion concentration)
Enhanced compatibility with cells and tissues	Additional cytotoxicity, due to the use of chemical agents and crosslinkers	Enhanced biocompatibility	Less precise control of the mechanical properties of hydrogels

### 1.2.3. Hydrogel properties

Hydrogels have a wide range of chemical and physical properties that make them suitable for a variety of biomedical applications. The chemical properties refer to the chemical composition of a hydrogel, polymer chains' molecular weight, degree of crosslinking, and functional groups. The physical properties of a hydrogel are referent to the characteristics related to its structure, such as porosity, swelling behavior, and degradation kinetics. Within the physical properties, the mechanical properties are based on the response of the hydrogel to the application of external forces, mainly compressive and tensile forces, being their elasticity/stiffness and strength the most important <sup>42</sup>.

Elasticity is a mechanical property that is related to the capacity of a material to suffer deformation in response to mechanical tension and to recover its original form when the tension is removed (elastic deformation). This is quantified by the

measurement of Young's modulus, which is a measure of the hydrogel's resistance to stretching. A stiffer hydrogel will have a higher Young's modulus and it will be harder to deform under a given force, while a more elastic hydrogel will have a lower Young's modulus and it will be easier to deform. Hydrogel's elasticity is dependent on the chemical composition of the polymeric network and on the degree of crosslinking. Hydrogels with higher crosslinking density and higher polymerization degrees are usually more elastic than those with lower crosslinking degrees and shorter polymeric chains. Hydrogel's elasticity is a very important property for many applications, including tissue engineering and drug delivery, since it may affect cell behavior, *in situ* controlled drug delivery kinetics, and general mechanical stability <sup>43</sup>.

Hydrogel strength is a more comprehensive mechanical property that also considers plastic deformation, which is normally expressed in terms of resistance to the compression or tension forces applied to the hydrogel, depending on the specific test method used. Hydrogel's mechanical strength is influenced by several factors, including the crosslinking density, molecular weight of the polymeric chains, and the presence of any load in the hydrogel <sup>44</sup>.

In terms of other physical properties of hydrogels, the porosity, the swelling behavior, and the degradation kinetics are also relevant. Porosity is a property that influences nutrients and residual product diffusion, as well as cellular infiltration and tissue integration. Higher porosity may make cellular migration and tissue integration easier but also may reduce the mechanical properties and hydrogel stability. So, it is important to find the ideal porosity for a specific application <sup>45</sup>.

Another physical property is the swelling behavior. When a hydrogel is placed in an aqueous solution, it absorbs water molecules in its structure, causing it to increase its weight and volume. This increase is promoted by the hydrogel swelling behavior depending on several factors, including hydrogel's chemical composition, crosslinking density, pH, and ionic strength of the surrounding solution <sup>45</sup>. Swelling behavior is very important for many hydrogel applications, such as drug delivery, tissue engineering, and wound healing <sup>45</sup>. This physical property can be characterized, by measuring the change in the hydrogel's mass or volume as a function of time, in response to changes in the surrounding solution.

Degradation kinetics refers to how quickly the hydrogel breaks down into the immersion fluid or is absorbed by the surrounding tissue. This parameter may be affected by several factors, including the hydrogel composition, the crosslinking method, and the conditions of the surrounding environment. It is a very important aspect of hydrogel

development for biomedical applications because it may affect hydrogel's longevity and effectiveness *in vivo* <sup>16</sup>.

These mechanical properties play a crucial role in applications where an efficient cellular penetration and resistance to deformation are necessary, ensuring a suitable performance in several biomedical applications, mostly in the tissue engineering area <sup>46</sup>.

### 1.3. Hyaluronic acid hydrogels

In recent years, natural hydrogels based on hyaluronic acid (HA) have received considerable attention. HA (Figure 2) is a linear anionic acidic polysaccharide composed of D-glucuronic acid and N-acetyl-D-glucosamine disaccharide repeating units linked by alternating  $\beta$ -1,3-glycosidic and  $\beta$ -1,4-glycosidic bonds, that, belongs to glycosaminoglycans (GAGs) that regulate cellular processes <sup>24</sup>.

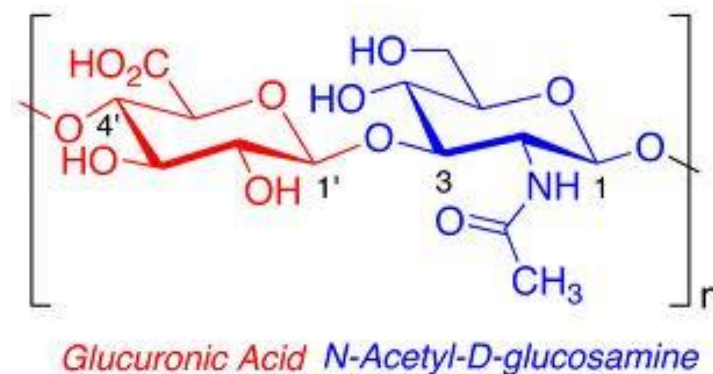


Figure 2- Chemical composition of HA <sup>47</sup>.

In its native form, HA chains are typically presented as long and coiled chains, adopting a conformation of random spiral in aqueous solutions <sup>48</sup>. The coiled structure is stabilized by intra and intermolecular hydrogen interactions between the hydroxyl and carboxyl groups of the sugar units. The HA chain's length and molecular weight can have significant effects on its activities and biological functions <sup>49</sup>. For example, high molecular weight HA is known to exhibit more viscoelasticity and swelling behavior, making it suitable for applications such as lubrication of joints, tissue hydration, and wound healing. On the other side, low molecular weight HA presents less viscosity and is responsible for different biological effects, acting as a signaling molecule in biological processes and anti-inflammatory activities <sup>50</sup>. HA widely exists in the vitreous, skin, umbilical cord, and synovial fluid of humans and animals, and was first isolated from the vitreous humor of bovine eyes in 1934. It has excellent moisturizing properties, biocompatibility, and biodegradability and has a variety of essential physiological

functions that are strictly related to many human physiological activities, such as cytokinesis and signal transduction <sup>51-53</sup>. As a crucial component of the extracellular matrix (ECM), HA can promote cellular adhesion and induce cellular differentiation. For that reason, HA can be used as a scaffold for cell culture <sup>45</sup>. HA can also be used as an important signaling molecule *in vivo*, since it can interact with the CD44, LYVE-1, and HARE receptors, being, for that reason, frequently used in drug delivery systems, for targeting delivery <sup>54-56</sup>. These properties and physiological functions make materials based on HA highlighted in the biomedicine field.

HA has been widely applied in ophthalmic treatment <sup>57,58</sup>, prevention of postoperative tissue adhesion <sup>59,60</sup>, and joint reparation <sup>61,62</sup> among other areas. Meanwhile, through further research, it is also found that HA itself still has several intrinsic defects. These defects include being susceptible to degradation by hyaluronidase and reactive oxygen species, short half-life *in vivo* and weak mechanical properties, mainly elasticity, stiffness, and swelling behavior, which limit the in-depth application of HA-based hydrogels in clinical practice, for orthopedic purposes, skin hydration and lubrication of joints <sup>63</sup>. To surpass these problems, it is possible to chemically modify HA through the introduction of carboxyl, hydroxyl, acetylamine groups, and other reactive groups <sup>64</sup>. The selection of suitable crosslinking strategies contributes to the improvement of their mechanical properties and expands their application in the biomedical domain.

In recent years, novel HA-based hydrogels with excellent properties have been developed and their applications in the biomedical area have been gradually extended to drug delivery <sup>65</sup>, wound healing <sup>66</sup>, cosmetics <sup>67</sup>, and tissue engineering, especially in cartilage repair <sup>68</sup>.

### **1.3.1. HA hydrogels crosslinking**

HA is readily biodegradable and exhibits relatively poor stability, which reduces its application potential. To avoid that limitation, physical and chemical crosslinking procedures have been developed. Chemical modification of HA macromolecules utilizing its carboxylic and/or hydroxyl groups allows for the adjustments of the physicochemical and biological properties of the obtained HA derivatives (Figure 3) for selected applications <sup>24</sup>.

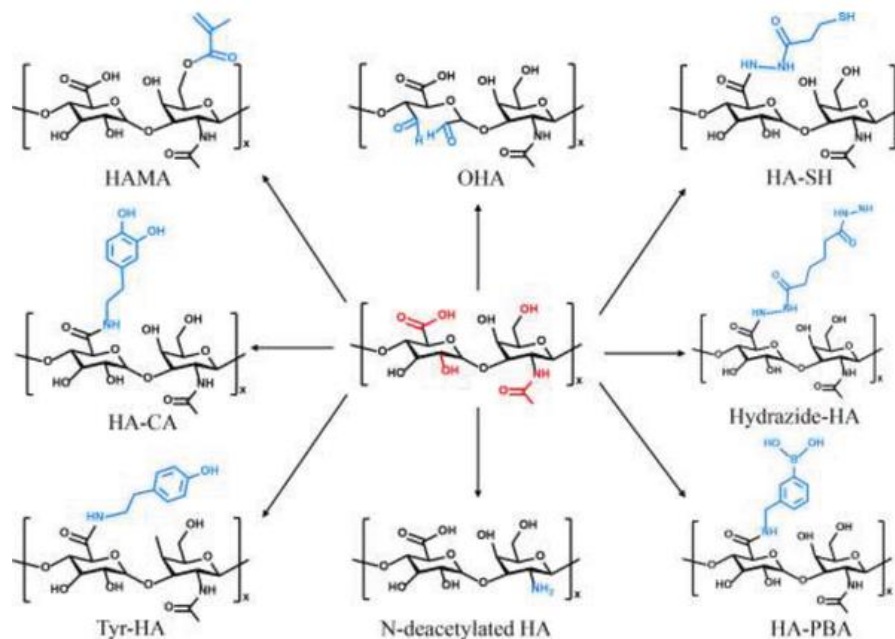


Figure 3 - Chemical structures of typical HA derivatives obtained from HA with different modification methods. HAMA – Hyaluronic acid methacrylate; OHA – Oxidized hyaluronic acid; HA-SH – Thiolated hyaluronic acid; HA-CA – Catechol-functionalized hyaluronic acid; Tyr-HA – Tyramine-modified hyaluronic acid and HA-PBA – Phenylboronic acid modified hyaluronic acid <sup>69</sup>.

There are several crosslinking agents commonly used to obtain HA hydrogels. The choice of the substance for the crosslinking procedure depends on several factors, such as the mechanism of desired crosslinking, biocompatibility, and desired application <sup>70</sup>. Table 2 shows examples of processes (chemical and physical) used for the preparation of HA-based hydrogels and their applications in the biomedicine domain.

Table 2- HA-based hydrogels and their applications in the biomedical domain.

HA-based hydrogels			
Crosslinking agent	Type of crosslinking	Applications	References
Divinyl sulfone (DVS)	Chemical	Tissue engineering	71
		Drug delivery	72
Genipin (Gen)	Chemical	Tissue engineering	73
		Drug delivery	74
		Wound healing	74
Glutaraldehyde (GA)	Chemical	Tissue engineering	75
		Drug delivery	76

		Wound healing	77
Butanediol diglycidyl ether (BDDE)	Chemical	Tissue engineering	78
		Drug delivery	79
		Wound healing	78
		Cosmetics	80
Adipic acid dihydrazide (ADH)	Chemical	Tissue engineering	81
		Drug delivery	82
		Wound healing	83
		Cosmetics	84
Polyethylene glycol (PEG)	Chemical	Tissue engineering	85
		Drug delivery	86
		Wound healing	87
		Three-dimensional cell culture	67
	Physical	Ophthalmology	88
Polyvinyl alcohol (PVA)	Physical	Tissue engineering	89
		Drug delivery	89
Hexamethylene diisocyanate (HMDI)	Physical	Tissue engineering	90
		Drug delivery	90

To prepare HA-based hydrogels with good mechanical stability and prolonged degradation profile, chemical crosslinking allows for the formation of strong covalent bonds between the functional groups of the polymeric chains. Among the crosslinkers listed in Table 2, polyethylene glycol (PEG) and genipin (Gen) have been originating hydrogels with enhanced properties, like hydrogels with a higher biocompatibility and swelling behavior in PEG's case, and hydrogels with a higher elasticity and mechanical strength in Gen's case. These unique and versatile properties make them popular choices in several biomedical applications, including tissue engineering and drug delivery<sup>91</sup>.

#### 1.3.1.1. Glutaraldehyde as crosslinker

Glutaraldehyde (GA) is an organic compound commonly used as hydrogel's crosslinking agent formed by substances of natural origin. This is because GA has two terminal carbonyl groups, which causes this to be reactive towards primary amine groups, and it

can work as a crosslinking agent for any substance with primary amine groups, such as chitosan, collagen, among others. However, it is important to notice that GA causes cytotoxicity in cells and biological tissues. So, GA is frequently used as a control or reference in studies to compare the effects of alternative methods of crosslinking<sup>92</sup>. This can include the evaluation of mechanical properties, swelling behavior, degradation speed, biocompatibility, and release kinetics of encapsulated substances<sup>93</sup>.

The GA concentration used to crosslink a hydrogel may vary depending on the application, desired crosslinking density, and the polymer's nature. According to the literature, the GA concentrations typically used for hydrogel crosslinking vary from 0.1% up to 5% (v/v)<sup>94</sup>. Lower concentrations, from 0.1% to 1%, are frequently used to obtain a more controlled crosslinking effect<sup>95</sup>. These concentrations are suitable for applications where minimal cytotoxicity or cellular compatibility is required, such as in tissue engineering or cell culture. Higher concentrations, such as 2% to 5%, can be used for more extensive crosslinking, especially in applications where higher mechanical strength and stability are required, like in drug delivery systems<sup>96</sup> and wound healing processes<sup>97,98</sup>.

HA hydrogels crosslinked with GA (HAGA) are notable for their mechanical stability and biocompatibility, making them suitable for a variety of biomedical applications. A study by Calles *et al.*<sup>99</sup>, demonstrated that the use of GA as a crosslinking agent significantly improved the integrity and the bioadhesiveness of HA hydrogels in aqueous environments. Crosslinked polymers showed more stability and increased porosity when the material had swelled. An example of a promising application of HAGA hydrogels in the biomedical area can be seen in the work reported by Nikjoo *et al.*<sup>76</sup>, which showed that HAGA hydrogels were used to assess the feasibility of using spray drying to produce inhalation powders from such HA hydrogels, including *in vitro* biodegradation and aerosolization performance and they revealed being promising scaffolds for pulmonary sustained drug delivery.

#### **1.3.1.2. Polyethylene glycol as crosslinker**

Polyethylene glycol (PEG) is a synthetic and soluble polymer composed of ethylene glycol repeated units. Even though ethylene glycol monomer is toxic, PEG is not and possesses a relevant importance in the biomedical area due to its unique combination of biocompatibility, hydrophilicity, and versatility<sup>100</sup>. PEG can crosslink several types of polymers, like HA, through a variety of mechanisms, including physical crosslinking (for example, by H-bond) and covalent bonds, originating hydrogels<sup>101</sup>.

In the HA-based hydrogels case, physical crosslinking occurs when PEG and HA chains link each other through H-bonds. These bonds can be established between the hydroxyl groups of the two polymers, between the HA's carboxyl groups and PEG's hydroxyl groups, or between the HA's hydroxyl groups and PEG's ether groups, contributing to the 3D network formation, increasing the hydrogel's mechanical strength. A covalent bond can be achieved by incorporating reactive groups, such as acrylate, epoxide, or thiol groups, in PEG's chains and crosslinking them with HA molecules that possess hydroxyl and carboxyl groups, with which they react, forming the 3D network<sup>101</sup>. A modification of HA can also be performed to promote the crosslinking with PEG's chains.

One of the most used PEG derivatives as a crosslinker for biomedical purposes is the polyethylene glycol diglycidyl ether (PEGDE), which is formed by introducing epoxide groups at the ends of the PEG's chains. Crosslinking by PEGDE has been more recently introduced and showed attractive features in terms of viscoelastic properties and reduced biodegradation. The incorporation of these reactive groups in the PEG's chains is an ideal strategy to promote the formation of ether bonds between the HA chains, which are very strong chemical bonds, leading to the formation of a hydrogel more resistant to *in vivo* hyaluronidase-promoted degradation, that is one of the most limiting factors of HA-based materials. These properties allowed for the HA-PEGDE hydrogels to become very useful in several biomedical applications, such as tissue engineering, drug delivery, etc.<sup>102</sup>.

Similar to PEGDE, ethylene glycol diglycidyl ether (EGDE), an epoxy-modified ethylene glycol (PEGDE monomer), has also been used to crosslink HA to reduce its biodegradation. EGDE is non-cytotoxic and hydrophilic, and it can form crosslinks in three different ways, depending on the pH. Under alkaline conditions, EGDE will react with the hydroxyl groups and under acidic conditions with the carboxyl groups. At neutral pH, EGDE would react with an amine, but this will not happen as unmodified HA does not have primary amine groups<sup>103</sup>.

The use of PEG as a crosslinker in HA hydrogels normally results in hydrogels with enhanced mechanical properties, especially in terms of mechanical stability, increasing its strength and durability, as well as its swelling behavior, being used in a variety of biomedical applications, including drug delivery, wound healing, and tissue engineering, mainly in joint lubrication and tissue hydration processes<sup>104</sup>. For example, Hussain *et al.* developed HA hydrogels with and without PEG and evaluated their capacity to deliver doxorubicin in a model of bladder cancer<sup>105</sup>. Results showed that HA-

PEG hydrogels presented a more controlled release of doxorubicin compared to HA hydrogels without PEG. In addition, HA-PEG hydrogels demonstrated higher effectiveness in the inhibition of tumoral growth and size reduction in comparison to HA hydrogels without PEG. This study highlighted the HA-PEG hydrogel's capability to improve drug delivery effectiveness, providing a more controlled and prolonged release of doxorubicin, which resulted in improved therapeutic results in the treatment of bladder cancer <sup>105</sup>.

#### 1.3.1.3. Genipin as crosslinker

Genipin (Gen) is a natural compound derived from the fruit of the gardenia plant (*Gardenia jasminoides*) (Figure 4). Chemically, it belongs to the class of iridoids, a type of secondary metabolites of a terpene nature, widely dispersed in the plant kingdom. Gen possesses alcohol, ester, and ether groups in its structure, and has been used as a low-cytotoxicity crosslinking agent that can establish bonds between macromolecules and primary amine groups <sup>106</sup>.

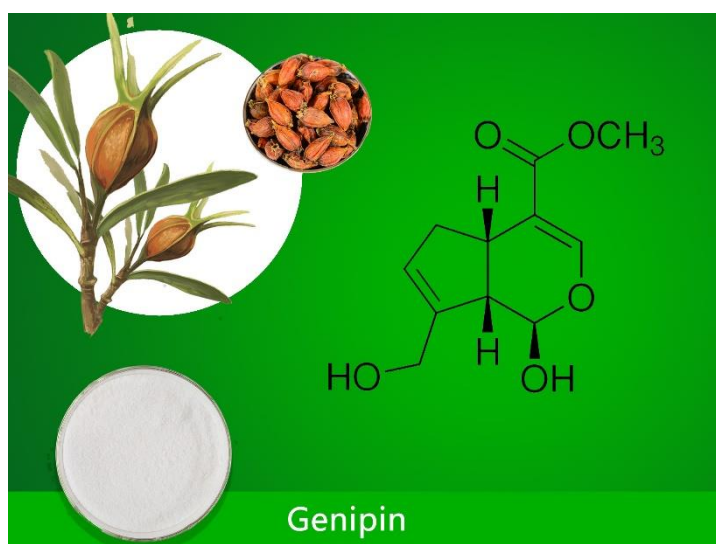


Figure 4 - Origin and chemical structure of genipin <sup>107</sup>.

The crosslinking mechanism (Figure 5) involves the attack of primary amine groups in the olefinic carbon atom in C-3 of Gen resulting in the opening of the ring, followed by the formation of bonds, with the participation of intermediate species of Gen <sup>108</sup>. The second reaction, slower, is the nucleophilic substitution of the ester group in Gen with amine groups, leading to the secondary amide formation <sup>109</sup>. In addition, it was reported that Gen can serve, not just as a crosslinking agent, but also as a therapeutic agent, due to its anti-inflammatory, antioxidant, and neuro-protective properties <sup>110</sup>.

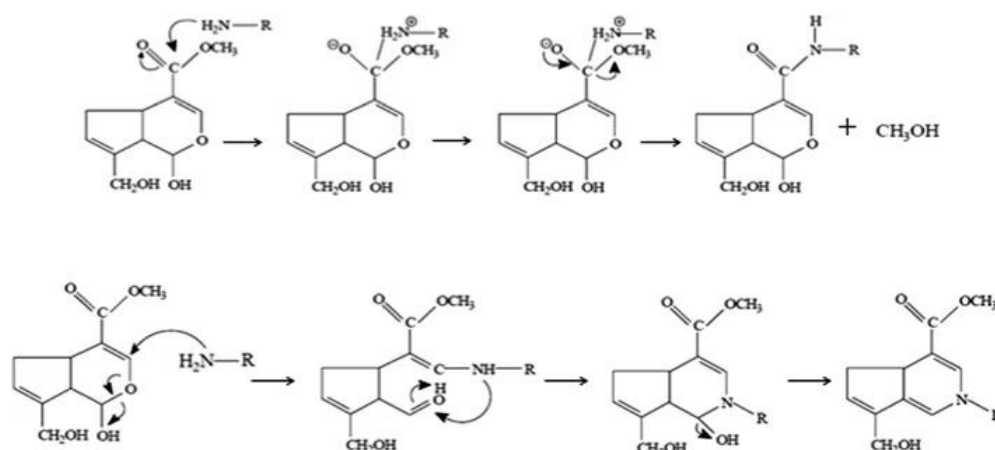


Figure 5 - Reaction of genipin crosslinking with primary amine groups <sup>111</sup>.

HA hydrogels crosslinked with Gen have been showing very promising results in the biomedical area, especially in terms of drug delivery. For example, Pérez *et al.* prepared HA hydrogels crosslinked with Gen and evaluated its potential for the controlled release of the anticancer drug methotrexate (MTX) <sup>112</sup>. They compared the drug-release behavior of Gen-crosslinked HA hydrogels with HA hydrogels without Gen as a control. Results showed that Gen-crosslinked HA hydrogels exhibited enhanced mechanical properties, especially in terms of strength, and higher stability in comparison with the HA hydrogels without Gen. The release of MTX from Gen-crosslinked hydrogels was more controlled and sustained over time, demonstrating the potential of Gen as a crosslinking agent to modulate drug delivery kinetics <sup>112</sup>.

### 1.3.2. HA hydrogel applications

According to the literature, HA-based hydrogels are non-toxic and non-immunogenic, both in *in vitro* and *in vivo* studies <sup>113</sup>, and have been used in a wide variety of applications, especially in the biomedical domain, because of their excellent physiological properties.

#### 1.3.2.1. Tissue engineering

Tissue engineering is a field that combines the domains of biology, engineering, and materials science and has as its objective the development of new therapies for the repair, substitution, or regeneration of damaged tissues and organs <sup>68</sup>.

In bidimensional cell culture (2D), cells are typically grown on flat, rigid surfaces, such as petri dishes or cell culture dishes. This does not supply the same 3D microenvironment that cells experience *in vivo*. The ECM is a complex 3D network of proteins and other molecules that supply structural support and signaling signs for cells

in tissues <sup>114</sup>. Hydrogels, on the other side, can be projected to have mechanical stiffness, porosity, and a chemical surface similar to those of ECM, allowing for cells to interact with the hydrogel's matrix in a way that resembles the structure of the tissue <sup>114</sup>.

In hydrogel's cell culture, the cell culture procedure can be considered a limiting factor for hydrogel application. Depending on the application-level point of view, cell culture may be held after hydrogel production or simultaneous with the hydrogel's fabrication process. The difference between making the hydrogel before cell culture and simultaneous with cell culture relies on the way cells are incorporated in the hydrogel and the chosen method/procedure applied to obtain the hydrogel is prepared <sup>115</sup>. In the first case, the hydrogel is prepared separately, and the cells are incorporated into or cultured on the hydrogel matrix after its formation. This method allows for the cells to be incorporated in a homogeneous and controlled way in the hydrogel, but it could present some challenges in cell distribution and viability, depending on the cell type, the reactions' type and conditions, and the hydrogel properties <sup>115</sup>. In the second case, the hydrogel and the cells are incorporated simultaneously, that is, the cells are added to the pre-hydrogel solution before it solidifies. This method allows for the cells to be distributed more uniformly in the hydrogel, but it could make it hard to control cellular density and hydrogel formation at the same time. It is important to say that this also is highly dependent on the crosslinking strategy, method, and chosen agent <sup>115</sup>. In addition, the choice between these methods could depend on the hydrogel type and the cell culture type used. For example, hydrogels that require incubation time to formation, generally are prepared before cell culture. Nonetheless, hydrogels that can be formed fast, like thermosensitive hydrogels, can be prepared and combined with cells simultaneously. It is important to refer that gelation temperature is an important aspect to be considered because it influences the thermosensitive hydrogel formation time <sup>115</sup>.

HA-based hydrogels have been investigated for their potential use as a matrix in tissue engineering applications (Figure 6). The hydrogel provides a 3D environment that mimics the tissues' ECM, promoting cellular fixation, proliferation, and differentiation <sup>68</sup>. The HA hydrogels have also the advantage of being biocompatible, biodegradable, and injectable, and it can be used to support the growth and differentiation of various cell types, including stem cells <sup>116</sup>. HA-based hydrogels can be functionalized with several bioactive molecules to provide factors that promote cellular differentiation towards a desired cellular type <sup>116</sup>. Besides that, HA hydrogels can be projected to have specific mechanical properties that correspond to the target properties, allowing for a better integration and tissue function where it was implanted <sup>68</sup>.

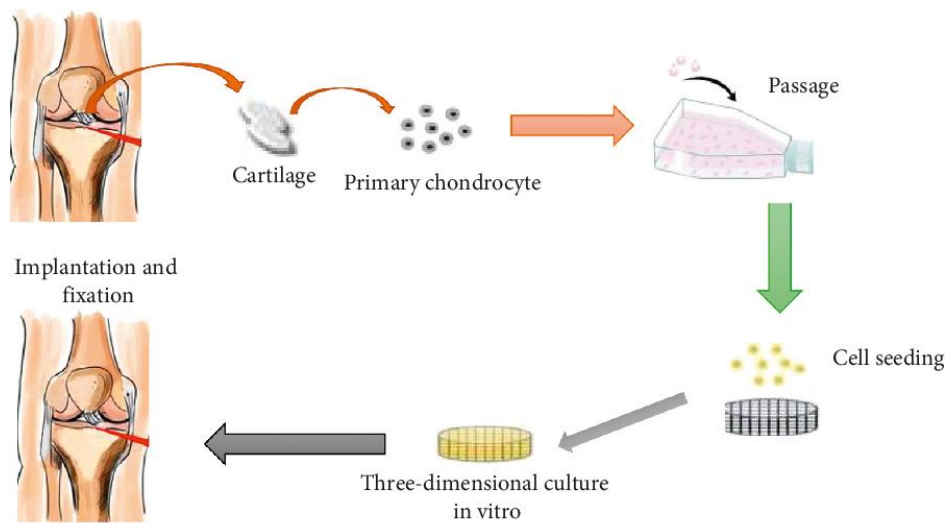


Figure 6 - Use of HA hydrogels as a matrix in tissue engineering applications <sup>117</sup>.

Some of the tissue engineering applications that have been investigated using HA-based hydrogels involve bone, cartilaginous, and neural tissue engineering processes. In bone tissue engineering, HA-based hydrogels have been used to promote the osteogenic differentiation of mesenchymal stem cells <sup>118</sup>. In cartilaginous tissue engineering, these hydrogels have been used to support the growth and differentiation of chondrocytes for the repair of damaged cartilage <sup>119</sup>. In neural tissue engineering, HA hydrogels have been used to support the growth and differentiation of neural stem cells for the repair of damaged neural tissue <sup>120</sup>.

Cell culture with 3D HA-based hydrogels is a promising approach for tissue engineering and regenerative medicine. HA hydrogels can be used as a matrix to provide mechanical support and a microenvironment that mimics the ECM *in vivo*, which promotes cellular adhesion, proliferation, and differentiation <sup>121</sup>. Besides that, HA hydrogels can be functionalized with bioactive molecules, like growth factors, allowing for a controlled release of these molecules, to modulate the cellular behavior <sup>122</sup>. For example, hydrogels can provide a platform for growth factor delivery, like BMP, cytokines, and other signaling molecules that can influence cellular behavior and promote tissue regeneration <sup>122</sup>. Besides that, hydrogels can be adapted to control the release of those molecules, providing a more controlled and sustainable delivery than other delivery systems, and providing a long-lasting effect over time <sup>123</sup>.

### 1.3.2.2. Drug delivery

Drug delivery refers to the process of administration of therapeutic agents to a patient. The goal is to deliver the drug to the cells or target tissue in the body, minimizing any

unwanted collateral effect. Drug administration relying on HA-based hydrogels has won significant attention in recent years due to its biocompatibility, biodegradability, and adjustable physical and chemical properties<sup>65</sup>. HA hydrogels can be used as carriers for the delivery of several types of drugs (Figure 7), including small molecules, proteins, and nucleic acids<sup>124</sup>. One of the main advantages of using HA hydrogels for drug delivery is its capability to form a 3D network structure that can provide a controlled release of the drug for a long period<sup>65</sup>.

Besides drug release and delivery to the target organs, HA hydrogels can carry growth factors such as bone morphogenetic proteins (BMP)<sup>122</sup>. BMPs are a group of growth factors that are part of the transforming growth factor beta family (TGF- $\beta$ ). These proteins have a fundamental role in bone formation and regeneration, as well as in other tissues, like cartilage and muscle. BMP-2 and BMP-7 are among the most widely studied growth factors and have been used in clinical applications for bone regeneration. They are normally used in combination with biomaterials, like hydrogels, to promote bone growth and repair, in case of bone defects or lesions<sup>125</sup>. Within the hydrogels, the HA nanogels are emerging as a promising platform for targeted drug delivery due to their unique properties and biocompatibility. These are a class of nanocarrier systems based on biodegradable polymers that can be applied in drug sustained release. These systems display prolonged blood circulation time, enhanced drug solubility, and selective accumulation at tumor tissues by enhanced permeability and retention (EPR) effect. With these properties, HA nanogels represent a versatile and promising approach for targeted drug delivery, offering the potential for more effective and safer therapies for a range of diseases<sup>126</sup>.

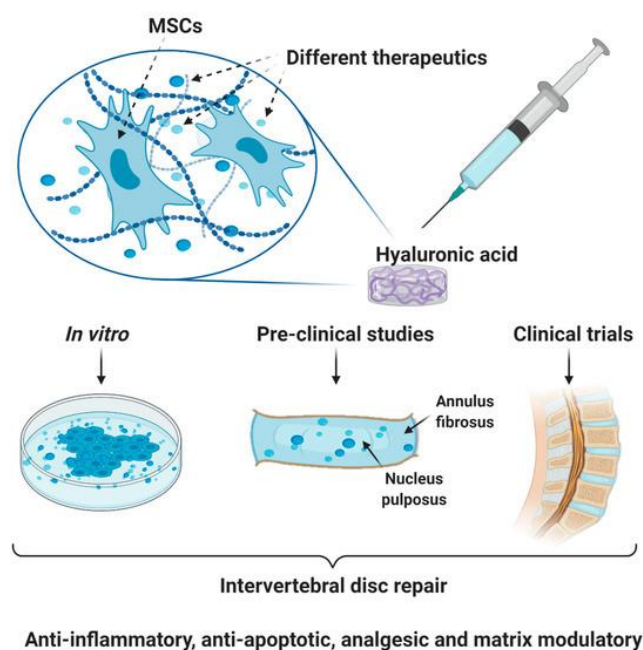


Figure 7 - The role of HA as a platform for cell and drug delivery in the Intervertebral disc repair (IVD). HA acts as a vehicle for adipose tissue and bone marrow isolated mesenchymal stem cells (MSC)s and drug delivery for disc repair <sup>127</sup>.

The release kinetics of the drug may be influenced by the crosslinking method, the crosslinking density, and the composition of the nanogel. In addition, HA nanogels can be modified with functional or conjugated groups with ligands to increase their specificity and targeting capability. This allows for the delivery of drugs that target specific cells or tissues, minimizing the side effects associated with their systemic administration <sup>65</sup>.

### 1.3.2.3. Wound healing

Wound healing is a natural process in which the body repairs and restores the damaged tissue structure and function. It involves a complex sequence of events that are rigidly regulated by several cells, cytokines, and growth factors <sup>66</sup>. HA hydrogels have been widely investigated because of their potential in wound healing applications (Figure 8) due to their biocompatibility, biodegradability, and capability to support cellular growth and tissue regeneration. HA hydrogels also can be easily functionalized with bioactive molecules to promote wound healing <sup>66</sup>. Hydrogels can also provide a humid environment that promotes cellular proliferation and migration, besides protecting the wound against infections and external factors. In addition, hydrogels can help to minimize the scars, promoting tissue regeneration and reducing inflammation <sup>128</sup>.

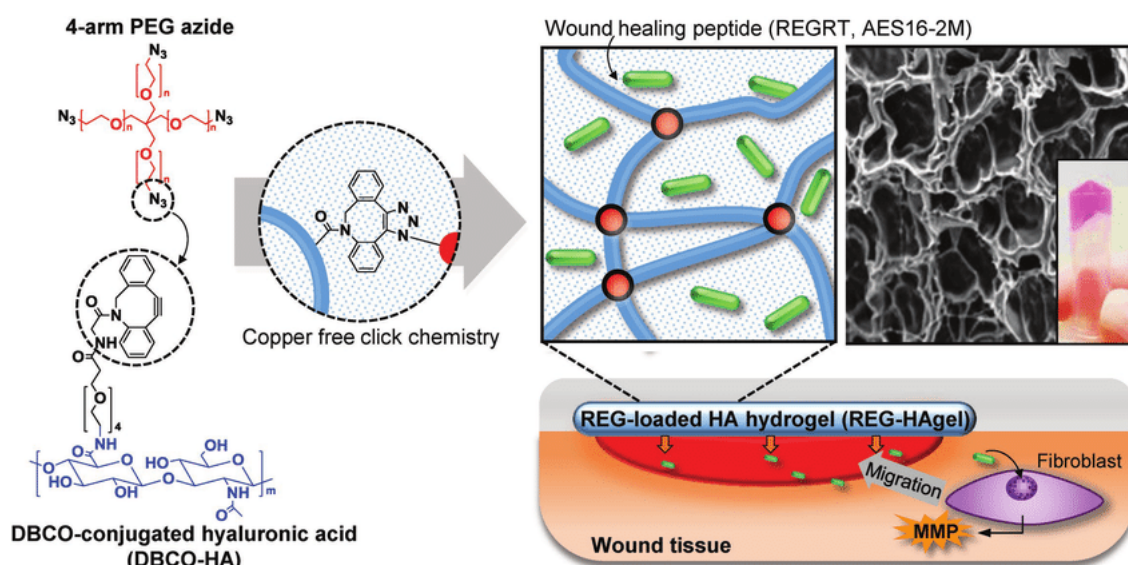


Figure 8 - Schematic illustration of HA hydrogel preparation through copper-free click chemistry, encapsulation of REG peptides, and its application in wound repair through activating cellular migration <sup>125</sup>.

Several studies showed HA hydrogel's efficacy in wound healing promotion. For example, a study by Hsu *et al.* reports that the application of a HA-based hydrogel in full-thickness wounds in mice resulted in accelerated wound healing and higher collagen deposition compared to control groups <sup>128</sup>. Similarly, a study by Poh *et al.* reports that the use of an HA hydrogel loaded with bone morphogenetic protein-2 (BMP-2) promoted the formation of granulation tissue and accelerated wound healing in mice <sup>129</sup>. The same research group also reports that the use of an HA hydrogel loaded with a nerve growth factor (NGF) promoted nerve regeneration and accelerated wound healing in mice <sup>130</sup>.

#### 1.3.2.4. Cosmetics

HA hydrogels have been used in several cosmetic applications due to their unique properties, including their high swelling behavior. They are commonly used in skin products, such as moisturizers, serums, and masks, to improve the skin's hydration and elasticity <sup>67</sup>. HA hydrogels have also been used as dermal fillers (Figure 9) to treat signs of aging. Due to its biocompatibility, HA hydrogels are a natural and more secure alternative to other types of dermal fillers made of synthetic materials. Injectable hydrogels can be prepared using a variety of natural and synthetic polymers, recombinant proteins, and peptides. These base materials have been crosslinked in the presence of cells, biologics, and tissues using chemical reactions or physical interactions. Such injectable hydrogels formed in situ have been used to deliver various therapeutic cells or biologics (e.g., growth factors, chemokines for modulating the

function of endogenous cells) to promote the regeneration of tissues, including bone, cartilage, and skin <sup>131</sup>.

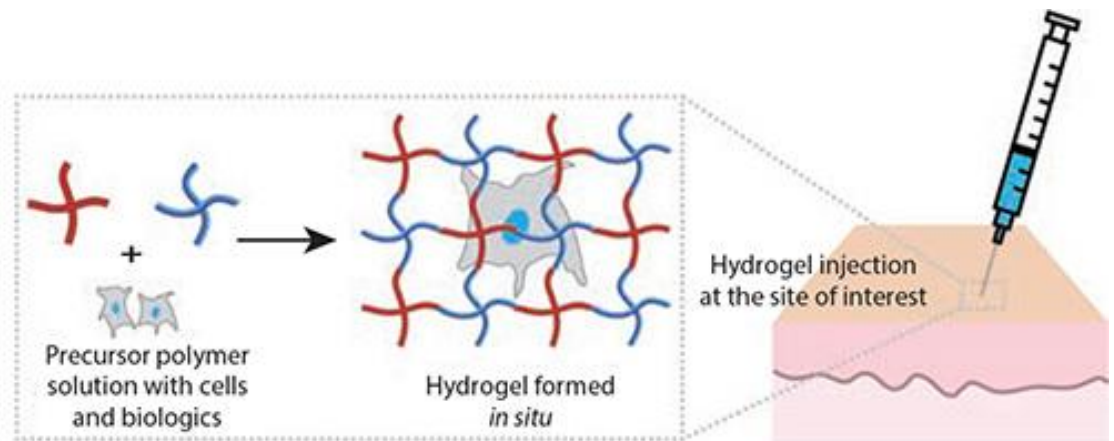


Figure 9 - Use of Injectable HA-based hydrogels as a novel, biocompatible and nontoxic dermal filler <sup>131</sup>.

## 1.4. Hydrogel Characterization

Hydrogels can be characterized by different instrumental techniques that evaluate their chemical composition, structure/morphology, and mechanical properties. Moreover, they can also be characterized through stability and degradation tests and assays for the determination of their toxicity and biocompatibility levels.

### 1.4.1. Instrumental tools for hydrogel characterization

Hydrogels can be characterized using a wide range of analytical methods, such as scanning electron microscopy (SEM), which is a technique used to visualize the hydrogel's morphology and structure at its surface <sup>132</sup>. Atomic force microscopy (AFM) is a technique that, along with surface topography analysis, is used to characterize the hydrogel's stability and mechanical properties, down to the nanometer scale <sup>133</sup>. Nuclear magnetic resonance (NMR) can be used to study the hydrogel components and to evaluate the success of the crosslinking process <sup>134</sup>. The Fourier transform infrared spectroscopy (FTIR) is a technique used to analyze the presence of functional groups in hydrogels, giving information about their chemical structure <sup>135</sup>. The Ultraviolet-Visible spectroscopy (UV-Vis) can be used to study the functional properties of hydrogels, including drug release, degradation, and chemical modifications, while also providing insights into their optical characteristics <sup>140</sup>.

#### 1.4.1.1. Scanning electron microscopy (SEM)

SEM is an analytical technique used to examine the surface of materials, such as hydrogels. This microscopy technique works by bombarding the sample surface with an electron beam and detecting backscattered and/or secondary electrons from the sample

surface. This information is used to generate a highly detailed 3D image of the sample's surface, with a high depth of field <sup>132</sup>.

In a hydrogel context, SEM can be used to examine the hydrogel's superficial topography. For example, SEM can be used to visualize the size, shape, and distribution of the hydrogel porous and fibrous network. It can also be used to evaluate the uniformity and consistency of crosslinking inside the hydrogel <sup>132</sup>.

SEM provides high-resolution images that can reveal details of micro and nanoscale. This fact makes SEM the ideal technique for the visualization of the surface's structure and hydrogel morphology. Additionally, SEM is a non-destructive technique to some extent, because it depends on the acceleration voltage of the electron beam and on the preparation and type of sample, which means that the same sample can be analyzed several times <sup>132</sup>. One limitation of this microscopy technique is that it requires a high vacuum environment, which means that the samples should be dehydrated or fixed before imaging. However, these pre-treatment steps of sample preparation can change the structure and morphology of the samples in the study, potentially affecting the efficacy of the results <sup>132</sup>.

One technique that is frequently coupled to SEM for hydrogel characterization corresponds to energy dispersion spectroscopy (EDS). EDS is an analytical technique that can be used to determine the presence and distribution of specific elements, like metallic ions or particles incorporated in the hydrogel. This can be useful to evaluate the nanoparticle incorporation or the distribution of elements of interest in drug delivery systems, for example. So, EDS can complement the hydrogel characterization, providing information about the elemental composition of the sample <sup>136</sup>.

#### **1.4.1.2. Atomic force microscopy (AFM)**

AFM is another analytical technique that can be used to examine the hydrogel's structure and mechanical properties. This microscopy technique works by scanning a probe over the surface of the sample while measuring the forces between the probe and the sample. This information is used to generate a 3D image of high resolution of the sample's surface <sup>133</sup>.

In the hydrogel context, AFM can be used to examine the surface topography and the roughness of the hydrogel. It can also be used to measure the hydrogel's mechanical properties, like its strength and elasticity and it can provide quantitative measures of the surface topography and mechanical properties <sup>133</sup>.

AFM can be operated in multiple modes, such as static mode or dynamic mode, depending on the specific requirements of the study in progress. In the static mode, the probe establishes physical contact with the sample, while, in the dynamic mode, the probe oscillates close to the surface of the specimen, making intermittent contact<sup>133</sup>. One AFM advantage is that it can operate in air or aqueous environments, without the need of high vacuum conditions, which makes it suitable for hydrogel analysis<sup>133</sup>. One AFM limitation is that this technique normally provides information only about the sample's surface and it cannot be used to examine the hydrogel's internal structure. In addition, this microscopy technique requires specialized equipment and experience in use by the operator, which can limit its accessibility for some researchers<sup>133</sup>.

#### **1.4.1.3. Nuclear magnetic resonance (NMR)**

NMR is a powerful analytical technique used to study the molecular structure of compounds, such as the hydrogel components. NMR spectroscopy is based on the interaction of specific atom's nuclei and a magnetic field<sup>134</sup>.

When addressing the hydrogels, NMR spectroscopy can be used to study the chemical composition and molecular structure of the components present in hydrogels, as well as the successful crosslinking reaction, by using, for example, proton NMR (<sup>1</sup>H) and carbon-13 NMR (<sup>13</sup>C)<sup>137</sup>.

NMR spectroscopy can provide detailed information about the hydrogel at the molecular level, including information about the chemical environment of specific atoms, the connectivity of different chemical groups, and the spatial arrangement of atoms within the hydrogel. Through NMR spectra analysis of a hydrogel before and after crosslinking, it is possible to quantify the extension of the established bonds, production of secondary products and to determine the structural changes that occur during the crosslinking process<sup>138</sup>. NMR spectroscopy is a non-destructive technique which means that the same sample can be analyzed several times. It is also a quantitative technique, which means that the results can be used to determine the amount of a specific component present in a sample. NMR is a well-established analytical method and is frequently used in the characterization of complex organic matrices, such as hydrogels<sup>134</sup>.

#### **1.4.1.4. Fourier transform infrared spectroscopy (FTIR)**

FTIR is an analytical technique widely used in hydrogel characterization. It allows for the identification of the functional groups in the material's chemical structure, providing information about its composition and chemical bonds. In FTIR, an infrared light beam is used to irradiate the sample, and the interaction of light with the molecules results in the absorption of energy at specific wavelengths. The resulting absorption/transmittance

spectrum is recorded and analyzed to identify the characteristic signals of the different functional groups <sup>135</sup>.

The obtained spectrum can be compared with reference spectral databases to identify the different functional groups in the sample, such as hydroxyl, amines, carboxy groups, etc. Besides functional group identification, this technique can also be used to check changes in chemical bonds during the formation or modification of hydrogels. For example, it is possible to observe the appearance of new signals or dislocations in the existing signals after the hydrogel's chemical crosslinking <sup>135</sup>.

Attenuated Total Reflection (ATR) is an extremely versatile measurement technique used in FTIR spectroscopy. It is easy to use and maintain and has plenty of options so that nearly any sample can be analyzed. In this method, a solid or liquid sample must be brought near the optical element where light is internally reflected and where the sample interacts with the evanescent wave. The effective path length for this interaction depends on several parameters and is typically a fraction of a wavelength <sup>139</sup>. Because of the small light penetration depth, the ATR technique is ideal for highly absorbing samples, surfaces, and thin film measurements. Generally, the ATR spectra are similar to regular transmission; nonetheless, for thick samples when spectra are recorded at angles greater than the critical one ( $40^\circ$ ), the wavelength dependence is observed. Moreover, ATR spectra possess not only absorption features but also reflection ones. Therefore, ATR spectra cannot be used in a quantitative manner (band shape analysis, determination of oscillator strengths...) directly <sup>139</sup>.

ATR-FTIR and FTIR are both valuable techniques for characterizing hydrogels, but they have some differences in terms of their application and advantages. Whereas FTIR requires thin, almost transparent samples, ATR-FTIR allows for direct analysis of samples in their native form, without the need for extensive preparation. While FTIR provides detailed information about the entire sample volume and is suitable for solid samples or samples with good transparency, ATR-FTIR requires minimal or no sample preparation, and provides surface-sensitive information, making it ideal for analyzing soft, wet, or irregular samples, like hydrogels. So, in hydrogel research, ATR-FTIR is often preferred for its simplicity and ability to handle soft, wet samples <sup>139</sup>.

#### **1.4.1.5. Absorption spectroscopy (UV-vis)**

Ultraviolet-visible (UV-vis) spectroscopy is an analytical technique that corresponds to a type of absorption spectroscopy in which UV-visible light is absorbed by molecules. Absorption of UV-visible radiation results in the excitation of the electrons from lower to higher energy levels. UV-vis spectroscopy is a versatile tool for characterizing hydrogels,

providing valuable information about their composition, structure, and behavior because it can be used to monitor the degree of crosslinking in hydrogels. Changes in absorbance at specific wavelengths can indicate the formation of crosslinking. This technique: can be used to measure the concentration of specific components within the hydrogel, provided these components absorb in the UV-vis range; can monitor chemical reactions involved in the formation or modification of hydrogels; can be used to study the kinetics of polymerization reactions involved in hydrogel formation, and, for hydrogels with optical transparency in the UV-vis range, can provide information about light transmission and absorption <sup>140</sup>.

#### **1.4.2. Physical and chemical stability**

Physical and chemical stability are two important parameters in the characterization of a hydrogel because they can affect the performance and lifespan of the material. For that, the storage conditions of a hydrogel are crucial and must be frequently monitored to maximize its lifespan <sup>141,142</sup>.

To evaluate the stability of a hydrogel, stability tests are often used, which are made to determine the lifespan and best storage conditions of a hydrogel. The test involves the monitoring of the physical, chemical, and biological properties of a hydrogel over time under different storage conditions <sup>143</sup>.

Parameters, such as hydrogel's appearance, texture and consistency, viscosity, or loss of gelation, could indicate a loss of physical stability as a function of time and environmental conditions. On the other hand, chemical stability can be evaluated by monitoring the production of degradation products as a function of changes in hydrogel's environmental conditions. The biological stability, which involves testing the biological properties of a hydrogel over time, including biocompatibility and sterility, can also be evaluated <sup>143</sup>. Temperature, for example, is a relevant environmental parameter that can affect the integrity of hydrogels. As such, the hydrogel can be stored at different temperatures over time to determine the effect of different storage conditions on the hydrogel's stability <sup>143</sup>.

Indeed, hydrogels must be stored at an appropriate temperature to avoid degradation and to maintain stability. Moreover, some hydrogels can be sensitive to light exposure and must be stored in dark containers or protected from light during storage. Hydrogels can also absorb the humidity in the environment, which can affect its stability and performance. To avoid microbe contamination, hydrogels must be stored in a sterile environment or container. In addition, the container must be well sealed to avoid contamination from the external environment <sup>143</sup>. The type and concentration of the used

crosslinking agent in the hydrogel can affect its lifespan too. Crosslinking agents that are unstable or degrade over time can reduce hydrogel's lifespan <sup>142</sup>. The packaging material should be compatible with the hydrogel and should protect the product from damage, contamination, and other environmental factors. The packaging materials commonly used to package hydrogels include glass or plastic bottles, ampoules, or syringes, which can be sealed with a lid or stopper to avoid contamination by microbial agents and other factors <sup>142</sup>.

To assess the level of chemical degradation of an HA-based hydrogel, namely the enzymatic degradation, the use of the enzyme hyaluronidase is often used. Hyaluronidase is an enzyme that specifically cleaves glycosidic bonds in HA, which is the main component of ECM. This enzyme leads to the degradation of HA into smaller fragments, such as oligosaccharides or monomers such as disaccharides composed of N-acetylglucosamine, and glucuronic acid <sup>144</sup>. This enzyme can be found in the connective tissues of animals and humans, where it helps to modulate the ECM. Indeed, in the context of hydrogels, hyaluronidase can be used as a reference enzyme to evaluate/compare the stability or degradation of HA-based hydrogels. In typical experiments, the hydrogel samples are normally incubated in a solution containing the enzyme, which breaks the polymeric chains, leading to the loss of the 3D network (loss of the hydrogel's structure). By comparing the behavior and degradation of hydrogel samples in the presence and absence of hyaluronidase, it is possible to assess the susceptibility of the hydrogel to enzymatic degradation <sup>145</sup>.

Several methods can be used to detect the hyaluronidase activity in a hydrogel matrix. For example, enzymatic assays can be performed with fluorescein-modified HA (or other compounds), and HA, when cleaved by hyaluronidase, results in a detectable change, such as colorimetric or fluorescent signals <sup>146</sup>. Also, the hyaluronidase activity can be determined by measuring the cleavage speed of the substrate, through the quantification of degradation products. It also can be assessed by microscopy techniques, such as confocal microscopy or SEM, which can be used to visualize the structural changes in the hydrogel's matrix after hyaluronidase degradation. These techniques provide high-resolution images that can reveal the induced changes by degradation in hydrogel's morphology and structure <sup>147</sup>. The hyaluronidase concentration used in all these experiments can vary depending on the configuration and the specific experimental objectives. Normally, according to the literature, it is used in concentrations varying between 10 U/mL to 100 U/mL. It is important to optimize the hyaluronidase

concentration based on the specific composition of the hydrogel, in the desired degradation rate and sensibility of the detection system <sup>148</sup>.

### **1.4.3. Biocompatibility**

The evaluation of the biocompatibility of a hydrogel is crucial to guarantee its safety and adaptation to biomedical applications. For that, several tests are performed, such as the *in vitro* toxicity <sup>149</sup> and *in vivo* tests <sup>150</sup>, first in animals and then in human beings (clinical trials) <sup>151</sup>, to achieve this purpose.

*In vitro* toxicity tests consist of laboratory techniques used to assess the potential toxicity of a substance, like a hydrogel, using cells or tissues in culture, in a controlled environment <sup>149</sup>. These types of tests are an important component in the biological assessment of a hydrogel as they can provide valuable information about the potential risks associated with its use. These tests can include different assays, such as cellular viability/cytotoxicity assays (assays to assess the potential of a hydrogel to cause damage to cells). The cytotoxicity assays commonly used include enzymatic assays (like the MTT and the resazurin reduction assays), which are colorimetric assays that evaluate, in an indirect way, the cell viability through the measure of the cell's metabolic activity, as well as assays that assess the damage to the plasmatic membrane, such as the LDH assay <sup>149</sup>.

For biomedical applications, hydrogels are often used as matrix materials for cell culture, for diverse studies, since they can mimic a more similar microenvironment to the *in vivo* conditions. The determination of cellular penetration and proliferation, and cell morphology in different hydrogels is an important analysis to assess the biocompatibility of the material within the organism. This assessment can be performed by *in vitro* assays with different types of cells, including fibroblast cell lineage, which is one of the most common cells in connective tissue <sup>152</sup>. To proceed with this analysis, hydrogels are prepared in formats suitable for cell culture, such as those adequate to be used in wells of culture plates. Then, cells are incubated with the hydrogel and maintained in culture under suitable conditions of temperature and humidity and appropriate nutrient supplementation. After a period of incubation, it is possible to assess the cellular penetration and proliferation in different hydrogels, as well as the cellular morphology by optic or electronic microscopy <sup>153</sup>. The obtained results can indicate the hydrogel's capacity to support cellular proliferation, as well as its capacity to allow for cell penetration and tissue formation. In addition, cellular morphology can provide information about the adhesion degree of cells to the material, as well as the possible occurrence of cell death or morphologic changes associated with cytotoxicity or

incompatibility of the material with cells <sup>154</sup>. This approach allows for the possibility of assessing the biocompatibility of hydrogels in a controlled and standardized environment, besides the possibility of assessing the cellular response to different formulations and conditions of hydrogel preparation. However, in *in vitro* conditions, cell cultures may not completely reflect the complexity of the biological processes that occur in tissues and live organisms, which can limit the ability to predict the *in vivo* responses of tissues to hydrogels <sup>153</sup>.

The genotoxicity assays are another type of *in vitro* assay that measures the toxicity level of hydrogels at the DNA level. These tests are used to assess the potential of the hydrogel to cause genetic damage to cells. There are several genotoxicity assays, being the most common the micronucleus assay, the Comet assay, and the Ames assay. The micronucleus assay consists of the observation of the cells exposed to a compound to verify if there is the formation of micronucleus, which are structures that indicate damage to DNA. The Comet assay is used to measure DNA fragmentation, and the Ames assay is a bacterial test used to assess the ability of a compound to cause genetic mutations <sup>155</sup>.

Lastly, other types of assays that are usually used to determine and evaluate the toxicity of hydrogels *in vitro* are the immunotoxicity assays, which assess the hydrogel's potential to cause an adverse immune response. There are several immunotoxicity assays that can be performed, being the most common the detection of the presence and quantity of specific proteins by ELISA, such as cytokines involved in immune processes<sup>156</sup>.

Regarding the *in vivo* toxicity tests, they involve the administration of a substance, in this case, the hydrogel, to live organisms. This type of test is an important component of the safety and toxicity evaluation of a material because it can provide valuable information about the potential risks associated with its use <sup>150</sup>.

The *in vivo* toxicity tests can involve several different types of studies, such as acute, sub-chronic, and chronic toxicity studies, as well as immunogenicity and carcinogenicity ones. The acute toxicity tests involve the administration of a unique dose of hydrogel to animals to assess the potential for immediate adverse effects <sup>157</sup>. The sub-chronic toxicity studies involve the repeated administration of a hydrogel to animals for weeks or even months to assess the potential for long-term adverse effects <sup>158</sup>. The chronic toxicity studies involve the repeated administration of a hydrogel to animals over an extended period, normally from several months to several years, to assess the toxicity potential in the long term <sup>159</sup>. Lastly, the immunogenicity studies assess the hydrogel

potential to cause an immune response in animals, and carcinogenicity studies, are those that assess its potential to cause cancer <sup>160</sup>.

## 1.5. OBJECTIVES OF THE THESIS

This thesis appears as a preliminary study to develop a new crosslinking strategy to prepare HA hydrogels with high efficiency, low toxicity, and good physical and chemical properties for biomedical applications. In particular, it was an important objective to obtain HA-based hydrogels double-crosslinked using genipin and PEGDE. In this context, to evaluate the impact of the different hydrogel formulations and preparation conditions on the final materials, several studies were performed, namely:

- (a) To establish the optimal conditions for HA hydrogels, different crosslinkers were used, such as polyethylene glycol diglycidyl ether (PEGDE), ethylene glycol diglycidyl ether (EGDE), genipin and glutaraldehyde (this one was used as a “classical” reference for crosslinking); the resulting hydrogels were tested through swelling and stability studies in different conditions (temperature and degradation media) over time.
- (b) Beyond macroscopic features evaluation, the morphology and topography of the hydrogels were analyzed by scanning electron microscopy, and the crosslinking process was studied by ATR-FTIR.
- (c) To determine hydrogels' susceptibility to degradation by the enzyme hyaluronidase, the carbazole assay was used. This allowed for the determination of the most stable hydrogel, based on the various crosslinkers used, in resisting degradation by this enzyme over time.
- (d) To evaluate hydrogels' cytotoxicity, NIH 3T3 cells were cultured in direct contact with hydrogels; with hydrogel's extracts and along with transwell inserts with the hydrogels within, being the results analyzed by the resazurin reduction assay and confocal microscopy.

## 2. MATERIALS AND METHODS

### 2.1. Cells, materials, reagents, and general equipment

For the preparation of the HA-based hydrogels, the reagents used were low molecular weight sodium hyaluronate (HA, 0.6-1.0 million DA, Biosynth), polyethylene glycol diglycidyl ether (PEGDE, Mn = 2000, 95% purity, Sigma-Aldrich), ethylene glycol diglycidyl ether (EGDE, MW = 174.1944 g/mol, Angene), glutaraldehyde (GA, MW = 100.12 g/mol, 50% aqueous solution, Sigma-Aldrich) and genipin (Gen, MW = 226.23 g/mol, 98% purity, BLDpharm). For the preparation of the HAGA and HA-Genipin hydrogels, a modification of the HA was performed. For that purpose, Lysine monohydrochloride (MW = 182.65 g/mol, 98% purity, Merck), 1-Ethyl-3-(3-dimethylaminopropyl)carbodiimide (EDC, 191.70 g/mol, 98% purity, ThermoFisher) and N-Hydroxysuccinimide (NHS, MW = 115.09 g/mol, 98% purity, Sigma-Aldrich) were used.

For the chemical characterization of the starting materials and HA-based hydrogels, Fourier-transform infrared spectroscopy coupled with attenuated total reflectance (FTIR-ATR, Perkin Elmer Spectrum Two Spectrometer) and nuclear magnetic resonance spectroscopy (Bruker AvanceCore spectrometer, 400MHz) were used. For the hydrogel's morphology characterization, the scanning electron microscopy (Bench SEM Phenom Pro X, Phenom World) was used, and all image treatment was done using Image J software v. 1.54 (NIH, Bethesda, MD, USA).

The NIH 3T3 cells used in the present work were provided by CQM cryopreservation cell bank (cells were previously acquired to DSMZ, Germany) and the cell number was then expanded by performing several cell passages when confluency was reached. For cell culture experiments, Dulbecco's Modified Eagle Medium (D-MEM, Gibco), phosphate buffered saline solution (PBS, Sigma-Aldrich), 100x antibiotic/antimycotic solution (AA, Gibco), and fetal bovine serum (FBS, Gibco) were used along with 100 mm tissue culture dishes, 24-well round bottom plates (Corning, Costar®). Cells and media were manipulated/cultured in a Laminar Flow Hood (Nuair, Model NU-425 class II type) and an incubator (Nuair, DH Autoflow Automatic CO<sub>2</sub> Air Jacked Incubator) at 37 °C, in a humidified atmosphere with 5 % CO<sub>2</sub>. Cell imaging throughout this work was acquired with a widefield and confocal microscopy platform (Mica, Leica Microsystems).

### 2.2. Preparation of HA-based hydrogels

HA-based hydrogels were prepared using HA (native or modified with lysine) and different crosslinkers (Figure 10). Five different types of HA-based hydrogels (Table 3)

were prepared, considering always a final volume of 1mL when performing the crosslinking reaction.

Table 3 - HA-based hydrogels and their crosslinking conditions.

HA-based hydrogels							
Crosslinker	Designation	Crosslinking conditions (%w/v)					
		HA native (%w/v)	HALys (%w/v)	GA (%w/v)	PEGDE (%w/v)	EGDE (%w/v)	Gen (mM)
Glutaraldehyde (GA)	HA1GA4		1	4			
	HA1GA8		1	8			
	HA1GA10		1	10			
Polyethylene glycol diglycidyl ether (PEGDE)	HA-PEGDE 20_5	20			5		
	HA-PEGDE 20_10	20			10		
	HA-PEGDE 10_10	10			10		
Ethylene glycol diglycidyl ether (EGDE)	HA-EGDE 20_1	20				1	
	HA-EGDE 20_5	20				5	
Genipin (Gen)	HA1Gen2		1				2
	HA1Gen10		1				10
	HA1Gen20		1				20
PEGDE and Gen	Gen20-HA10-PEGDE10		10		10		20

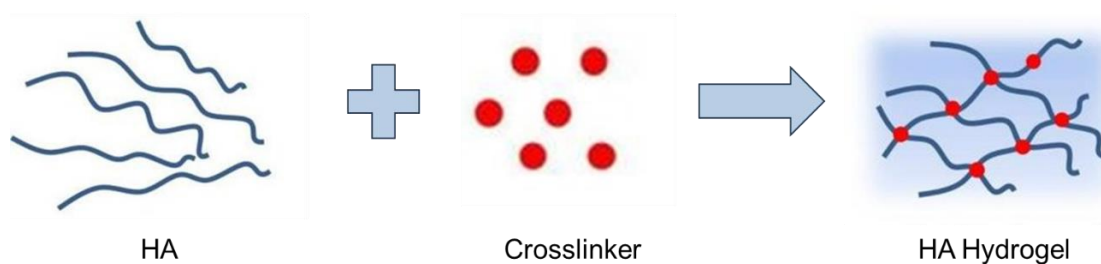


Figure 10 - Schematic representation of the HA-based hydrogels formulation.

### 2.2.1. HA-lysine functionalization

To obtain HAGA, HA-Gen, and Gen-HA-PEGDE hydrogels, a functionalization of the HA with the amino acid lysine was performed, in order to introduce primary amine groups in the polysaccharide that are necessary to react with Gen and GA since only the polymers with primary amine groups can be crosslinked by these molecules <sup>161,162</sup>.

For this purpose, 100 mg of HA was dissolved in 20 mL of PBS buffer (1x; pH = 6). Next, 72 mg of EDC, 44 mg of NHS, and 146 mg of lysine were separately dissolved, each in 1 mL of PBS, and added to the HA solution. To avoid the intermolecular amination, and thus to minimize the probability of a concomitant crosslinking process, a large excess of lysine in respect to the amount of HA was used. The reaction mixture was then stirred for 24h at room temperature (RT) of 22°C using a magnetic stirrer. After this time, the mixture was transferred to a dialysis membrane (MWCO 12000 Da) and dialyzed for the first 12 h against 0.1 M aqueous solution of Na<sub>2</sub>CO<sub>3</sub> and then for 8 days against deionized water. Finally, the obtained purified solution of the product was lyophilized (Labconco 4.5L Freeze Drier). The obtained product (HALys) was characterized by <sup>1</sup>H NMR spectroscopy using deuterated water <sup>162</sup>.

### 2.2.2. HAGA hydrogel

To obtain HAGA hydrogels, an adaptation of the method used by Gilarska *et al.* was made <sup>162</sup>. A solution of 1% HALys was dissolved in 3mL of 10x PBS buffer (pH = 7.4), and different amounts of GA was added to the HA solution to obtain variable crosslinker concentrations (4, 8, and 10% w/v). The solutions were stirred for 30min and then incubated at 37°C until gel formation (usually 24h) to obtain HA1GA4, HA1GA8 and HA1GA10 hydrogels.

### 2.2.3. HA-PEGDE and HA-EGDE hydrogels

The method of Liu *et al.* <sup>163</sup> was followed. To obtain HA-PEGDE hydrogels, HA was dissolved at 20% (w/v) in 0.3 M NaOH overnight. To crosslink HA, different amounts of PEGDE (5 and 10% w/v) and EGDE (1 and 5% w/v) were added, separately, to the HA solution, and the resulting mixtures were kept at 25°C for 24 h, under stirring (1500 rpm).

### 2.2.4. HA-Gen hydrogel

To obtain HA-Gen hydrogels, an adaptation of the method used by Gilarska *et al.* was made <sup>162</sup>. HALys was dissolved at 1% in 10x PBS buffer overnight. To crosslink HALys, different concentrations of Gen (2, 10, and 20 mM) were added to the HALys solution and stirred for 30 min. The obtained HA-Gen solutions were incubated at 37°C until gel formation, usually 24h.

### **2.2.5. Gen – HA – PEGDE hydrogel**

The process to obtain Gen – HA – PEGDE hydrogel involved two steps: the first one consisted of the crosslinking between HALys with PEGDE, and the second one consisted of the crosslinking between the HA-PEGDE hydrogel with Gen. For the first step, HALys was dissolved at a concentration of 10% w/v in 0.3 M NaOH overnight and then PEGDE (10% w/v) was added to the HALys solution and kept at 25°C for 24 h, under stirring. After HA-PEGDE crosslinking, the hydrogel was carefully washed several times with 10x PBS buffer and an adequate amount of an aqueous solution of 50 mM Gen was added to the solution to reach a final concentration of 20mM, and stirred for 30 min. The obtained Gen20-HA10-PEGDE10 solution was incubated at 37°C until gel formation.

## **2.3. HA-based hydrogels characterization**

### **2.3.1. NMR spectroscopy**

For NMR measurements, 250 µL of HALys was previously diluted in 200 µL of distilled water with vortex homogenization. Then, 50 µL of D<sub>2</sub>O was added to the sample with vortex homogenization. <sup>1</sup>H NMR measurements were carried out for the samples in D<sub>2</sub>O. NMR analysis: <sup>1</sup>H NMR (400 MHz, D<sub>2</sub>O), δ 4.79 (residual D<sub>2</sub>O; reference). For all samples, the <sup>1</sup>H NMR measurements were carried out with water suppression (NOESY-1D), according to Gilarska *et al.* <sup>162</sup>.

### **2.3.2. Scanning Electron Microscopy (SEM)**

The surface morphology of HA1GA4, HA-EGDE and HA-PEGDE hydrogels was examined by SEM, using a Bench SEM Phenom-Pro X (PhenomWorld) microscope. The samples were swelled in distilled water (HA1GA4 and HA-EGDE) or 1x PBS (HA-PEGDE) until reached their maximum swollen state, at 22°C. Subsequently, they were freeze-dried before observation (Labconco 4.5L Freeze Drier). The different hydrogel samples, prepared as previously stated, were swelled in distilled water or 1X PBS for a certain period at 22°C until the weight was stable. The surface morphology of the samples was examined by scanning electron microscopy, using a Bench SEM Phenom Pro X (Phenom World), with the Backscatter Electron Detector (BSD Full), the electron beam at 10kV, and Map intensity. Images were taken at different magnifications, from 250x to 2000x.

### **2.3.3. ATR-FTIR Spectroscopy**

Attenuated Total Reflectance Fourier-Transform Infrared spectroscopy (ATR-FTIR) was conducted to characterize HA-EGDE, HA-PEGDE and Gen-HA-PEGDE hydrogels. EGDE, PEGDE and Gen stock solutions were analyzed by ATR-FTIR to be used as standards for the HA-based hydrogels characterization. Also, Gen exposed to alkaline and acidic conditions were analyzed by FTIR to assess the possibility of degradation

under these conditions, due to a color change of the Gen-crosslinked HA hydrogel from blue to dark amber color. The spectra were acquired in a range of 4000 to 500  $\text{cm}^{-1}$  with a total of 32 scans per sample.

#### 2.4. Swelling studies

Swelling studies were performed to determine the extent to which the hydrogel absorbed water or 1x PBS. The HA-based hydrogels in this study were washed with approximately 10 mL of distilled water and stored in 3 mL of distilled water for 24h. After 24h, the gels were frozen in liquid nitrogen and lyophilized overnight. The lyophilized gels were then weighed, and the dry weight ( $m_d$ ) was registered. The hydrogel was then submerged in 10 mL of distilled water or PBS and allowed to swell for 48 h. After 48 h, the hydrogels were removed from the swelling solution, placed on a paper, dabbed gently with the paper to remove any excess water or PBS, and immediately weighed. The weight obtained was recorded as the swollen weight ( $m_s$ ). The swelling ratio was determined by use of the formula (eq.1), according to Pulat *et al.*<sup>164</sup>.

$$\text{Swelling Ratio (\%)} = \frac{m_s - m_d}{m_d} \times 100\% \quad \text{eq.1}$$

#### 2.5. Stability studies

The stability behavior of the hydrogels was studied in water and PBS (1x, pH=7.4) at 37°C. To perform this study, dried and pre-weighed hydrogel samples were first left to swell in water or PBS. Swollen gels were removed from the swelling solution at the end of 48h (except the HA-Gen hydrogels that were removed after 24h), dried superficially with paper, and weighed. This weight ( $m_m$ ) was recorded as the maximum swollen state of hydrogels. Then, they were placed into the fresh water and PBS solutions, and weighting was continued at regular intervals until the hydrogels completely disintegrated ( $m_t$ ). The stability ratio (%) was determined using the formula (eq.2), according to Pulat *et al.*<sup>164</sup>.

$$\text{Stability Ratio (\%)} = \frac{m_m - m_t}{m_m} \times 100\% \quad \text{eq.2}$$

#### 2.6. Degradation studies using hyaluronidase

*In vitro* degradation of HA-based hydrogels was performed by incubating the hydrogels with hyaluronidase (HAase) at 37°C. Samples of HA-based hydrogels were cut into defined shapes with similar weight (approx. 10mg), placed in 3mL of a 100 U/mL solution of HAase, and incubated at 37°C until the hydrogels were completely degraded. Aliquots

(200  $\mu\text{L}$ ) of each supernatant were taken at predetermined time points and replaced with fresh 100 U/mL HAase solution (200  $\mu\text{L}$ ). The collected supernatants were analyzed for uronic acid content according to the carbazole assay, using D-glucuronic acid lactone as the standard <sup>165</sup>. The degree of degradation was calculated by dividing the amount of uronic acid released at a given time point ( $u_t$ ) by the final amount of uronic acid collected when the hydrogel was completely degraded ( $u_f$ ), using the formula (eq.3), according to Segura *et al.* <sup>165</sup>.

$$\text{Degradation Ratio (\%)} = \frac{u_t}{u_f} \times 100\% \quad \text{eq.3}$$

## 2.7. Cell culture

For the preparation of the 3D cell culture, NIH 3T3 cells were used. First, cryopreserved NIH 3T3 cells were thawed, and centrifuged at 300 g for 8 min at 20°C. The pelleted cells were then resuspended in 1 mL of D-MEM containing 10% v/v FBS, and 1% v/v AA (henceforth also referred to as complete medium) and cultured in 100 mm culture dishes with 10 mL of complete culture medium and maintained in the incubator. The medium was changed 3 times a week. Before maximum confluency, cells were trypsinized. Succinctly, the culture medium was removed, and the cells were washed with PBS. After that, 1 mL trypsin solution (0.25% v/v trypsin-EDTA, ThermoFisher™ LIFETechnologies) was added to each culture dish, and incubated at 37°C for 5 min. After cell detachment, 2 mL of complete medium was added to stop trypsin action. Viability and cell density were determined in a cell suspension aliquot using 0.2% w/v trypan blue (Sigma-Aldrich) dye and a hemocytometer (Neubauer chamber). These cell suspensions were then used for the 3D cell culture preparation.

## 2.8. Metabolic activity

The NIH 3T3 embryonic mouse fibroblasts were seeded in three separately 24-well tissue culture plate at a density of  $4 \times 10^4$  cells/well in 1mL of complete medium and incubated at 37 °C in 5% CO<sub>2</sub> for 24h. Three different procedures were used to access the NIH 3T3 cells' metabolic activity upon exposure to the hydrogels: the direct contact method, which consisted of exposing the HA-based hydrogels directly with the cells; the extracts method, which involved exposing hydrogel's extracts (the solution constituted by the products released from the hydrogels to the D-MEM) to the cells; and, lastly, the transwell insert method, that consisted in placing the hydrogels in a transwell insert to be applied on top of the cell monolayer, in order to avoid direct contact between the hydrogels and the cells.

For the first two methods (direct contact and extract method), the HA-based hydrogels were prepared as previously described and transferred to a 24-well tissue culture plate, with the assistance of a scalpel and a tweezer, where they were incubated/stored at 4°C, with 1mL of 1x AA-containing PBS, followed by 1mL of complete medium, for 24h each, allowing for their simultaneous swelling and sterilization. For the third method (transwells), the hydrogels were incubated with the AA-PBS followed by the complete medium, directly in the transwell. Next, in the direct contact method, the hydrogels were transferred to the 24-well tissue culture plates directly on top of the pre-seeded cells and incubated at 37 °C in 5% CO<sub>2</sub>. In the case of the extract method, 100µl of the solution constituted by the products released from the hydrogels to the D-MEM (for 24h) was transferred to the 24-well tissue culture plates with the pre-seeded cells. Lastly, in the transwell insert method, the inserts with the hydrogels were transferred to the 24-well tissue culture plates with the pre-seeded cells as described above. After an incubation time of 48 h, the cells were washed, and the metabolic activity was assessed by the resazurin reduction assay. For this, the 0.1 mg/mL resazurin was diluted in 1:10 in complete medium and added to the cells in the wells <sup>166</sup>. The cells were incubated for 2 h at 37 °C incubator after which 100µL were transferred to a white opaque 96-well plate. Fluorescence intensity was measured using a microplate reader at  $\lambda_{ex} = 530$  nm and  $\lambda_{em} = 590$  nm (VICTOR3™ Multilabel Plate Counter). Metabolic activity was determined using the following formula:

$$Metabolic\ Activity\ (\%) = \frac{\overline{sample}}{\overline{cells\ control}} \times 100\% \quad eq.4$$

## 3. RESULTS AND DISCUSSION

### 3.1. HA-based hydrogels

#### 3.1.1. HA-lysine functionalization

In order to promote the crosslinking reaction of HA with Gen, the functionalization reaction of HA with the amino acid lysine was performed to introduce primary amines into the polymer chain structure.

Analyzing the  $^1\text{H}$  NMR spectrum of functionalized HA (Figure 11) the functionalization occurred with success, as can be seen by the presence of the lysine corresponding signals in the spectrum and by the presence of the protons of the amide group (8.10 ppm), as a result of the covalent bonding between the carboxyl group from HA with the amine group of lysine. Based on the integrations obtained for the two L5 protons of the lysine unit and the three protons of the methyl group in the HA backbone, the substitution degree was calculated as 23.5%. This is in agreement with the results obtained by Gilarska *et al.*<sup>162</sup>.

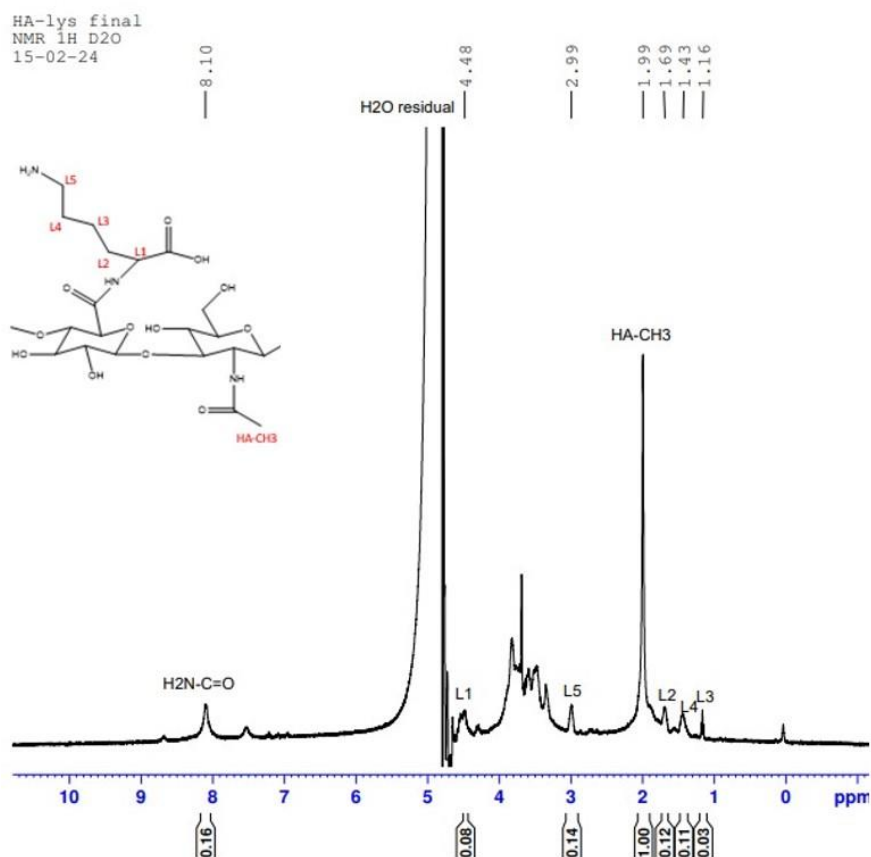


Figure 11 -  $^1\text{H}$  NMR spectrum of HALys with lysine unit signals assigned. Molecular structure of the reaction product in the insert on the top left.

### 3.1.2. Hydrogel's macroscopic features

Hydrogels based on HA were successfully prepared at different experimental conditions using glutaraldehyde (HAGA hydrogels), ethylene glycol diglycidyl ether (HA-EGDE hydrogels), polyethylene glycol diglycidyl ether (HA-PEGDE hydrogels) and genipin (HA-Gen hydrogels) as crosslinkers. In addition, Gen-HA-PEGDE hydrogel was also obtained by a dual crosslinking strategy, that is, using both genipin and PEGDE as crosslinkers. Figure 12 shows macroscopic images of the obtained materials.

The HAGA hydrogels (Figure 12, a-c) present a well-defined circular form due to the shape of the container in which they were prepared, are colorless, and show a gel-like texture which indicates the formation of a stable polymeric 3D network within the material, confirming the success of the crosslinking reaction. According to Alavarse *et al.*<sup>167</sup>, the covalent bonds formed between GA and primary amines should have resulted in a color change to yellow, but instead, the obtained hydrogels were colorless. This can be due to the complexity of the associated reaction mechanisms (e.g., many equilibrium structures of GA can exist in aqueous solution) that may affect the hydrogel's final characteristics, such as their color. Also, low concentrations of GA were used for crosslinking, which could probably contribute to the absence of color.

The HA-PEGDE hydrogels (Figure 12, d-f) are very elastic gels, with a defined 3D structure and with a yellowish color due to the high crosslinker concentration (5 and 10%) used for the hydrogel formation reaction. According to Lee *et al.*<sup>168</sup>, HA-PEGDE hydrogel color is dependent on its crosslinker concentration because increasing PEGDE concentration enhances the crosslinking density within the hydrogel, which means that a higher density can lead to a more tightly packed network, which might cause changes in the optical properties of the hydrogel, such as its color, changing it from transparent to a yellowish coloration.

The HA-EGDE hydrogels (Mw EGDE = 174.1944 g/mol; Figure 12, g-h) are very stiff compared to the HA-PEGDE (Mn PEGDE = 2000) hydrogels due to the size of the crosslinker chains, because the smaller the chain size, the less flexible will be the network<sup>169</sup>, contributing to a stiffer hydrogel<sup>103</sup>.

HA-Gen hydrogels (Figure 12, i-k) have a disc-like form, due to the shape of the vial used for the preparation of the hydrogels, with a blue color that resulted from the crosslinking between Gen (its original color is light brown) and the primary amine groups from HALys<sup>170</sup>. The Gen-HA-PEGDE hydrogel (Figure 12, l) results from a double crosslinking reaction and presents a brownish color, instead of blue. Gen reaction with amines is thought to occur via a nucleophilic attack by the free N-electron pair on the

olefinic carbon of the dihydropyran ring, resulting in ring opening and reclosure to incorporate the amine nitrogen. Crosslinking then proceeds via polymerization (Figure A1). The polymerization of Gen at strong alkaline conditions (pH 13.6) is quick, leading the color of aqueous Gen to change from blue to brownish immediately <sup>171</sup>. As a result, the clear/yellowish HA-PEGDE submerged in the blue Gen solution becomes an amber-like color after the crosslinking reaction.

a) HA1GA4



b) HA1GA8



c) HA1GA10



d) HA-PEGDE 20\_5



e) HA-PEGDE 20\_10



f) HA-PEGDE 10\_10



g) HA-EGDE 20\_1



h) HA-EGDE 20\_5





Figure 12 - HA-based hydrogels. HALys was used for HAGA, HA-Gen and Gen-HA-PEGDE hydrogels formation, meanwhile native HA (0.6-1.0 million Da) was used for the formation of HA-PEGDE and HA-EGDE hydrogels.

### 3.1.3. Characterization by ATR-FTIR Spectroscopy

The FTIR spectra of the different formulations of HA-EGDE and HA-PEGDE hydrogels (Figure 13, A-E) revealed multiple peaks characteristic of crosslinked HA. The peak at  $1600\text{ cm}^{-1}$  corresponds to the HA carbonyl group (C=O) (Table A1 and Figure A5). The broad peak observed at  $1020\text{--}1120\text{ cm}^{-1}$  indicates the C–O–C and C–O stretches, typical of the ether bonds formed during crosslinking with EGDE and PEGDE (Figures A3 and A4), though absorbance from HA can have partly contributed to the peak. These findings confirm the successful formation of crosslinked HA gels, utilizing both EGDE and PEGDE as crosslinkers <sup>172</sup>.

The spectrum of Gen powder (Figure A2) showed an absorption peak at  $1680\text{ cm}^{-1}$ , which was assigned to stretching vibrations of the carbonyl group (C=O), and another absorption peak at  $1621\text{ cm}^{-1}$  that was attributed to C=C vibration of the olefin ring in Gen. The peak that appeared in the region around  $2800\text{--}3000\text{ cm}^{-1}$  was attributed to C-H stretching vibration. The double peak between  $3000$  and  $3600\text{ cm}^{-1}$  in the Gen spectrum is most probably due to the overlapping of aromatic C–H and O–H vibration bands <sup>173</sup>. To test the possibility of degradation of Gen under acidic and alkaline conditions, Gen was dissolved in 10x PBS (pH=6) and 0.3M NaOH (pH=12). The spectra of Gen in acidic solution (Figure A6) and in alkaline solution (Figure A7), showed no differences from the spectrum of Gen powder (Figure A2), meaning that the pH of the Gen solution is not a factor that influenced in the color change of the Gen-crosslinked HA hydrogel from blue to dark amber color. Genipin crosslinking with primary amine

groups is thought to occur via a nucleophilic attack by the free N-electron pair on the olefinic carbon of the dihydropyran ring, resulting in ring opening and reclosure to incorporate the amine nitrogen, substituting the C=O group in the ring. In the Gen20-HA10-PEGDE10 hydrogel spectrum (Figure 14) it is not possible to see the absorption peak at  $1680\text{ cm}^{-1}$ , which was assigned to stretching vibrations of the C=O group, indicating that the crosslink between Gen and the primary amine group of HALys occurred with success. This is in agreement with Slusarewicz *et al.*<sup>171</sup> which reported genipin crosslinking mechanisms.

The remaining hydrogels (HAGA and HA-Gen) were not characterized by ATR-FTIR due to lack of starting material (HA native).

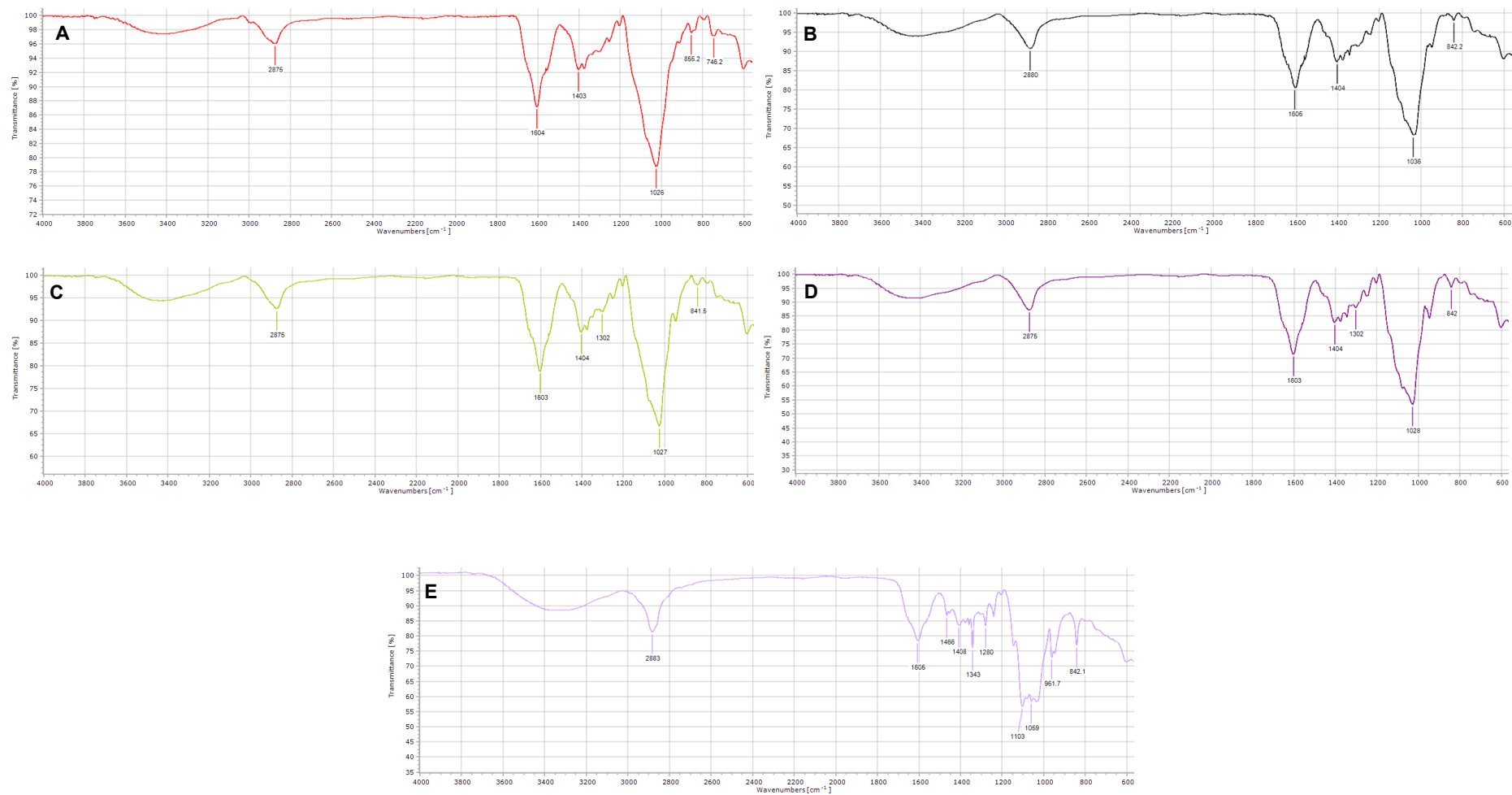


Figure 13 – ATR-FTIR spectra of A) HA-EGDE 20\_1; B) HA-EGDE 20\_5; C) HA-PEGDE 20\_5; D) HA-PEGDE 20\_10 and E) HA-PEGDE 10\_10 hydrogels.

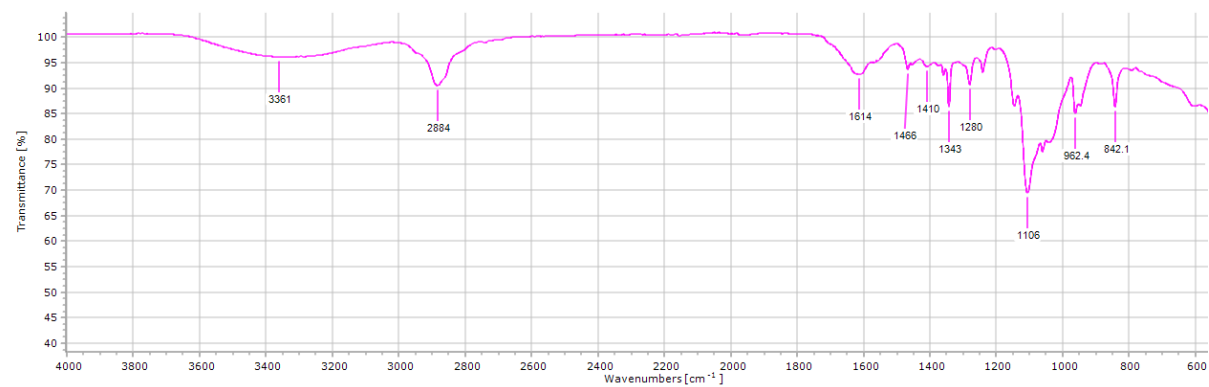


Figure 14 – ATR-FTIR spectrum of Gen20-HA10-PEGDE10 hydrogel.

#### **3.1.4. Characterization by Scanning Electron Microscopy (SEM)**

SEM images of the HA1GA4 hydrogel (Figure 15) indicated that the HA-based hydrogel presented a very rough surface, with many pores of large size. The hydrogel pores are interconnected, channel-free, and sponge-like, as can be seen in the work reported by Calles *et al.*<sup>99</sup>. The porosity of materials plays an essential role in the potential application in regenerative medicine since it is a property that has a significant impact on the cell adhesion and proliferation as well as on the permeation of nutrients and oxygen.

HA-PEGDE hydrogels (Figure 15) have well-defined porous structures with interconnected pores and a surface similar to that of a leaf/sheet, as reported in the work of Liu *et al.*<sup>163</sup>. Some bright particles can be seen in the images corresponding to salt crystals from PBS. Based on these results, it is clear that the increase in the crosslinking density (PEGDE from 5 to 10) leads to the reduction of the hydrogel's porosity. Meanwhile, similarly to HA-PEGDE hydrogels, HA-EGDE hydrogels (Figure 15) also present well-defined porous structures with interconnected pores and a fibrous surface structure<sup>174</sup>.

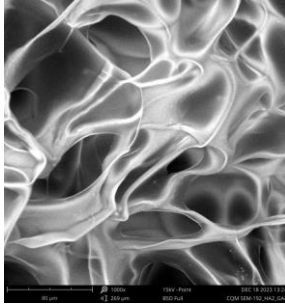
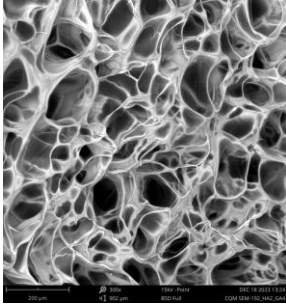
The remaining hydrogels (HAGA swelled in PBS, HA1GA8 and HA1GA10 swelled in H<sub>2</sub>O; HA-PEGDE swelled in H<sub>2</sub>O; HA-EGDE swelled in PBS; and HA-Gen and Gen-HA-PEGDE swelled in both H<sub>2</sub>O and PBS) were not characterized by SEM due to the lack of starting material (HA native).

**Hydrogel**

**300x**

**1000x**

HA1GA4 (water)



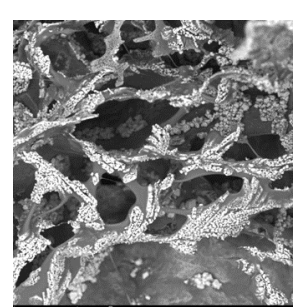
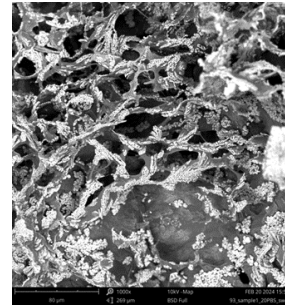
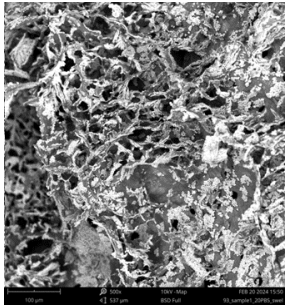
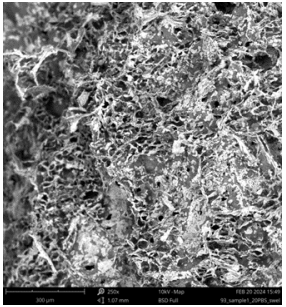
**250x**

**500x**

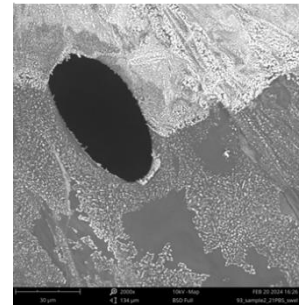
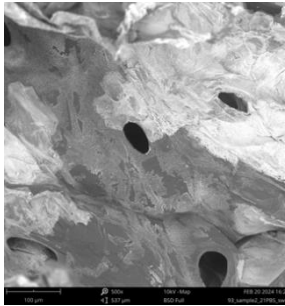
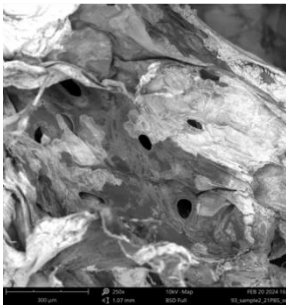
**1000x**

**2000x**

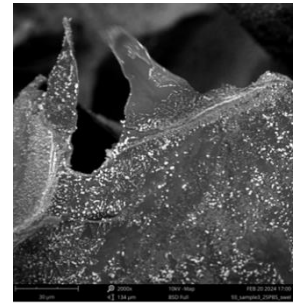
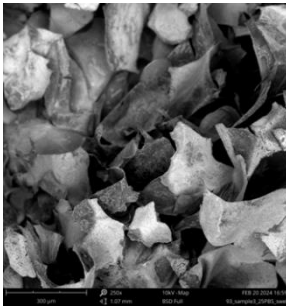
HA-PEGDE 20\_5 (PBS)



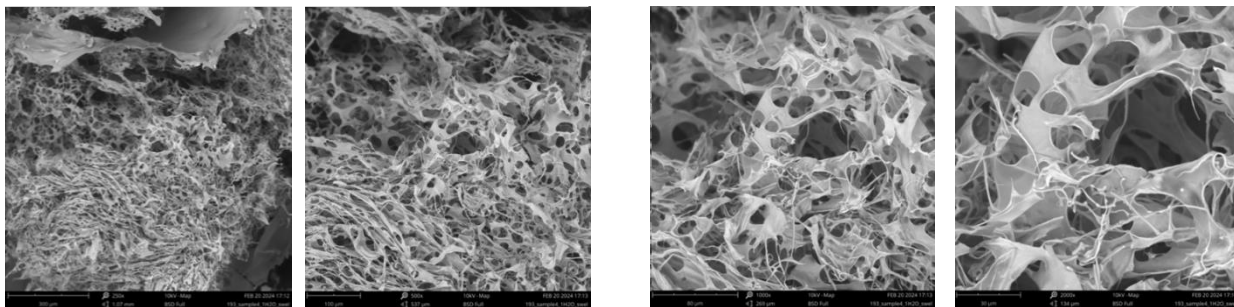
HA-PEGDE 20\_10 (PBS)



HA-PEGDE 10\_10 (PBS)



HA-EGDE 20\_5 (water)



HA-EGDE 20\_1 (water)

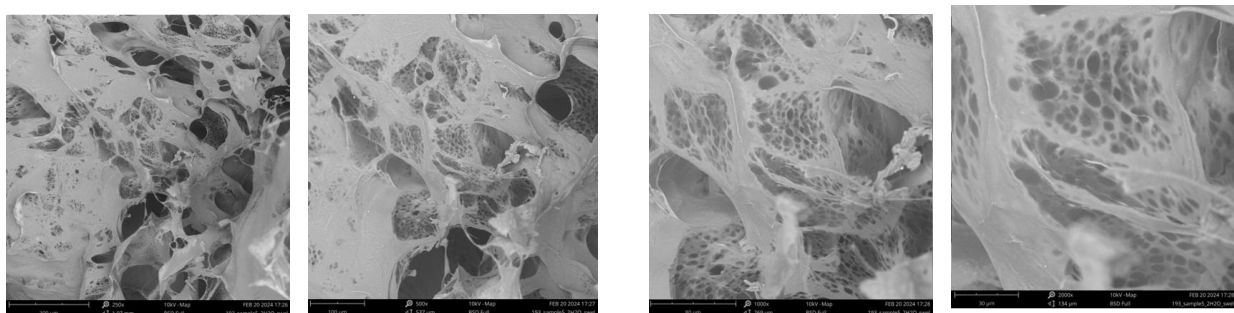


Figure 15 - SEM images of lyophilized HA-based hydrogels after swelling in water and PBS (pH = 7.4) at different magnifications. Scale: 250x (300  $\mu$ m), 300x (200  $\mu$ m), 500x (100  $\mu$ m), 1000x (80 $\mu$ m) and 2000x (30  $\mu$ m).

### 3.1.5. Hydrogels' swelling behavior

The swelling behavior of a hydrogel is influenced by several factors, including the polymer composition, crosslinking length and density, and the nature of the surrounding environment. So, the choice between water and PBS (phosphate-buffered saline) as the swelling medium can impact the extent of swelling. In this work, the swelling behavior of the HA-based hydrogels prepared with different crosslinkers was evaluated.

#### HAGA hydrogels

Figure 16 presents the swelling ratio (in percentage, S%) in water and PBS as a function of time for several HAGA hydrogel formulations. Regarding the impact of the hydrogel formulation on the swelling behavior in water, values were shown to be  $1355 \pm 130\%$  for the most swollen hydrogel, HA1GA4, and  $301 \pm 10\%$  for the least swollen hydrogel, HA1GA10. S% values, in PBS, were determined to be  $935 \pm 150\%$  for the most swollen hydrogel, HA1GA4, and  $352 \pm 75\%$  for the least swollen hydrogel, HA1GA10. Thus, in terms of S% trend, one can observe: HA1GA4 > HA1GA8 > HA1GA10, in both water and PBS media.

It can be observed that the swelling behavior of HAGA hydrogel is different in water and PBS. HAGA hydrogel exhibited a S% in water that increased rapidly within the first 5 hours, steadily increasing until 24-25h, after which it stabilized. Meanwhile, the swelling in PBS tended to stabilize faster, leading to a lower swelling percentage compared with the swelling process in water. All HAGA hydrogel formulations reached

an equilibrium state after approximately 20 to 25 hours. This happens because PBS is a buffer that contains salts such as sodium chloride (NaCl) and potassium chloride (KCl), which increase the osmotic pressure of the external solution. This reduces the osmotic gradient between the hydrogel and the surrounding solution, resulting in less water influx and thus less swelling. Meanwhile, pure water has no solutes, so the osmotic pressure is lower. This creates a larger gradient for water to enter the hydrogel, causing it to swell more. In addition, ionic strength is a parameter that can influence the swelling capacity of a hydrogel. The ions in PBS (e.g., Na<sup>+</sup>, Cl<sup>-</sup>) can shield the negative charges on the HA chains. This shielding reduces the electrostatic repulsion between the HA molecules, allowing them to come closer together. As a result, the hydrogel network contracts and swells less. Meanwhile, in pure water, there are no ions to screen the charges on the HA molecules. The negatively charged carboxylate groups on the HA chains repel each other, which pushes the polymer chains apart, leading to an expanded hydrogel structure and more swelling <sup>76</sup>.

This is in agreement with the literature, as Horlay *et al.* <sup>175</sup> reported that hydrogels, when submitted to swelling media with different concentrations of salts, result in a change in their swelling behavior, with the swelling media with higher salts concentration causing hydrogels to swell less, due to the increase of the osmotic pressure of the external solution caused by the presence of salts, while swelling media with less concentration of salts, results in a lower osmotic pressure, leading to create a larger gradient for the swelling medium to enter the hydrogel, causing to swell more, meaning that osmotic pressure is a parameter that influences the hydrogel's swelling behavior. In addition, Shah *et al.* <sup>176</sup> reported that besides the influence of the osmotic pressure on swelling behavior of HA hydrogels, it is also dependent on the ionic strength of the swelling media because the ions present in the swelling media neutralize some of the negative charges of the HA molecules through ionic interactions, leading to a reduction of the electrostatic repulsion and allowing for the polymer network to be more compact and thus reduce swelling, while without ions to neutralize the charges, the electrostatic repulsion is higher, which increases the volume of the hydrogel and, consequently, its swelling capacity.

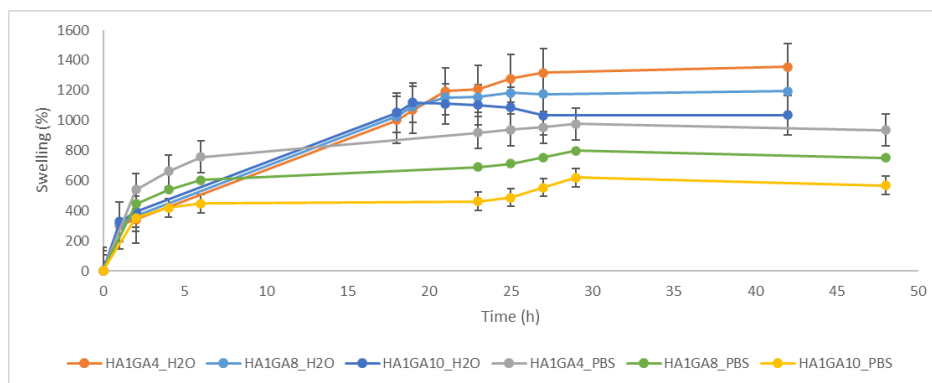


Figure 16 - Swelling behavior of HAGA hydrogels in water and 1x PBS as a function of time.

### HA-EGDE and HA-PEGDE hydrogels

Figure 17 presents the swelling behavior (S%) of HA-EGDE (A) and HA-PEGDE (B) hydrogels in water and PBS as a function of time. In the case of HA-EGDE hydrogels, the S% values, in water, were  $3323 \pm 1189\%$  for the most swollen hydrogel, HA-EGDE 20\_1, and  $891 \pm 192\%$  for the least swollen hydrogel, HA-EGDE 20\_5. S% values, in PBS, were  $2926 \pm 607\%$  for the most swollen hydrogel, HA-EGDE 20\_1, and  $1095 \pm 133\%$  for the least swollen hydrogel, HA-EGDE 20\_5. Therefore, in terms of S% trend, it can be observed: HA-EGDE 20\_1 > HA-EGDE 20\_5, in both water and PBS media.

Regarding the HA-PEGDE, S% values, in water, were  $5760 \pm 1279\%$  for the most swollen hydrogel HA-PEGDE 20\_5, and  $1484 \pm 227\%$  for the least swollen hydrogel HA-PEGDE 10\_10. S% values, in PBS, were  $2402 \pm 109\%$  for the most swollen hydrogel HA-PEGDE 20\_5, and  $524 \pm 172\%$  for the least swollen hydrogel HA-PEGDE 10\_10. Thus, in terms of S% trend, one can observe: HA-PEGDE 20\_5 > HA-PEGDE 20\_10 > HA-PEGDE 10\_10, in both water and PBS media.

Similarly to HAGA hydrogels, HA-PEGDE hydrogels also have a higher swelling behavior in water than in PBS buffer due to the osmotic pressure and ionic strength influence in the swelling studies explained above. In addition, the degree of crosslinking is also a factor that influences the swelling behavior of a hydrogel. As the degree of crosslinking increases, the percentage of swelling decreases, because the 3D hydrogel's network becomes stiffer and more resistant to the intake of swelling medium, contributing to a lower swelling behavior. In addition, it can be seen that PEGDE is a crosslinker agent that provides elasticity to hydrogels. Indeed, as can be seen, it was this crosslinker that led to the highest swelling percentage values, indicating that PEGDE is a crosslinker that originates elastic hydrogels <sup>163</sup>.

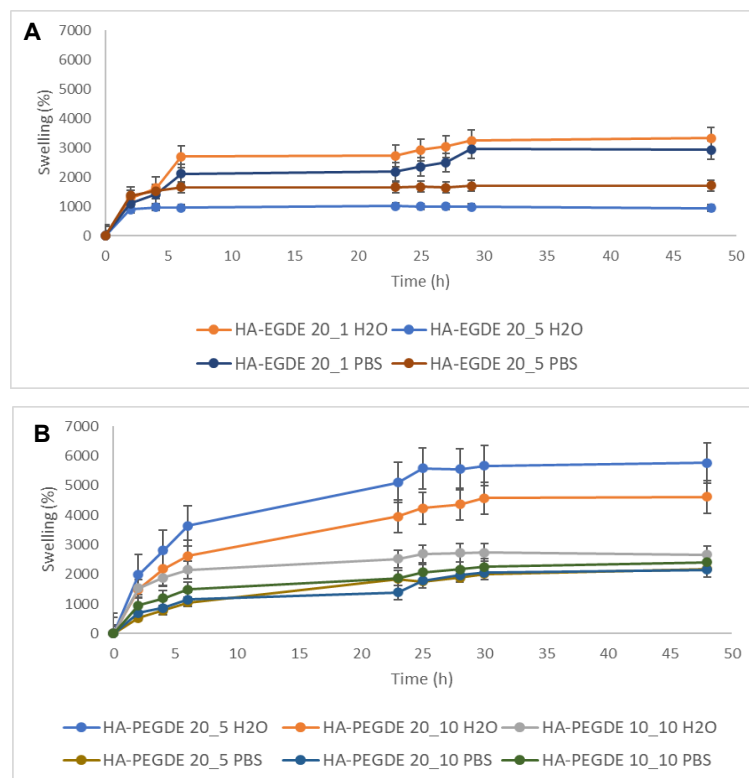


Figure 17 - Swelling behavior in water and PBS as a function of time. (A) HA-EGDE and (B) HA-PEGDE. Note: The y-axes on both graphs have different scales.

Comparing the results of the swelling behavior of HA-PEGDE and HA-EGDE, it can be observed that the swelling behavior in water is far superior than in PBS due to the presence of salts in PBS. This happens since PBS has a higher osmotic pressure due to the presence of sodium, chlorine, potassium, and phosphate ions, which affect the water uptake and the swelling behavior of HA. Not only the swelling of the hydrogel can be due to the difference in osmotic pressure, but also driven by the possible interaction of the cations with the negatively charged HA polymer chains. Meanwhile, hydrogels tend to absorb water, leading to an increase in volume or swelling.

It can be seen that the swelling behavior of HA-EGDE hydrogel tends to stabilize faster than that of HA-PEGDE hydrogels. This is attributed to the length of the crosslinker chains. EGDE is lengthwise smaller than PEGDE, which leads to less expansion capability and, thus less swelling power, with the hydrogel reaching a maximum swollen state (EGDE chain extension at its maximum) first than when using PEGDE. On the other hand, PEGDE has longer chains, so it confers more flexibility to the hydrogels, extending their swelling stabilization time. HA-EGDE hydrogels tend to stabilize their swelling behavior in both water and PBS after 6h, while the HA-PEGDE hydrogels usually tend to stabilize later, around the 25h time point.

It is clear that the HA-PEGDE hydrogels reached superior values of swelling than HA-EGDE hydrogels due to the aforementioned length of the polymer chains. Alongside with the crosslinker chain length, it can also be seen that the degree of crosslinking is a factor that influences the swelling behavior of the hydrogels. As the degree of crosslinking increases, the swelling behavior decreases, because the obtained hydrogels present a denser mesh (higher crosslinking point density), and their network is more resistant to expansion and to the intake of the swelling medium. For the hydrogels in the same conditions of crosslinker concentration (HA-PEGDE 20\_5 and HA-EGDE 20\_5 hydrogels), it can be seen that the swelling behavior of HA-PEGDE 20\_5 hydrogel in water is higher than that of the HA-EGDE 20\_5 hydrogel, but lower in PBS, due to the size of the chains and due to osmotic pressure and ionic strength as described above.

### **HA-Gen and Gen-HA-PEGDE hydrogels**

Figure 18 presents the swelling behavior (S%) of HA-Gen (A) and Gen-HA-PEGDE (B) hydrogels in water and PBS as a function of time. Regarding the impact of the hydrogel formulation on the swelling behavior of HA-Gen hydrogels in water, S% values were  $1553 \pm 174\%$  for the most swollen hydrogel, HA1Gen2, and  $692 \pm 156\%$  for the least swollen hydrogel, HA1Gen20. S% values, in PBS, were  $616 \pm 175\%$  for the most swollen hydrogel, HA1Gen2, and  $35 \pm 3\%$  for the least swollen hydrogel, HA1Gen20. Hence, in terms of S% trend, it can be observed: HA1Gen2 > HA1Gen10 > HA1Gen20, in both water and PBS media. Regarding the Gen-HA-PEGDE hydrogel, S% values, in water, were  $1385 \pm 364\%$  for the most swollen state and  $947 \pm 189\%$  for the least swollen state. S% values, in PBS, were  $645 \pm 228\%$  for the most swollen state and  $477 \pm 134\%$  for the least swollen state.

It can be confirmed that, similarly to the other hydrogels, the degree of crosslinking is a factor that influences the swelling behavior of hydrogels, and also that Gen is a crosslinker agent that provides stiffness to hydrogels as it leads to lower swelling percentage values. In addition, it can be noticed that this is a highly swellable hydrogel, because it has a rapid increase in the swelling value in the first 2 hours, starting to stabilize after that until reaching its maximum swollen state.

Summarizing, the swelling behavior of the hydrogels is influenced by the formulation composition and swelling media, where lower concentrations of crosslinker lead to greater swelling. Also, hydrogels swell more in water compared to PBS<sup>176,177</sup>.

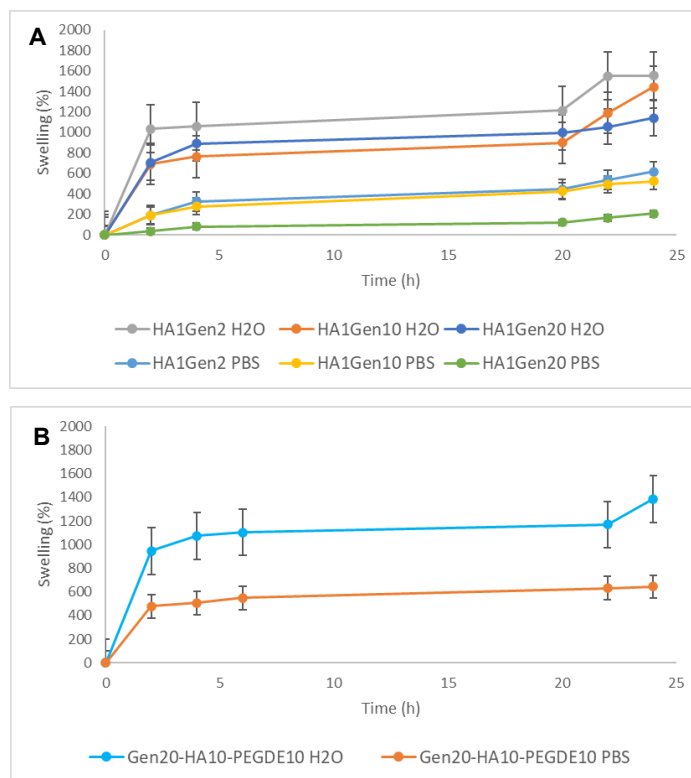


Figure 18 - Swelling behavior in water and PBS as a function of time. (A) HA-Gen and (B) Gen-HA-PEGDE.

It can be observed that, in a general way, independently of the crosslinker used (GA, PEGDE, EGDE, or Gen), the swelling percentage is lower in PBS than in water due to the presence of ions that influence the swelling behavior of hydrogels because they can interact with the polymer network and affect the osmotic pressure. It can also be noticed that the swelling ratio decreases with the increase of the degree of crosslinking in both water and PBS, which is due to the change in polymer volume fraction and thus the size of hydrogel pores<sup>163</sup>. In addition, it is also important to note that the crosslinker length also has a significant impact on the swelling behavior, because the swelling ratio decreases with the decrease of the length of the crosslinker, in both water and PBS, which is associated with the crosslinking density, the hydrogel pore's size, and it's the hydrogel's mechanical strength. From all the hydrogels prepared, the HA1Gen20 demonstrated to have the less swelling capacity, however, the HA-PEGDE 20\_5 presented to have the most swelling capacity.

## 3.2. Stability and Degradation Studies

### 3.2.1. *In vitro* stability studies

To evaluate how the hydrogel maintains its 3D structure under physiological conditions over time, hydrogels were subjected to incubation in water and PBS, at 37°C. The results presented in Figures 19-21 indicate that the stability increases with the crosslinking density. For the hydrogels crosslinked with the same molecule (such as GA: 4, 8 and

10%; PEGDE: 5 and 10%; EGDE: 1 and 5% and Gen: 2, 10 and 20mM), as expected, the HA1GA10 (61 days) is more stable than HA1GA8 (55 days) and than HA1GA4 (40 days); the HA-PEGDE 20\_10 (84 days) is more stable than HA-PEGDE 20\_5 (77 days) and than HA-PEGDE 10\_10 (63 days); the HA-EGDE 20\_5 (91 days) is more stable than HA-EGDE 20\_1 (70 days); and also the HA1Gen20 (62 days) is more stable than HA1Gen10 (55 days) and than HA1Gen2 (48 days).

Comparing the different HA-based hydrogels (Figure 19-21), it can be seen that the most stable hydrogels are the ones crosslinked with EGDE, and the HAGA hydrogels are the most susceptible to degradation, degrading more rapidly than the others. Comparing the HA-based hydrogels in the same conditions but with different crosslinkers (HA-EGDE 20\_5 and HA-PEGDE 20\_5), it can be seen that the HA-EGDE 20\_5 (91 days) is more resistant to degradation than the HA-PEGDE 20\_5 (77 days), which indicates that a hydrogel crosslinked with a smaller chain molecule such as EGDE (compared with PEGDE) form a stronger and less flexible crosslinking between the HA chains, making the resulting hydrogel less susceptible to degradation, i.e. more stable.

The Gen20-HA10-PEGDE10 hydrogel (Figure 22) showed the slowest weight loss rate of all the HA-based hydrogels (106 days). The Gen20-HA10-PEGDE10 hydrogel showed a slower weight loss rate than the HA-PEGDE and HA-Gen hydrogels, due to sufficient crosslinking because as this hydrogel involves 2 different types of crosslinking mechanisms, this increases the crosslinking density within the hydrogel <sup>178</sup>.

In addition, another different condition was also assessed that consisted of a step of lyophilization after the swelling study, in order to see if a hydrogel that is dried prior to the stability study presents different results regarding its stability compared to a hydrogel without being previously dried and being continuously in the swelling medium. The results presented in Figure 23 A and B showed that there is no difference between the hydrogels previously dried and the hydrogels being continuously in the swelling bath, indicating that an extra step of lyophilization does not make any difference in hydrogel's stability <sup>164</sup>. For biomedical applications purposes, these HA-based hydrogels could be commercialized in a dried state, which would increase its lifespan and also its stability, because its stability time will only start counting from the moment the hydrogel was hydrated, making lyophilization a very important process in hydrogel's shelf life <sup>179</sup>.

This stability study was also performed in different media (water and PBS, pH=7.4), in order to see the influence of the medium on the hydrogel's resistance to degradation over time. Results showed that the hydrogel's degradation is initially more rapid in water than in PBS, being more uniform in PBS. However, in the long term, there

is no difference between them, as it can be seen, in a general way, that the hydrogels, independently of the medium used for the stability test, eventually degrade within the same time interval for both media.

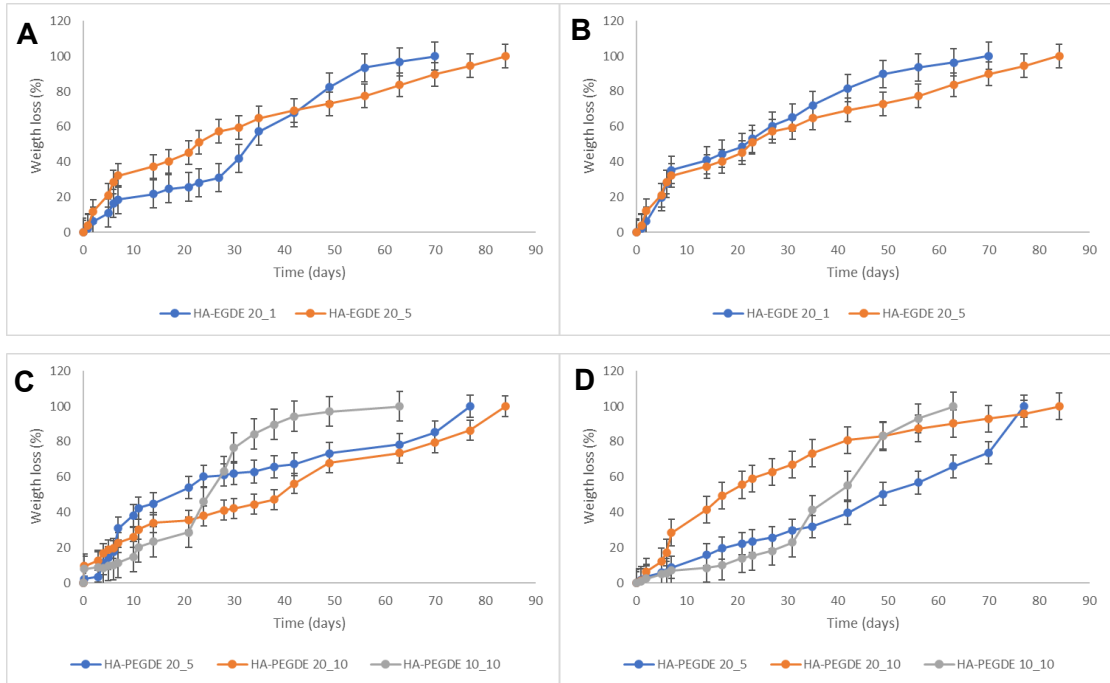


Figure 19 - Stability studies, determined by weight loss (%) of prepared hydrogels. (A) swelled and lyophilized HA-EGDE in water, 37°C; (B) swelled and lyophilized HA-EGDE in PBS (pH=7.4), 37°C; (C) swelled and lyophilized HA-PEGDE in water, 37°C; and (D) swelled and lyophilized HA-PEGDE in PBS (pH=7.4), 37°C.

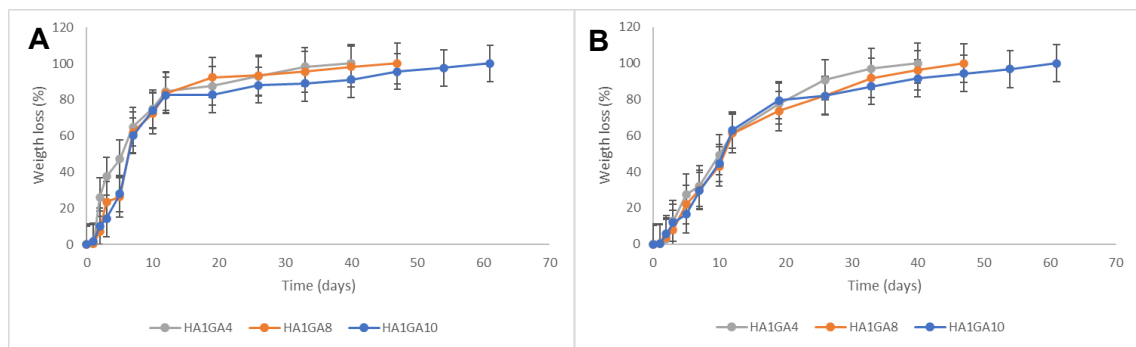


Figure 20 - Stability studies, determined by weight loss (%) of prepared hydrogels. (A) swelled and lyophilized HAGA in water, 37°C and (B) swelled and lyophilized HAGA in PBS (pH=7.4), 37°C.

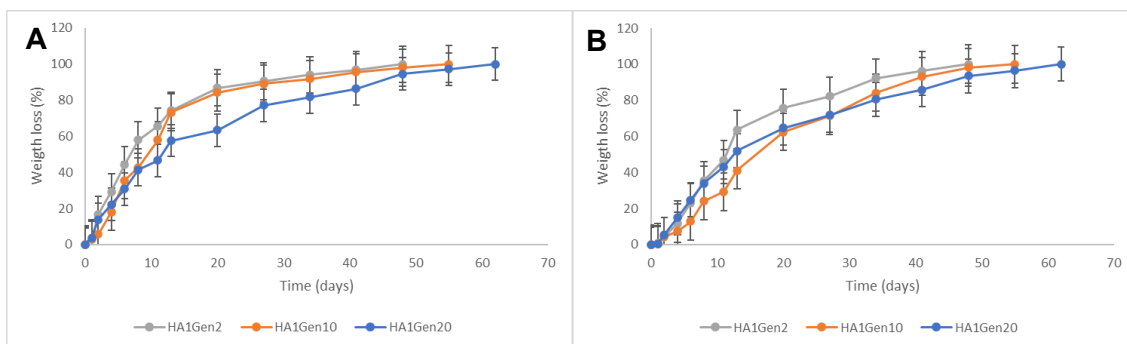


Figure 21 - Stability studies, determined by weight loss (%) of prepared hydrogels. (A) swelled and lyophilized HA-Gen in water, 37°C and (B) swelled and lyophilized HA-Gen in PBS (pH=7.4), 37°C.

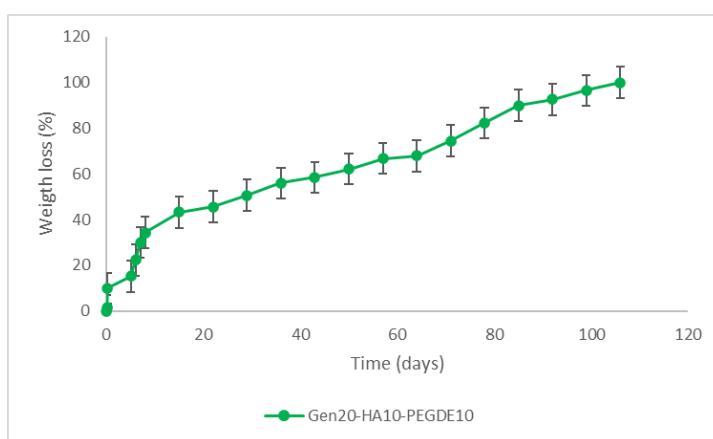


Figure 22 - Stability studies, determined by weight loss (%) of Gen20-HA10-PEGDE10 hydrogel.

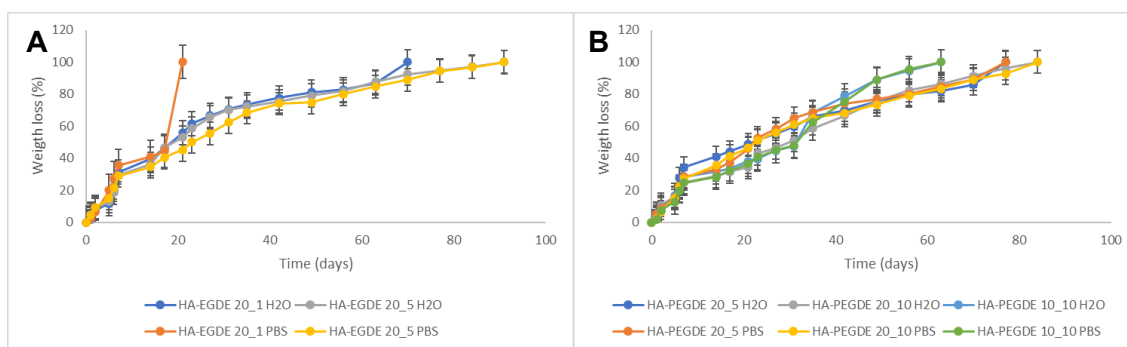


Figure 23 - Stability studies, determined by weight loss (%) in water and PBS at 37°C, of prepared hydrogels previously swelled and then lyophilized. (A) HA-EDGE and (B) HA-PEGDE.

### 3.2.2. *In vitro* degradation studies

To evaluate whether the HA-based hydrogels are biodegradable, the sensitivity of the gels to hyaluronidase (HAase) was determined. HAase is an endohexosaminidase that randomly cleaves HA into smaller polysaccharide fragments. For these studies, the glucuronic acid at the nonreducing end of the fragments that resulted from the enzymatic digestion was quantified by the carbazole assay, according to Burdick *et al*<sup>180</sup>.

According to the *in vitro* degradation tests (Figure 24), in a general way, the HA-based hydrogels in study present a good resistance against HAase degradation. As expected, the higher the degree of crosslinking, the more resistant the hydrogel becomes against HAase degradation, as can be seen for Gen20-HA10-PEGDE10 hydrogel, which was the hydrogel that showed the most resistance to degradation (864h/36 days), for HA-PEGDE, that HA-PEGDE 20\_10 (672h/28 days) resists the degradation longer than HA-PEGDE 20\_5 (576h/24 days) and HA-PEGDE 10\_10 (384h/16 days), for HA-EGDE hydrogels, that HA-EGDE 20\_1 (480h/20 days) hydrogel degraded more rapidly than HA-EGDE 20\_5 (720h/30 days), for HA-Gen hydrogels, that HA1Gen20 (624h/26 days) resists to degradation longer than HA1Gen10 (480h/20 days) and HA1Gen2 (240h/10 days) and HAGA hydrogels, that HA1GA10 (336h/14 days) are less susceptible to degradation than HA1GA8 (288h/12 days) and HA1GA4 (192h/8 days).

Expectedly, a double crosslinked hydrogel as the Gen20-HA10-PEGDE10 demonstrated to be more resistant to enzymatic degradation than the other HA-based hydrogels because a denser network makes it more difficult for HAase to access and cleave HA chains because the chemical modification to the HA chains can alter the recognition and cleavage sites for HAase, resulting in a more resilient hydrogel <sup>178</sup>.

It can be concluded that the time for complete enzymatic degradation of the hydrogels in the presence of HAase depended on the equivalents of crosslinker, with the highest degree of crosslinking producing the most stable hydrogels <sup>181</sup>.

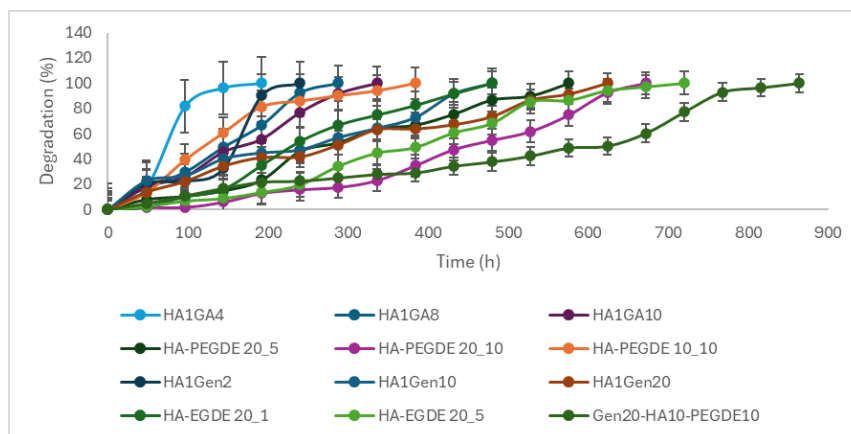


Figure 24 - Hyaluronidase digestion of HA-based hydrogels. Gels were incubated with 100U/mL of HAase for the indicated time and the degradation of the gels was determined by the quantification of the released glucuronic acid residues into the supernatant using the carbazole method.

Importantly, a linear relationship was seen when comparing the concentration of HA with the concentration of uronic acid (or glucuronic acid) over time (Figure 25), because the longer the gels are incubated with HAase, the more HA will be degraded

and the concentration of HA available for the carbazole assay will be higher, so more uronic acid will be quantified during this assay.

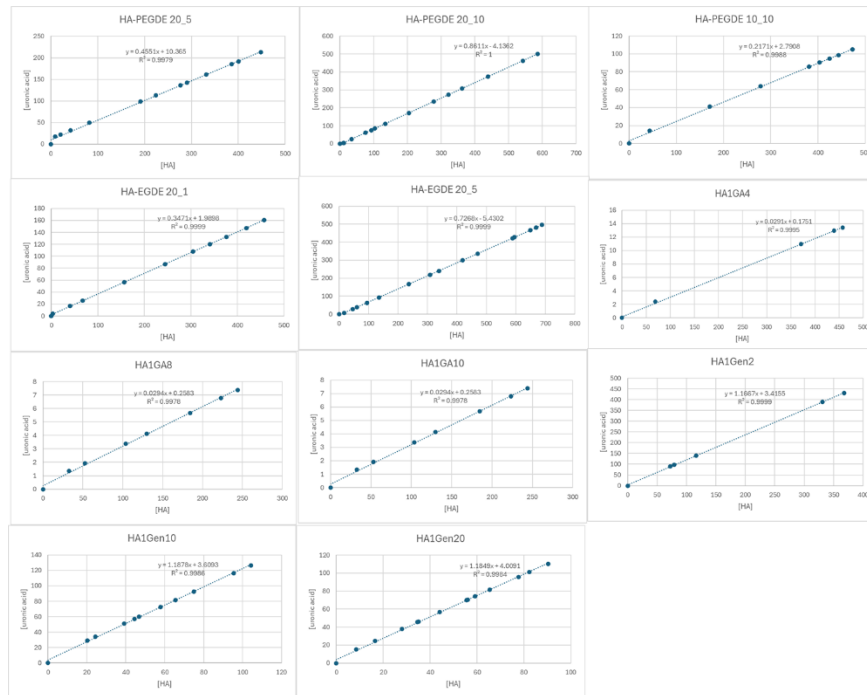


Figure 25 - Uronic acid vs HA in vitro degradation studies.

### 3.3. *In vitro* Cytotoxicity Evaluation

In these experiments, the potential cytotoxicity caused by the HA-based hydrogels was indirectly assessed using the resazurin reduction assay which measures the metabolic activity of the cells. For the direct contact method, HA-based hydrogels were prepared and added to culture wells containing NIH 3T3 cells previously seeded for 24h. Initially, it was attempted to culture the NIH 3T3 cells in the hydrogel's surface, but the resazurin reduction assay (Figure A8) showed very incongruent results. On one hand, the HA-PEGDE and HA-EGDE hydrogels had a high cytotoxic impact on the cell's viability, and on the other hand, the Gen20-HA10-PEGDE10 hydrogel showed a very high positive impact on the cell's metabolic activity, having a metabolic activity of  $244 \pm 13\%$ . As shown in Figure 26, the increase of PEGDE in the HA-PEGDE hydrogels resulted in an improvement of cell metabolic activity, as can be seen when comparing the hydrogels with the same HA concentration (HA-PEGDE 20\_5 and HA-PEGDE 20\_10 hydrogels) (Figure 27, b and c). In addition, it can be seen that the introduction of Gen in the HA-based hydrogels led to an increase in the metabolic activity, as shown by the experiments with the Gen20-HA10-PEGDE10 hydrogel (Figure 27, g) <sup>166</sup>. In all cases, the metabolic

activity of cells exposed to HA hydrogels was significantly lower than the control values (cells cultured only with cell culture medium).

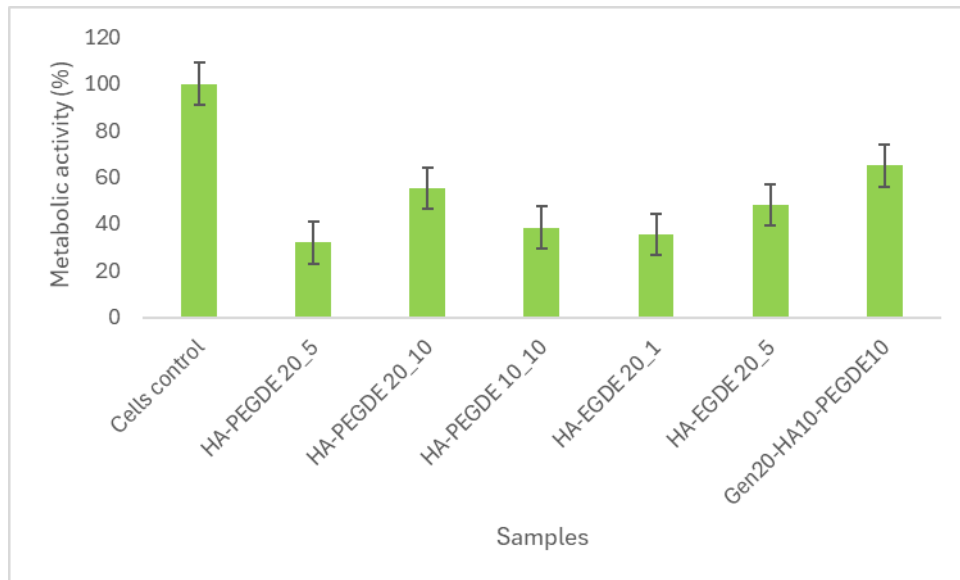
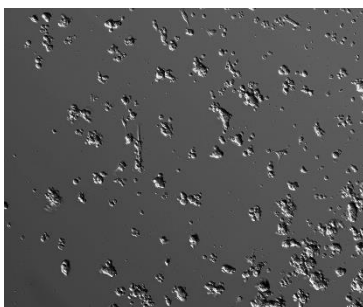


Figure 26 - Metabolic activity of embryo mouse fibroblasts (NIH 3T3) in direct contact with HA-PEGDE, HA-EGDE, and Gen-HA-PEGDE hydrogels as measured by the resazurin reduction assay.

According to Figure 27, and the results obtained through the mentioned resazurin reduction assay, the metabolic activity was relatively low due to the direct contact of the hydrogel to the cells, with fewer cells adhering to the plate, and no evidence of cell adhesion to the hydrogels, perhaps due to the absence of cell adhesion-specific ligands in the hydrogels<sup>182,183</sup>. As such, another approach to access the hydrogels' *in vitro* cytotoxicity was considered which consisted of exposing the cells directly to hydrogel's extracts.

a) Cells control



b) HA-PEGDE 20\_5

c) HA-PEGDE 20\_10

d) HA-PEGDE 10\_10

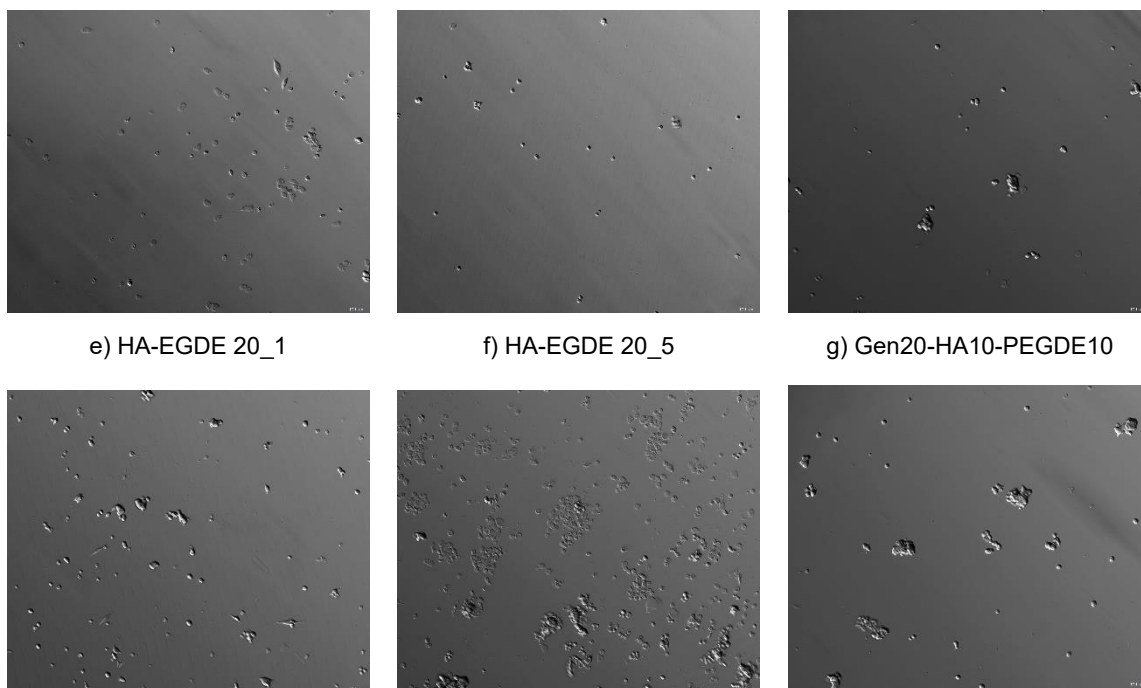


Figure 27 - Optical microscopy images of cells control (a) and cells exposed directly with the HA-based hydrogels ((b-d) HA-PEGDE; (e-f) HA-EGDE and (g) Gen-HA-PEGDE hydrogels).

So, the metabolic activity of cells exposed to extracts of the hydrogels was analyzed. For this purpose, hydrogels were incubated for 24h in a solution of sterile PBS with 1% AA, and then incubated with complete medium for another 24h; the solution constituted by the products released from the hydrogels to the complete medium (i.e. the extract) was then incubated with the NIH3T3 cells. In this case, as shown in Figure 28, the metabolic activity of cells was always above 80% of the control value. These experiments reveal that the apparent toxicity previously observed when the cells were cultured in direct contact with the hydrogels cannot be attributed to the products of degradation of these hydrogels <sup>166</sup>.

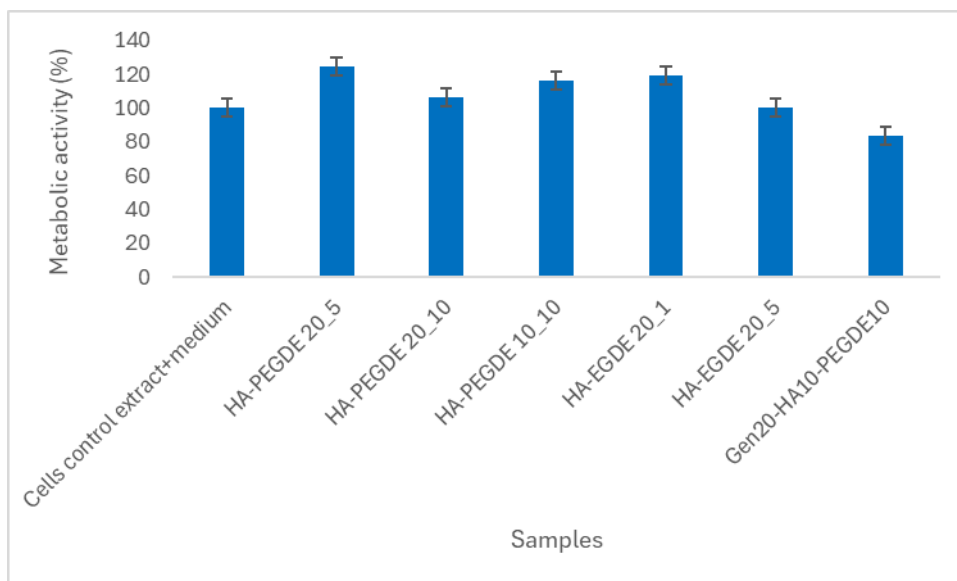


Figure 28 - Metabolic activity of embryo mouse fibroblasts (NIH 3T3) in the presence of HA-PEGDE, HA-EGDE, and Gen-HA-PEGDE hydrogel extracts as measured by the resazurin reduction assay.

Figure 29 shows the metabolic activity of cells in direct contact with HA-Gen and HAGA hydrogels. As can be seen and as expected, the HAGA hydrogels led to very low values of metabolic activity because the HAGA hydrogel is a hydrogel crosslinked by GA, known for its impact on viability <sup>167</sup>. The HA-Gen hydrogels showed low metabolic activity values too, which was not expected because Gen is a molecule that has been used recently in several studies to improve hydrogel's biocompatibility <sup>184</sup>.

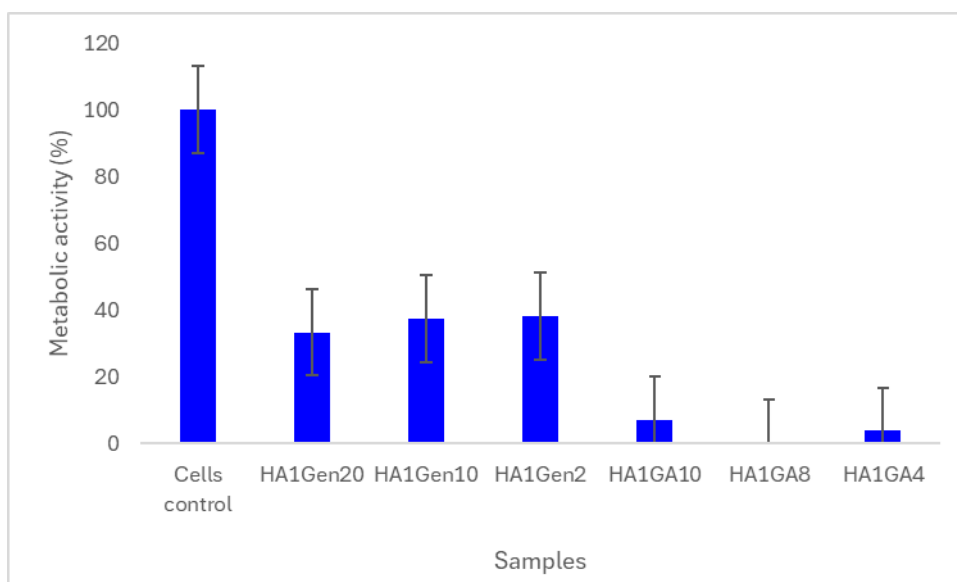


Figure 29 - Metabolic activity of embryo mouse fibroblasts (NIH 3T3) in direct contact with HA-Gen and HAGA hydrogels as measured by the resazurin reduction assay.

To evaluate the effect of Gen on cell metabolic activity, NIH 3T3 cells were incubated with Gen solutions at increasing concentrations (0.1 – 20mM). As shown in Figure 30, it can be noticed that the Gen solutions have an important impact on the cell's

metabolic activity in the range of concentrations studied. These results clearly show that, for these conditions, Gen is a cytotoxic molecule<sup>184</sup>. In fact, a study by Wang *et al.*<sup>185</sup> recommended keeping the dosage of Gen below 0.5 mM in most tissue engineering practices.

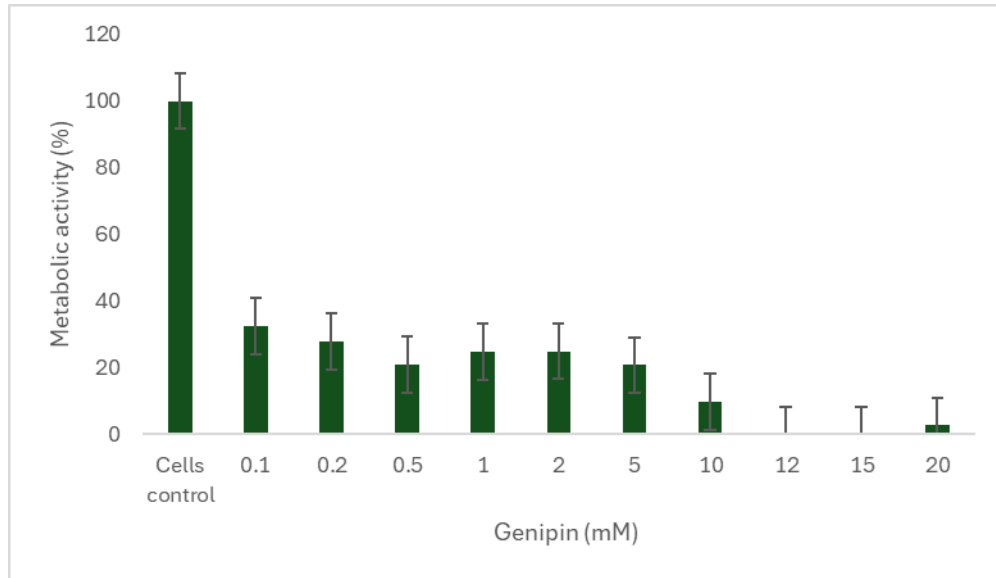


Figure 30 - Metabolic activity of embryo mouse fibroblasts (NIH 3T3) in the presence of Gen solutions of different concentrations (0.1 – 20mM) as measured by the resazurin reduction assay.

A different approach to evaluate hydrogel cytotoxicity was further tested that consisted of the use of transwell inserts. For this purpose, hydrogels (HA1Gen2) were placed in a transwell insert to be applied on top of the cell monolayer, avoiding direct contact between the hydrogels and the cells. As can be seen in Figure 31, there is a difference between the results of the transwell insert method, direct contact, and the use of extracts.

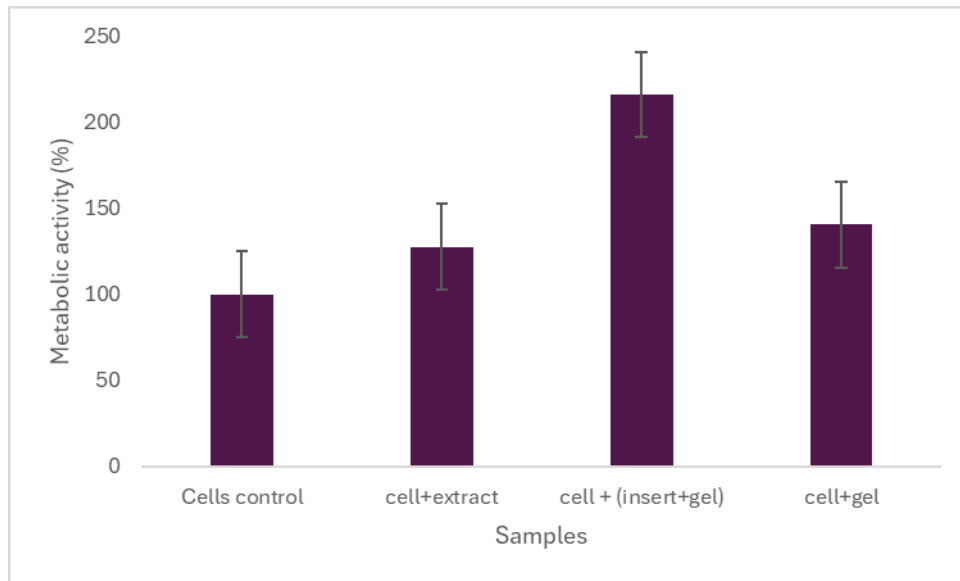


Figure 31 - Metabolic activity of embryo mouse fibroblasts (NIH 3T3) in the presence of HA1Gen2 hydrogel in transwell inserts as measured by the resazurin reduction assay.

These results showed that the method that conducted the highest metabolic activity values was the transwell insert method. Nevertheless, this method only proceeded with one hydrogel type (HA1Gen2), because the inserts are non-reusable and very expensive, not justifying its use for preliminary tests, such as the one described in this thesis and, in addition, this method is very difficult to execute, due to the difficult in maneuver the hydrogels inside the insert. In fact, more studies will be necessary in the future to allow for more explicit conclusions about hydrogel's cytocompatibility.

## 4. CONCLUSIONS AND FUTURE PERSPECTIVES

HA is a biomaterial that has been widely used in the synthesis of hydrogels and, despite still presenting several intrinsic defects, such as being susceptible to degradation by HAase, has received considerable attention due to its unique physiological properties and functions, which have made it stand out, especially in the biomedicine domain. In recent years, HA-based hydrogels have been applied even more in the biomedical field, especially in drug delivery, wound healing, cosmetics, and tissue engineering, and are being recognized as promising materials in the biomedical area.

The susceptibility to degradation by HAase represents the major limitation when using HA-based hydrogels. Therefore, to prepare HA-based hydrogels with improved stability and prolonged degradation profile, several crosslinking strategies have been used. From these, the use of PEG and genipin as crosslinking agents can be highlighted, giving rise to promising soft materials.

In this thesis, different HA-based hydrogels were prepared, physiochemically characterized and *in vitro* biologically assayed. The idea was to develop a possible new crosslinking strategy to obtain HA hydrogels with high efficiency, low toxicity, and enhanced mechanical properties. Indeed, HA hydrogels like the one dually crosslinked with PEGDE and Gen described in this thesis have never been reported in the literature.

The functionalization of HA with the amino acid Lys was accomplished in order to attain HA hydrogels crosslinked with GA and Gen, as they only react with compounds with primary amines. The synthesis proved to be successful by the presence of the amide group, which indicates the bond between HA and Lys detected in the  $^1\text{H}$  NMR spectrum.

The preparation of the different HA-based hydrogels, including the dual-crosslinked hydrogel - the Gen20-HA10-PEGDE10 - was successful. All HA-based hydrogels exhibited great swelling capacity and good stability in both water and PBS over time, with Gen20-HA10-PEGDE10 hydrogel standing out for demonstrating to be a highly swellable hydrogel and having a high stability over time (106 days).

The swelling behavior of the hydrogels was influenced by the formulation composition, degree of crosslinking, crosslinker length, and swelling media, with lower concentrations of crosslinker resulting in less crosslinked hydrogels that, independently of the crosslinker used, led to greater swelling (swelling was higher in water compared to PBS).

*In vitro* stability studies showed that hydrogel's stability increases with the crosslinking density. In a general way, HA-based hydrogels, independently of the

medium used for the stability test, always degrade within the same time interval. The Gen20-HA10-PEGDE10 hydrogel showed a slower weight loss rate than the HA-PEGDE and HA-Gen hydrogels, due to sufficient crosslinking because as this hydrogel is dual-crosslinked, it involves two different types of crosslinking mechanisms, leading to an increase of the crosslinking density within the hydrogel.

To assess the morphology and topography of the hydrogels, SEM was used. The results reported showed that the HA-based hydrogels have very rough surfaces, with many pores, which makes them a promising material to be used in the biomedicine domain, particularly in tissue engineering. In fact, porosity is a property that has a significant impact on cell adhesion and proliferation, as well as on the permeation of nutrients and oxygen.

Importantly, the degradation studies of HA-based hydrogels by HAase demonstrated that the time for complete enzymatic degradation is dependent on the equivalents of crosslinker used in the process, with the highest degree of crosslinking producing the most stable hydrogels.

Finally, the cytotoxicity impact of HA-based hydrogels on NIH 3T3 cells was evaluated using the resazurin assay, revealing a significant cytotoxic effect. The results indicated low cell metabolic activity and no evidence of cell adhesion to the hydrogels. Contrary to what is reported in the literature, HA-PEGDE and HA-EGDE hydrogels exhibited a high cytotoxic impact on cell viability. Surprisingly, HA-Gen hydrogels also showed significant cytotoxicity, despite Gen's recent use in enhancing hydrogel biocompatibility<sup>186</sup>. Although the Gen20-HA10-PEGDE10 hydrogel demonstrated high stability and improved properties, its significant cytotoxic impact makes it unsuitable for biomedical applications.

In the near future, further studies are needed with the HA-based hydrogels, particularly with the Gen20-HA10-PEGDE10 hydrogel, which was the main focus of this work, to obtain more definitive conclusions about their cytocompatibility. It is important to note that this work was a preliminary study, and that deeper and different approaches are required to advance the application of these hydrogels. To complement this preliminary work, several studies could be conducted. For instance, analyzing the mechanical properties of HA-based hydrogels using AFM would aid in designing and optimizing these materials for biomedical applications, ensuring their safety, efficacy, and long-term performance. Additionally, rheological studies are essential to confirm their mechanical reliability and improve interactions with biological systems. These studies also provide valuable insights into the material's mechanical and viscoelastic properties,

which directly impact its performance in biomedical applications. A deeper understanding of HA viscosity would further enhance hydrogel formulation conditions, optimizing the overall development process.

Also, by optimizing hydrogel formulation conditions through rheological studies, it is possible to enhance the interaction between HA and the CD44 receptor, which promotes cell adhesion to the hydrogel, facilitating 3D cell culture. Excessive crosslinking density can hinder this interaction and lead to poor cell adhesion. With an optimized hydrogel formation process, it would be feasible to simultaneously carry out 3D cell culture during the hydrogel fabrication.

Besides the resazurin reduction assay, other methods such as the MTT assay, Live/Dead assay, and LDH assay could be employed to assess cell viability, offering alternative approaches to evaluate the cytocompatibility of HA-based hydrogels with NIH 3T3 cells, beyond just measuring metabolic activity. Additionally, a different cell type, like hMSCs, could be used. Chemically modifying HA hydrogels can influence hMSCs differentiation into specific lineages, such as osteogenic cells, which are useful for bone regeneration procedures.

Lastly, one possible alternative is to explore the hemocompatibility of HA-based hydrogels to assess their potential in tissue engineering applications and even study any possible antimicrobial properties.

## 5. BIBLIOGRAPHY

1. Bashir S., Hina M., Iqbal J., Rajpar A., Fundamental concepts of hydrogels: synthesis, properties, and their applications, *Polymers*, 12 (11), **2020**, 2702-2713, <https://doi.org/10.3390/polym12112702>
2. Daly A., Riley L., Segura T., Burdick J., Hydrogel microparticles for biomedical applications, *Nature Reviews Materials*, 5 (7), **2020**, 20-43, <https://doi.org/10.1038/s41578-019-0148-6>
3. Hu W., Wang Z., Xiao Y., Zhang S., Wang J., Advances in crosslinking strategies of biomedical hydrogels, *Biomaterials Science*, 7 (3), **2019**, 843-855, <https://doi.org/10.1039/C8BM01246F>
4. Maitra J., Shukla V., Cross-linking in Hydrogels - A Review, *American Journal of Polymer Science*, 4 (2), **2014**, 25-31, DOI: 10.5923/j.ajps.20140402.01
5. Sharma S., Tiwari S., A review on biomacromolecular hydrogel classification and its applications, *International Journal of Biological Macromolecules*, 162 (1), **2020**, 737-747, <https://doi.org/10.1016/j.ijbiomac.2020.06.110>
6. Varaprasad K., Raghavendra G., Jayaramudu T., Yallapu M., Sadiku R., A mini review on hydrogels classification and recent developments in miscellaneous applications, *Materials Science and Engineering*, 79 (1), **2017**, 958-971, <https://doi.org/10.1016/j.msec.2017.05.096>
7. Basu A., Kunduru K., Doppalapudi S., Domb A., Khan W., Poly (lactic acid) based hydrogels, *Advanced Drug Delivery Reviews*, 107 (15), **2016**, 192-205, <https://doi.org/10.1016/j.addr.2016.07.004>
8. Madduma-Bandarage U., Madihally S., Synthetic hydrogels: synthesis, novel trends, and applications, *Journal of Applied Polymer Science*, 10 (2), **2021**, 190-214, <https://doi.org/10.1002/app.50376>
9. Jian X., Feng X., Luo Y., Li F., Tan J., Development, preparation, and biomedical applications of DNA-based hydrogels, *Frontiers in Bioengineering and Biotechnology*, 9 (2), **2021**, 661-679, <https://doi.org/10.3389/fbioe.2021.661409>
10. Gul K., Gan R., Sun C., Jiao G., Fang Y., Recent advances in the structure, synthesis, and applications of natural polymeric hydrogels, *Food Science & Nutrition*, 62 (14), **2022**, 3817-3832, <https://doi.org/10.1080/10408398.2020.1870034>
11. Feng X., Luo Y., Li F., Jian X., Liu Y., Development of natural-drugs-based low-molecular weight supramolecular gels, *Gels*, 7 (3), **2021**, 105-117, <https://doi.org/10.3390/gels7030105>
12. Yang Z., Peng H., Wang W., Liu T., Crystallization behavior of poly( $\epsilon$ -caprolactone)/layered double hydroxide nanocomposites, *Journal of Applied Polymer Science*, 10 (2), **2010**, 2658-2667, <https://doi.org/10.1002/APP.31787>
13. Yang L., Chu J., Fix J., Colon-specific drug delivery: New approaches and in vitro/in vivo evaluation, *International Journal of Pharmaceutics*, 1 (2), **2002**, 1-15, [https://doi.org/10.1016/S0378-5173\(02\)00004-2](https://doi.org/10.1016/S0378-5173(02)00004-2)
14. Villalba-Rodríguez A., Martínez-González S., Sosa-Hernández J., Parra-Saldívar R., Bilal M., Nanoclay/polymer-based hydrogels and enzyme-loaded nanostructures for wound healing applications, *Gels*, 7 (2), **2021**, 1-13, <https://doi.org/10.3390/gels7020059>
15. Maolin Z., Jun L., Min Y., Hongfei H., The swelling behavior of radiation prepared semi-interpenetrating polymer networks composed of polyNIPAAm and hydrophilic polymers,

*Radiation Physics and Chemistry*, 58 (4), **2000**, 397-400, [https://doi.org/10.1016/S0969-806X\(99\)00491-0](https://doi.org/10.1016/S0969-806X(99)00491-0)

16. Ghasemiyeh P., Mohammadi-Samani S., Hydrogels as Drug Delivery Systems; Pros and Cons, *Trends in Pharmaceutical Science*, 30 (76), **2019**, 7-24, <https://doi.org/10.30476/TIPS.2019.81604.1002>
17. Rebers L., Reichsöllner R., Regett S., Tovar G., Borchers K., Differentiation of physical and chemical cross-linking in gelatin methacryloyl hydrogels, *Scientific Reports*, 11 (1), **2021**, 1-12, <https://doi.org/10.1038/s41598-021-82393-z>
18. Wang Z., Chen J., Lu B., Tang L., Chen X., A bioinspired hydrogen bond crosslink strategy toward toughening ultrastrong and multifunctional nanocomposite hydrogels, *Journal of Materials Chemistry*, 20 (18), **2020**, 4002-4015, <https://doi.org/10.1039/d0tb00424c>
19. Jiang H., Duan L., Ren X., Gao G., Hydrophobic association hydrogels with excellent mechanical and self-healing properties, *European Polymer Journal*, 112 (19), **2019**, 660-669, <https://doi.org/10.1016/j.eurpolymj.2018.10.031>
20. Tasnim T., Adkins M., Lim T., Feng H., Zhang H., Thermally tunable hydrogel crosslinking mediated by temperature sensitive liposome, *Biomedical Materials*, 16 (6), **2021**, 680-692, <https://doi.org/10.1088/1748-605X/ac246c>
21. Yang J., Chen Y., Zhao L., Zhang J., Luo H., Constructions and Properties of Physically Crosslinked Hydrogels Based on Natural Polymers, *Polymer Reviews*, 63 (3), **2022**, 1-39, <https://doi.org/10.1080/15583724.2022.2137525>
22. Akhtar M., Hanif M., Ranjha N., Methods of synthesis of hydrogels ... A review, *Saudi Pharmaceutical Journal*, 24 (5), **2016**, 554-559, <https://doi.org/10.1016/j.jsps.2015.03.022>
23. Singh B., Kumar A., Hydrogel formation by radiation induced crosslinked copolymerization of acrylamide onto moringa gum for use in drug delivery applications, *Carbohydrate Polymers*, 200 (15), **2018**, 262-270, <https://doi.org/10.1016/j.carbpol.2018.08.018>
24. Xu J., Liu X., Ren X., Gao G., The role of chemical and physical crosslinking in different deformation stages of hybrid hydrogels, *European Polymer Journal*, 100 (18), **2018**, 86-95, <https://doi.org/10.1016/j.eurpolymj.2018.01.020>
25. Abdelkader A., White J., Water Absorption in Epoxy Resins: The Effects of the Crosslinking Agent and Curing Temperature, *Journal of Applied Polymer Science*, 29 (20), **2005**, 2544-2549, <https://doi.org/10.1002/app.22400>
26. Hua S., Ma H., Li X., Yang H., Wang A., pH-sensitive sodium alginate/poly(vinyl alcohol) hydrogel beads prepared by combined Ca<sup>2+</sup> crosslinking and freeze-thawing cycles for controlled release of diclofenac sodium, *International Journal of Biological Macromolecules*, 46 (5), **2010**, 517-523, <https://doi.org/10.1016/j.ijbiomac.2010.03.004>
27. Qin X., Lu A., Zhang L., Gelation behavior of cellulose in NaOH/urea aqueous system via cross-linking, *Springer Science*, 20 (7), **2013**, 1669-1677, <https://doi.org/10.1007/s10570-013-9961-z>
28. Li Z., Guan J., Thermosensitive hydrogels for drug delivery, *Expert Opinion on Drug Delivery*, 20 (13), **2011**, 991-1007, <https://doi.org/10.1517/17425247.2011.581656>
29. Ekenseair A., Boere K., Tzouanas S., Vo T., Mikos A., Structure-Property Evaluation of Thermally and Chemically Gelling Injectable Hydrogels for Tissue Engineering, *Biomacromolecules*, 13 (9), **2012**, 2821-2830, <https://doi.org/10.1021/bm300797m>

30. Liu C., Li M., Liu Z., Shi Z., Wang X., Chitosan thermogelation and cascade mineralization via sequential CaCO<sub>3</sub> incorporations for wound care, *International Journal of Biological Macromolecules*, 266 (2), **2024**, 1-11, <https://doi.org/10.1016/j.ijbiomac.2024.131076>
31. Abdelgawad A., Hudson S., Chitosan nanoparticles: Polyphosphates cross-linking and protein delivery properties, *International Journal of Biological Macromolecules*, 62 (6), **2019**, 133-142, <https://doi.org/10.1016/j.ijbiomac.2019.06.062>
32. Mi F., Shyu S., Wong T., Jang S., Lee S., Chitosan–Polyelectrolyte Complexation for the Preparation of Gel Beads and Controlled Release of Anticancer Drug. II. Effect of pH-Dependent Ionic Crosslinking or Interpolymer Complex Using Tripolyphosphate or Polyphosphate as Reagent, *Journal of Applied Polymer Science*, 74 (5), **1999**, 1093-1107, [https://doi.org/10.1002/\(SICI\)1097-4628\(19991031\)74:5%3C1093::AID-APP6%3E3.0.CO;2-C](https://doi.org/10.1002/(SICI)1097-4628(19991031)74:5%3C1093::AID-APP6%3E3.0.CO;2-C)
33. Berger J., Reist M., Mayer J., Felt O., Gurny R., Structure and interactions in chitosan hydrogels formed by complexation or aggregation for biomedical applications, *European Journal of Pharmaceutics and Biopharmaceutics*, 57 (1), **2003**, 35-52, [https://doi.org/10.1016/S0939-6411\(03\)00160-7](https://doi.org/10.1016/S0939-6411(03)00160-7)
34. Nasution H., Harahap H., Dalimunthe N., Ginting M., Jaafar M., Hydrogel and Effects of Crosslinking Agent on Cellulose-Based Hydrogels: A Review, *Gels*, 8 (9), **2022**, 425-432, <https://doi.org/10.3390/gels8090568>
35. Han C., Zhang H., Wu Y., He X., Chen X., Dual-crosslinked hyaluronan hydrogels with rapid gelation and high injectability for stem cell protection, *Scientific Reports*, 10 (1), **2020**, 1-7, <https://doi.org/10.1038/s41598-020-71462-4>
36. Moody C., Palvai S., Brudno Y., Click cross-linking improves retention and targeting of refillable alginate depots, *Acta Biomaterialia*, **2020**, 10 (16), 112-121, <https://doi.org/10.1016/j.actbio.2020.05.033>
37. Lofty V., Basta A., Optimizing the chitosan-cellulose based drug delivery system for controlling the ciprofloxacin release versus organic/inorganic crosslinker, characterization and kinetic study, *International Journal of Biological Macromolecules*, 165 (15), **2020**, 1496-1506, <https://doi.org/10.1016/j.ijbiomac.2020.10.047>
38. Cintas P., Barge A., Tagliapietra S., Boffa L., Cravotto G., Alkyne–azide click reaction catalyzed by metallic copper under ultrasound, *Nature Protocols*, 5 (3), **2010**, 607-616, <https://doi.org/10.1038/nprot.2010.1>
39. Wang Q., Shi Y., Li Q., Wu C., Toughening, recyclable and healable nitrile rubber based on multi-coordination crosslink networks after “tetrazine click” reaction, *European Polymer Journal*, 150 (5), **2021**, 1-13, <https://doi.org/10.1016/j.eurpolymj.2021.110415>
40. Gregoritz M., Brandl F., The Diels–Alder reaction: A powerful tool for the design of drug delivery systems and biomaterials, *European Journal of Pharmaceutics and Biopharmaceutics*, 97 (15), **2015**, 438-453, <https://dx.doi.org/10.1016/j.ejpb.2015.06.007>
41. Lee Y., Kurra Y., Liu W., Phospha-Michael Addition as a New Click Reaction for Protein Functionalization, *ChemBioChem*, 12 (16), **2016**, 456-461, <https://doi.org/10.1002/cbic.201500697>
42. Ahmed E., Hydrogel: Preparation, characterization, and applications: A review, *Journal of Advanced Research*, 6 (2), **2015**, 105-121, <https://doi.org/10.1016/j.jare.2013.07.006>
43. Oyen M., Mechanical characterisation of hydrogel materials, *International Materials Reviews*, 54 (1), **2014**, 44-59, <https://doi.org/10.1179/1743280413Y.0000000022>

44. Lin P., Ma S., Wang X., Zhou F., Molecularly Engineered Dual-Crosslinked Hydrogel with Ultrahigh Mechanical Strength, Toughness, and Good Self-Recovery, *Advanced Materials*, 27 (11), **2015**, 2054-2059, <https://doi.org/10.1002/adma.201405022>
45. Kaczmarek B., Nadolna K., Owczarek A., The physical and chemical properties of hydrogels based on natural polymers, *Elsevier*, 25 (9), **2019**, 220-232, <https://doi.org/10.1016/B978-0-12-816421-1.00006-9>
46. Khademhosseini A., Langer R., Borenstein J., Vacanti J., Microscale technologies for tissue engineering and biology, *Proceedings of the National Academy of Sciences*, 103 (8), **2006**, 2480-2487, <https://doi.org/10.1073/pnas.0507681102>
47. Ernest Z., "What type of acid is in synovial fluid?", **2016**, <https://socratic.org/questions/what-type-of-acid-is-in-synovial-fluid> (accessed November 21, 2023)
48. Garantziotis S., Savani R., Hyaluronan biology: a complex balancing act of structure, function, location, and context, *Matrix Biology*, 79 (1), **2019**, 1-10, <https://doi.org/10.1016/j.matbio.2019.02.002>
49. Dovedytis M., Liu Z., Bartlett S., Hyaluronic acid and its biomedical applications: A review, *Engineered Regeneration*, 1 (2), **2020**, 102-113, <https://doi.org/10.1016/j.engreg.2020.10.001>
50. Chistyakov D., Astakhova A., Azbukina N., Goriainov S., Chistyakov V., High and low molecular weight hyaluronic acid differentially influences oxylipins synthesis in course of neuroinflammation, *International Journal of Molecular Sciences*, 20 (16), **2019**, 490-512, <https://doi.org/10.3390/ijms20163894>
51. Dicker K., Gurski L., Pradhan-Bhatt S., Witt R., Farach-Carson M., Hyaluronan: a simple polysaccharide with diverse biological functions, *Acta Biomaterialia*, 10 (4), **2014**, 1558-1570, <https://doi.org/10.1016/j.actbio.2013.12.019>
52. Valachov'a K., Volpi N., Stem R., Soltes L., Hyaluronan in medical practice, *Current Medicinal Chemistry*, **2016**, 23 (31), 3607-3617, <https://doi.org/10.2174/0929867323666160824162133>
53. Nakka K., Hachmer S., Mokhtari Z., Kovac R., Bandukwala H., JMJD3 activated hyaluronan synthesis drives muscle regeneration in an inflammatory environment, *Science*, 377 (5), **2022**, 666-669, <https://doi.org/10.1126/science.abm9735>
54. Passi A., Vigetti D., Hyaluronan as tunable drug delivery system, *Advanced Drug Delivery Reviews*, 146 (14), **2019**, 83-96, <https://doi.org/10.1016/j.addr.2019.08.006>
55. Toole B., Hyaluronan-CD44 interactions in cancer: paradoxes and possibilities, *Clinical Cancer Research*, 15 (24), **2009**, 7462-7468, <https://doi.org/10.1158/1078-0432.CCR-09-0479>
56. Dosio F., Arpicco S., Stella B., Fattal E., Hyaluronic acid for anticancer drug and nucleic acid delivery, *Advanced Drug Delivery Reviews*, 97 (1), **2016**, 204-236, <https://doi.org/10.1016/j.addr.2015.11.011>
57. Raia N., Jia D., Ghezzi C., Muthukumar M., Kaplan D., Characterization of silk-hyaluronic acid composite hydrogels towards vitreous humor substitutes, *Biomaterials*, 10 (16), **2020**, 119-129, <https://doi.org/10.1016/j.biomaterials.2019.119729>
58. Chae J., Jung J., Zhu W., Gerberich B., Bahrani Fard M., Drug-free, nonsurgical reduction of intraocular pressure for four months after suprachoroidal injection of hyaluronic acid hydrogel, *Advanced Science*, 8 (2), **2021**, 200-208, <https://doi.org/10.1002/advs.202001908>

59. Li Z., Liu L., Chen Y., Dual dynamically crosslinked thermosensitive hydrogel with self-fixing as a postoperative anti-adhesion barrier, *Acta Biomaterialia*, 110 (1), **2020**, 119-128, <https://doi.org/10.1016/j.actbio.2020.04.034>
60. Cai Z., Tang Y., Wei Y., Wang P., Zhang H., Physically cross-linked hyaluronan-based ultrasoft cryogel prepared by freeze–thaw technique as a barrier for prevention of postoperative adhesions, *Biomacromolecules*, 22 (12), **2021**, 4967-4979, <https://doi.org/10.1021/acs.biomac.1c00878>
61. Galarraga J., Locke R., Witherel C., Stoecki B., Castilho M., Fabrication of MSC-laden composites of hyaluronic acid hydrogels reinforced with MEW scaffolds for cartilage repair, *Biofabrication*, 14 (1), **2021**, 1758-1772, <https://doi.org/10.1088/1758-5090/ac3acb>
62. Jin Y., Koh R., Kim S., Park G., Hwang N., Injectable anti-inflammatory hyaluronic acid hydrogel for osteoarthritic cartilage repair, *Materials Science and Engineering*, 115 (11), **2020**, 1110-1126, <https://doi.org/10.1016/j.msec.2020.111096>
63. Kim M., Park J., Nguyen D., Kim S., Jeong D., Hyaluronidase inhibitor-incorporated cross-linked hyaluronic acid hydrogels for subcutaneous injection, *Pharmaceutics*, 13 (2), **2021**, 1-16, <https://doi.org/10.3390/pharmaceutics13020170>
64. Momose T., Amadio P., Sun Y., Zhao C., Kai-Nan A., Surface modification of extrasynovial tendon by chemically modified hyaluronic acid coating, *Journal of Biomedical Materials Research*, 59 (2), **2001**, 219-224, <https://doi.org/10.1002/jbm.1235>
65. Trombino S., Servidio C., Curcio F., Cassano R., Strategies for hyaluronic acid-based hydrogel design in drug delivery, *Pharmaceutics*, 11 (8), **2019**, 1-17, <https://doi.org/10.3390/pharmaceutics11080407>
66. Ding Y., Wang Z., Ren Z., Zhang X., Wei D., Advances in modified hyaluronic acid-based hydrogels for skin wound healing, *Biomaterials Science*, 10 (13), **2022**, 3393-3409, <https://doi.org/10.1039/d2bm00397j>
67. Mitura S., Sionkowska A., Jaiswal A., Biopolymers for hydrogels in cosmetics: review, *Journal of Materials Science: Materials in Medicine*, 31 (6) **2020**, 580-602, <https://doi.org/10.1007/s10856-020-06390-w>
68. Saravanakumar K., Park S., Santosh S., Ganeshalingam A., Thiripuranathar G., Application of hyaluronic acid in tissue engineering, regenerative medicine, and nanomedicine: A review, *International Journal of Biological Macromolecules*, 222 (4), **2022**, 2744-2760, <https://doi.org/10.1016/j.ijbiomac.2022.10.055>
69. Luo Z., Wang Y., Li J., Wang J., Zhao Y., Tailoring Hyaluronic Acid Hydrogels for Biomedical Applications, *Advanced Functional Materials*, 23 (7), **2023**, 1-28, <https://dx.doi.org/10.1002/adfm.202306554>
70. Kenne L., Gohil S., Nilsson E., Karlsson A., Ericsson D., Modification and cross-linking parameters in hyaluronic acid hydrogels - Definitions and analytical methods, *Carbohydrate Polymers*, 91 (1), **2013**, 410-418, <https://doi.org/10.1016/j.carbpol.2012.08.066>
71. Hinsenkamp A., Ézsiás B., Pál É., Hricisák L., Fülöp Á., Crosslinked Hyaluronic Acid Gels with Blood-Derived Protein Components for Soft Tissue Regeneration, *Tissue Engineering Part A*, 27 (11), **2021**, 806-820, <https://doi.org/10.1089/ten.tea.2020.0197>
72. Andrade del Olmo J., Alonso J., Sáez Martínez V., Ruiz-Rubio L., Pérez González R., Biocompatible hyaluronic acid-divinyl sulfone injectable hydrogels for sustained drug release with enhanced antibacterial properties against *Staphylococcus aureus*, *Materials Science and Engineering C*, 12 (2), **2021**, 732-738, <https://doi.org/10.1016/j.msec.2021.112102>

73. Roether J., Oelschlaeger C., Willenbacher N., Hyaluronic acid cryogels with non-cytotoxic crosslinker genipin, *Materials Letters: X*, 4 (9), **2019**, 100-117, <https://doi.org/10.1016/j.mlblux.2019.100027>
74. Karavasili C., Komnenou A., Katsamenis L., Charalampidou G., Fatouros D., Self-Assembling Peptide Nanofiber Hydrogels for Controlled Ocular Delivery of Timolol Maleate, *ACS Biomaterials Science & Engineering*, 12 (3), **2017**, 3386–3394, <https://doi.org/10.1021/acsbiomaterials.7b00706>
75. Ma B., Wang X., Wu C., Chang J., Crosslinking strategies for preparation of extracellular matrix-derived cardiovascular scaffolds, *Regenerative Biomaterials*, 1 (1), **2014**, 81-89, <https://doi.org/10.1093/rb/rbu009>
76. Morimoto K., Metsugi K., Katsumata H., Iwanaga K., Kakemi M., Effects of Low-Viscosity Sodium Hyaluronate Preparation on the Pulmonary Absorption of rh-Insulin in Rats, *Drug Development and Industrial Pharmacy*, 27 (4), **2001**, 365-371, <https://doi.org/10.1081/DDC-100103737>
77. Zhao X., Sun X., Yildirimer L., Lang Q., Lin Z., Cell infiltrative hydrogel fibrous scaffolds for accelerated wound healing, *Acta Biomaterialia*, 56 (7), **2017**, 66-77, <https://doi.org/10.1016/j.actbio.2016.11.017>
78. Xue Y., Chen H., Xu C., Yu D., Hu Y., Synthesis of hyaluronic acid hydrogels by crosslinking the mixture of high-molecular-weight hyaluronic acid and low-molecular-weight hyaluronic acid with 1,4-butanediol diglycidyl ether, *RSC Advances*, 7 (12), **2020**, 7206-7213, <https://doi.org/10.1039/c9ra09271d>
79. Mondon K., Dadras M., Influence of the Macro- and/or Microstructure of Cross-Linked Hyaluronic Acid Hydrogels on the Release of Two Model Drugs, *Journal of Glycobiology*, 19 (3), **2016**, 1-7, <https://doi.org/10.4172/2168-958x.1000119>
80. Fidalgo J., Deglesne P., Arroyo R., Sepúlveda L., Ranneva E., Detection of a new reaction by-product in BDDE cross-linked autoclaved hyaluronic acid hydrogels by LC–MS analysis, *Medical Devices: Evidence and Research*, 15 (11), **2018**, 367-376, <https://doi.org/10.2147/MDER.S166999>
81. Kalia J., Raines R., Hydrolytic stability of hydrazones and oximes, *Angewandte Chemie*, 47 (39), **2008**, 7523-7526, <https://doi.org/10.1002/anie.200802651>
82. Luo Y., Kirker K., Prestwich G., Cross-linked HA hydrogel film new biomaterials for drug delivery, *Journal of controlled release*, 69 (1), **2000**, 169-184, [https://doi.org/10.1016/s0168-3659\(00\)00300-x](https://doi.org/10.1016/s0168-3659(00)00300-x)
83. Cho E., Sun B., Doh K., Wilson E., Yeo Y., Intraperitoneal delivery of platinum with in-situ crosslinkable hyaluronic acid gel for local therapy of ovarian cancer, *Biomaterials*, 37 (9), **2015**, 312-319, <https://doi.org/10.1016/j.biomaterials.2014.10.039>
84. Friedmann D., Kurian A., Fitzpatrick R., Delayed granulomatous reactions to facial cosmetic injections of polymethylmethacrylate microspheres and liquid injectable silicone: A case series, *Journal of Cosmetic and Laser Therapy*, 18 (3), **2016**, 1-14, <https://doi.org/10.3109/14764172.2015.1114642>
85. Hardy J., Lin P., Schmidt C., Biodegradable hydrogels composed of oxime crosslinked poly (ethylene glycol), hyaluronic acid and collagen: A tunable platform for soft tissue engineering, *Journal of Biomaterials Science*, 26 (3), **2015**, 143-161, <https://doi.org/10.1080/09205063.2014.975393>
86. Yu B., Zhan A., Liu Q., Ye H., Huang X., A designed supramolecular cross-linking hydrogel for the direct, convenient, and efficient administration of hydrophobic drugs, *International*

87. Zhao W., Li Y., Zhang X., Zhang R., Xu F., Photo-responsive supramolecular hyaluronic acid hydrogels for accelerated wound healing, *Journal of Controlled Release*, 323 (10), 2020, 24-35, <https://doi.org/10.1016/j.jconrel.2020.04.014>
88. McTiernan C., Simpson F., Hunter D., Lewis P., Griffith M., LiQD Cornea: Pro-regeneration collagen mimetics as patches and alternatives to corneal transplantation, *Science Advances*, 25 (6), 2020, 1-12, <https://doi.org/10.1126/sciadv.aba2187>
89. Sonker A., Rathore K., Nagarale R., Verma V., Crosslinking of Polyvinyl Alcohol (PVA) and Effect of Crosslinker Shape (Aliphatic and Aromatic) Thereof, *Journal of Polymers and the Environment*, 26 (3), 2018, 1782-1794, <https://doi.org/10.1007/s10924-017-1077-3>
90. Lee J., Kim S., Synthesis and characterization of biopolyurethane crosslinked with castor oil-based hyperbranched polyols as polymeric solid–solid phase change materials, *Scientific Reports*, 12 (4), 2022, 1-14, <https://doi.org/10.1038/s41598-022-17390-x>
91. Gilarska A., Lewandowska-Łańcucka J., Horak W., Nowakowska M., Collagen/chitosan/hyaluronic acid – based injectable hydrogels for tissue engineering applications –design, physicochemical and biological characterization, *Colloids and Surfaces B: Biointerfaces*, 17 (8), 2018, 152-162, <https://doi.org/10.1016/j.colsurfb.2018.06.004>
92. Sallach R., Chaikof E., Electrospun elastin and collagen nanofibers and their application as biomaterials, *Natural-Based Polymers for Biomedical Applications*, 53 (18), 2008, 315-336, <https://doi.org/10.1533/9781845694814.3.315>
93. Richbourg N., Wancura M., Gilchrist A., Toubbeh S., Harley B., Precise control of synthetic hydrogel network structure via linear, independent synthesis-swelling relationships, *Science Advances*, 7 (7), 2021, 2032-2045, <https://doi.org/10.1126/sciadv.abe3245>
94. Bigi A., Cojazzi G., Panzavolta S., Rubini K., Roveri N., Mechanical and thermal properties of gelatin films at different degrees of glutaraldehyde crosslinking, *Biomaterials*, 22 (8), 2001, 763-768, [https://doi.org/10.1016/S0142-9612\(00\)00236-2](https://doi.org/10.1016/S0142-9612(00)00236-2)
95. Ruijgrok J., De Wijn J., Optimizing glutaraldehyde crosslinking of collagen: effects of time, temperature and concentration as measured by shrinkage temperature, *Journal of Materials Science: Materials in Medicine*, 5 (8), 1994, 80-87, <https://doi.org/10.1007/BF00121695>
96. Mirzaei E., Ramazani A., Shafiee S., Danaei M., Studies on Glutaraldehyde Crosslinked Chitosan Hydrogel Properties for Drug Delivery Systems, *International Journal of Polymeric Materials and Polymeric Biomaterials*, 62 (11), 2013, 605-611, <https://doi.org/10.1080/00914037.2013.769165>
97. Teixeira M., Antunes J., Teresa M., Amorim P., Felgueiras H., Green Optimization of Glutaraldehyde Vapor-Based Crosslinking on Poly(Vinyl Alcohol)/Cellulose Acetate Electrospun Mats for Applications as Chronic Wound Dressings, *Proceedings of the National Academy of Sciences*, 69 (30), 2021, 1-6, <https://doi.org/10.3390/CGPM2020-07193>
98. Neves M., Araújo M., Barrias C., Granja P., Sousa A., Multiplatform Protein Detection and Quantification Using Glutaraldehyde-Induced Fluorescence for 3D Systems, *Journal of Fluorescence*, 29 (11), 2019, 1171-1181, <https://doi.org/10.1007/s10895-019-02433-w>
99. Calles J., Ressia J., Llabot J., Vallés E., Palma S., Hyaluronan–Itaconic Acid–Glutaraldehyde Films for Biomedical Applications: Preliminary Studies, *Scientia Pharmaceutica*, 84 (1), 2016, 61-72, <https://dx.doi.org/10.3797/scipharm.1504-17>

100. Thi T., Pilkington E., Nguyen D., Lee J., Truong N., The Importance of Poly(ethylene glycol) Alternatives for Overcoming PEG Immunogenicity in Drug Delivery and Bioconjugation, *Polymers*, 12 (2), **2020**, 1-21, <https://dx.doi.org/10.3390/polym12020298>
101. Fu S., Dong H., Deng X., Zhuo R., Zhong Z., Injectable hyaluronic acid/poly (ethylene glycol) hydrogels crosslinked via strain-promoted azide-alkyne cycloaddition click reaction, *Carbohydrate Polymers*, 169 (1), **2017**, 332-340, <https://doi.org/10.1016/j.carbpol.2017.04.028>
102. Monticelli D., Martina V., Mocchi R., Rauso R., Zerbinati U., Chemical Characterization of Hydrogels Crosslinked with Polyethylene Glycol for Soft Tissue Augmentation, *Macedonian Journal of Medical Sciences*, 7 (7), **2019**, 1077-1081, <https://doi.org/10.3889/oamjms.2019.279>
103. Tine Jansen, *PREPARATION OF SOFT MACROPOROUS HYALURONAN GELS*, First Master of Pharmaceutical Care, CHALMERS UNIVERSITY OF TECHNOLOGY, **2012**, [https://libstore.ugent.be/fulltxt/RUG01/002/063/827/RUG01-002063827\\_2013\\_0001\\_AC.pdf](https://libstore.ugent.be/fulltxt/RUG01/002/063/827/RUG01-002063827_2013_0001_AC.pdf)
104. Yu F., Cao X., Li Y., Zeng L., Zhu J., Wang G., Diels–Alder crosslinked HA/PEG hydrogels with high elasticity and fatigue resistance for cell encapsulation and articular cartilage tissue repair, *Polymer Chemistry*, 14 (17), **2014**, 689-705, <https://doi.org/10.1039/C4PY00473F>
105. Hussain Z., PEGylation: a promising strategy to overcome challenges to cancer-targeted nanomedicines: a review of challenges to clinical transition and promising resolution, *Drug Delivery and Translational Research*, 9 (3), **2019**, 721-734, <https://doi.org/10.1007/s13346-019-00631-4>
106. Zhang J., Yong H., Sigen A., Xu Q., Wang W., Structural design of robust and biocompatible photonic hydrogels from an in situ crosslinked hyperbranched polymer system, *Chemistry of Materials*, 30 (17), **2018**, 6091-6098, <https://doi.org/10.1021/acs.chemmater.8b02542>
107. King Tiger, Genipin 98%, <https://www.king-tiger.com/Genipin98-1.html> (accessed March 17, 2024)
108. Mi F., Sung H., Shyu S., Drug release from chitosan and alginate complex beads reinforced by a naturally occurring cross-linking agent, *Carbohydrate Polymers*, 48 (1), **2002**, 61-72, [https://doi.org/10.1016/S0144-8617\(01\)00212-0](https://doi.org/10.1016/S0144-8617(01)00212-0)
109. Deb S., Abueva C., Kim B., Taek B., Chitosan – hyaluronic acid polyelectrolyte complex scaffold crosslinked with genipin for immobilization and controlled release of BMP-2, *Carbohydrate Polymers*, 115 (9), **2015**, 160-169, <https://doi.org/10.1016/j.carbpol.2014.08.077>
110. MacAya D., Ng K., Spector M., Injectable collagen-genipin gel for the treatment of spinal cord injury: In vitro studies, *Advanced Functional Materials*, 89 (18), **2011**, 4788-4797, <https://doi.org/10.1002/adfm.201101720>
111. Miyagusuku-Cruzado G., Voss D., Carpio-Jiménez C., Lao F., Giusti M., The Amazing Colors of Peruvian Biodiversity: Select Peruvian Plants for Use as Food Colorants, *Anales Científicos*, 83 (1), **2022**, 1-17, <https://dx.doi.org/10.21704/ac.v83i1.1888>
112. Pérez L., Hyaluronic Acid Hydrogels Crosslinked in Physiological Conditions: Synthesis and Biomedical Applications, *Biomedicines*, 9 (9), **2021**, 1113-1133, <https://doi.org/10.3390/biomedicines9091113>
113. Kazezian Z., Joyce K., Pandit A., The role of hyaluronic acid in intervertebral disc regeneration, *Applied Sciences*, 10 (18), **2020**, 1-25, <https://doi.org/10.3390/APP10186257>

114. Mahboubian A., Villasaliu D., Dorkoosh F., Stolnik S., Temperature-Responsive Methylcellulose-Hyaluronic Hydrogel as a 3D Cell Culture Matrix, *Biomacromolecules*, 21 (12), **2020**, 4737-4746, <https://doi.org/10.1021/acs.biomac.0c00906>
115. Kim M., Nguyen D., Kim D., Recent studies on modulating hyaluronic acid-based hydrogels for controlled drug delivery, *Journal of Pharmaceutical Investigation*, 52 (9), **2022**, 397-413, <https://doi.org/10.1007/s40005-022-00568-w>
116. Khayambashi P., Iyer J., Pillai S., Upadhyay A., Zhang Y., Hydrogel Encapsulation of Mesenchymal Stem Cells and Their Derived Exosomes for Tissue Engineering, *International Journal of Molecular Sciences*, 22 (2), **2021**, 1-15, <https://doi.org/10.3390/ijms22020684>
117. Li H., Qi Z., Zheng S., Chang Y., Pan S., The Application of Hyaluronic Acid-Based Hydrogels in Bone and Cartilage Tissue Engineering, *Advances in Materials Science and Engineering*, 20 (2), **2019**, 1-13, <https://doi.org/10.1155/2019/3027303>
118. Wu A., Aoki T., Sakoda M., Ohta S., Ichimura S., Enhancing Osteogenic Differentiation of MC3T3-E1 Cells by Immobilizing Inorganic Polyphosphate onto Hyaluronic Acid Hydrogel, *Biomacromolecules*, 16 (1), **2015**, 166-173, <https://dx.doi.org/10.1021/bm501356c>
119. Kim I., Mauck R., Burdick J., Hydrogel design for cartilage tissue engineering: A case study with hyaluronic acid, *Biomaterials*, 32 (34), **2011**, 8771-8782, <https://dx.doi.org/10.1016/j.biomaterials.2011.08.073>
120. Wang X., He J., Wang Y., Cui F., Hyaluronic acid-based scaffold for central neural tissue engineering, *Interface Focus*, 2 (3), **2012**, 278-291, <https://doi.org/10.1098/rsfs.2012.0016>
121. Xiao W., Ehsanipour A., Sohrabi A., Seidlits S., Hyaluronic-acid based hydrogels for 3-dimensional culture of patient-derived glioblastoma cells, *Journal of Visualized Experiments*, 138 (24), **2018**, 1-9, <https://doi.org/10.3791/58176>
122. Shan B., Wu F., Hydrogel-Based Growth Factor Delivery Platforms: Strategies and Recent Advances, *Advanced Materials*, 36 (5), **2024**, 1-40, <https://doi.org/10.1002/adma.202210707>
123. Xu H., Yu Y., Zhang L., Zheng F., Xu P., Sustainable release of nerve growth factor for peripheral nerve regeneration using nerve conduits laden with Bioconjugated hyaluronic acid-chitosan hydrogel, *Composites Part B: Engineering*, 230 (1), **2022**, 5090-6008, <https://doi.org/10.1016/j.compositesb.2021.109509>
124. Huang G., Huang H., Application of hyaluronic acid as carriers in drug delivery, *Drug Delivery*, 25 (1), **2018**, 766-772, <https://doi.org/10.1080/10717544.2018.1450910>
125. Wang S., Kim H., Kwak G., Yoon H., Jo S., Development of Biocompatible HA Hydrogels Embedded with a New Synthetic Peptide Promoting Cellular Migration for Advanced Wound Care Management, *Advanced Science*, 5 (11), **2018**, 1-12, <https://doi.org/10.1002/advs.201800852>
126. Pedrosa S., Gonçalves C., David L., Gama M., A Novel Crosslinked Hyaluronic Acid Nanogel for Drug Delivery, *Macromolecular Bioscience*, 14 (11), **2014**, 1556-1568, <https://doi.org/10.1002/mabi.201400135>
127. Ashworth J., Morgan R., Lis-Slimak K., Meade K., Merry C., Preparation of a user-defined peptide gel for controlled 3d culture models of cancer and disease, *Journal of Visualized Experiments*, 166 (3), **2020**, 1-19, <https://doi.org/10.3791/61710>
128. Hsu S., Huang T., Cheng Y., Young T., Clinical-grade manufacturing of therapeutic proteins for the cell therapy industry, *Biotechnology journal*, 7 (1), **2013**, 908-921, <https://doi.org/10.1038/s41392-022-00904-4>

129. Poh Z., Goh J., Stylios G., Advances in hyaluronic acid-based scaffold for tissue engineering applications, *Journal of Materials Chemistry B*, 22 (10), **2019**, 5679-5700, <https://doi.org/10.3389/fbioe.2022.910290>
130. Poh Z., Liew J., Yusoff N., Nordin N., Ahmad I., In situ-forming hydrogels for ophthalmic drug delivery: A review, *Journal of Controlled Release*, 11 (6), **2019**, 11-26, <https://doi.org/10.1016/j.jconrel.2007.07.009>
131. Kharkar P., Kloxin A., Injectable Hydrogels for Cell Delivery and Tissue Regeneration, *Materials Science and Engineering*, **2018**, <https://www.sigmaaldrich.com/PT/en/technical-documents/technical-article/materials-science-and-engineering/tissue-engineering/injectable-hydrogels> (accessed May 29, 2024)
132. Anguiano M., Castilla C., Maška M., Ederra C., Peláez R., Characterization of three-dimensional cancer cell migration in mixed collagen-Matrigel scaffolds using microfluidics and image analysis, *PLOS ONE*, 12 (2), **2017**, 905-912, <https://doi.org/10.1371/journal.pone.0171417>
133. Solbu A., Koernig A., Kjesbu J., Zaytseva-Zotova D., Sletmoen M., High resolution imaging of soft alginate hydrogels by atomic force microscopy, *Carbohydrate Polymers*, 276 (15), **2022**, 850-864, <https://doi.org/10.1016/j.carbpol.2021.118804>
134. Raghuwanshi V., Garnier G., Characterisation of hydrogels: Linking the nano to the microscale, *Advances in Colloid and Interface Science*, 274 (12) **2019**, 6875-6890, <https://doi.org/10.1016/j.cis.2019.102044>
135. Garcia H., Barros A., Gonçalves C., Gama F., Gil A., Characterization of dextrin hydrogels by FTIR spectroscopy and solid-state NMR spectroscopy, *European Polymer Journal*, 44 (7), **2008**, 2318-2329, <https://doi.org/10.1016/j.eurpolymj.2008.05.013>
136. Fernandes R., de Moura M., Glenn G., Aouada F., Thermal, microstructural, and spectroscopic analysis of Ca<sup>2+</sup> alginate/clay nanocomposite hydrogel beads, *Journal of Molecular Liquids*, 265 (1), **2018**, 327-336, <https://doi.org/10.1016/j.molliq.2018.06.005>
137. Bian L., Hou C., Tous E., Rai R., Burdick J., The influence of hyaluronic acid hydrogel crosslinking density and macromolecular diffusivity on human MSC chondrogenesis and hypertrophy, *Biomaterials*, 34 (2), **2013**, 413-421, <https://dx.doi.org/10.1016/j.biomaterials.2012.09.052>
138. Pouyani T., Harbison G., Prestwich G., Novel Hydrogels of Hyaluronic Acid: Synthesis, Surface Morphology, and Solid-state NMR, *Journal of the American Chemical Society*, 116 (17), **1994**, 7515-7522, <https://doi.org/10.1021/ja00096a007>
139. Grdadolnik J., ATR-FTIR Spectroscopy: Its Advantages and Limitations, *Acta Chimica Slovenica*, **2002**, 49 (3), 631-642 (accessed June 11, 2024)
140. Passos L., Saraiva M., Detection in UV-visible spectrophotometry: Detectors, detection systems, and detection strategies, *Measurement*, 135 (15), **2019**, 896-904, <https://doi.org/10.1016/j.measurement.2018.12.045>
141. Luong P., Browning M., Bixter R., Cosgriff-Hernandez E., Drying and storage effects on poly (ethylene glycol) hydrogel mechanical properties and bioactivity, *Journal of Biomedical Materials Research - Part A*, 102 (9), **2014**, 3066-3076, <https://doi.org/10.1002/jbm.a.34977>
142. Leyva-Jiménez F., Oliver-Simancas R., Castangia I., Rodríguez-García A., Alañón M., Comprehensive review of natural based hydrogels as an upcoming trend for food packing, *Food Hydrocolloids*, 135 (18), **2023**, 278-293, <https://doi.org/10.1016/j.foodhyd.2022.108124>

143. Shoichet M., Li R., White M., Winn S., Stability of hydrogels used in cell encapsulation: An in vitro comparison of alginate and agarose, *Biotechnology and Bioengineering*, 50 (4), **1996**, 374-381, [https://doi.org/10.1002/\(sici\)1097-0290\(19960520\)50:4%3C374::aid-bit4%3E3.0.co;2-i](https://doi.org/10.1002/(sici)1097-0290(19960520)50:4%3C374::aid-bit4%3E3.0.co;2-i)
144. Jung H., Hyaluronidase: An overview of its properties, applications, and side effects, *Archives of Plastic Surgery*, 47 (9), **2020**, 297-300, <https://doi.org/10.5999/aps.2020.00752>
145. Patterson J., Siew R., Herring S., Lin A., Guldberg R., Hyaluronic acid hydrogels with controlled degradation properties for oriented bone regeneration, *Biomaterials*, 31 (26), **2010**, 6772-6781, <https://doi.org/10.1016/j.biomaterials.2010.05.047>
146. Huang X., Liu Q., Wu C., Lin Z., Huang A., Controllable release ratiometric fluorescent sensor for hyaluronidase via the combination of Cu<sup>2+</sup>-Fe-N-C nanozymes and degradable intelligent hydrogel, *Talanta*, 237 (15), **2022**, 340-354, <https://doi.org/10.1016/j.talanta.2021.122961>
147. Al-Sibani M., Al-Harrasi A., Neubert R., Effect of hyaluronic acid initial concentration on cross-linking efficiency of hyaluronic acid - Based hydrogels used in biomedical and cosmetic applications, *Pharmazie*, 72 (2), **2017**, 81-86, <https://doi.org/10.1691/ph.2017.6133>
148. Xu K., Lee F., Gao S., Tan M., Kurisawa M., Hyaluronidase-incorporated hyaluronic acid – tyramine hydrogels for the sustained release of trastuzumab, *Journal of Controlled Release*, 216 (28), **2015**, 47-55, <https://doi.org/10.1016/j.jconrel.2015.08.015>
149. Zemlyakova E., Samokhin A., Korel A., Kuznetsov V., Pestov A., Preparation and cytotoxicity evaluation of hydrogels based on poly (trimethylene carbonate) and carboxyalkyl chitosans for regenerative medicine applications, *Materials Today: Proceedings*, 25 (3), **2019**, 470-473, <https://doi.org/10.1016/j.matpr.2019.12.182>
150. Shazeeb M., Corazzini R., Konowicz P., Fogle R., Bangari D., Assessment of in vivo degradation profiles of hyaluronic acid hydrogels using temporal evolution of chemical exchange saturation transfer (CEST) MRI, *Biomaterials*, 78 (26), **2018**, 326-338, <https://doi.org/10.1016/j.biomaterials.2018.05.037>
151. Kim J., Lee D., Kim T., Song Y., Cho N., Biocompatibility of hyaluronic acid hydrogels prepared by porous hyaluronic acid microbeads, *Metals and Materials International*, 20 (5), **2014**, 555-563, <https://doi.org/10.1007/s12540-014-3022-5>
152. Wang H., Tibbitt M., Langer S., Leinwand L., Anseth K., Hydrogels preserve native phenotypes of valvular fibroblasts through an elasticity-regulated PI3K/AKT pathway, *Proceedings of the National Academy of Sciences of the United States of America*, 110 (48), **2013**, 19336-19341, <https://doi.org/10.1073/pnas.1306369110>
153. Hazur J., Endrizzi N., Schubert D., Boccaccini A., Fabry B., Stress relaxation amplitude of hydrogels determines migration, proliferation, and morphology of cells in 3-D culture, *Biomaterials Science*, 10 (1), **2022**, 270-280, <https://doi.org/10.1039/d1bm01089a>
154. Lei Y., Gojgini S., Lam J., Segura T., The spreading, migration and proliferation of mouse mesenchymal stem cells cultured inside hyaluronic acid hydrogels, *Biomaterials*, 32 (1), **2011**, 39-47, <https://dx.doi.org/10.1016/j.biomaterials.2010.08.103>
155. Pereira I., Fraga S., Silva S., Teixeira J., Gama M., In vitro genotoxicity assessment of an oxidized dextrin-based hydrogel for biomedical applications, *Journal of Applied Toxicology*, 28 (7), **2019**, 639-649, <https://doi.org/10.1002/jat.3754>
156. Vigata M., Meinert C., Hutmacher D., Bock N., Hydrogels as drug delivery systems: A review of current characterization and evaluation techniques, *Pharmaceutics*, 7 (12), **2020**, 1-45, <https://doi.org/10.3390/pharmaceutics12121188>

157. Gong C., Wu Q., Dong P., Shi S., Fu S., Acute Toxicity Evaluation of Biodegradable In Situ Gel-Forming Controlled Drug Delivery System Based on Thermosensitive PEG-PCL-PEG Hydrogel, *Journal of Biomedical Materials Research - Part B*, 91 (1), **2009**, 26-36, <https://doi.org/10.1002/jbm.b.31370>
158. Unnikrishnan V., Venugopal A., Sivadasan S., Fernandez F., Arumugam S., Cellular and sub-chronic toxicity of hydroxyapatite porous beads loaded with antibiotic in rabbits, indented for chronic osteomyelitis, *International Journal of Pharmaceutics*, 616 (12), **2022**, 1-11, <https://doi.org/10.1016/j.ijpharm.2022.121535>
159. Mukhopadhyay P., Bhattacharya S., Nandy A., Bhattacharyya A., Mishra R., Assessment of in vivo chronic toxicity of chitosan and its derivatives used as oral insulin carriers, *Toxicology Research*, 16 (12), **2015**, 281-290, <https://doi.org/10.1039/c4tx00102h>
160. Chen X., Butt A., Amin M., Molecular Evaluation of Oral Immunogenicity of Hepatitis B Antigen Delivered by Hydrogel Microparticles, *Molecular Pharmaceutics*, 16 (9), **2019**, 3853-3872, <https://dx.doi.org/10.1021/acs.molpharmaceut.9b00483>
161. Yibin Y., Shuo X., Sanming L., Hao P., Genipin-cross-linked hydrogels based on biomaterials for drug delivery: a review, *Biomaterials Science*, 9 (5), **2021**, 1583-1597, <https://doi.org/10.1039/d0bm01403f>
162. Gilarska A., Lewandowska-Łańcucka J., Guzdek-Zajac K., Nowakowska M., Bioactive yet antimicrobial structurally stable collagen/chitosan/lysine functionalized hyaluronic acid – based injectable hydrogels for potential bone tissue engineering applications, *International Journal of Biological Macromolecules*, 38 (9), **2020**, 938-950, <https://doi.org/10.1016/j.ijbiomac.2019.11.052>
163. Liu S., Cong H., Yu B., Shen Y., Screening of a short chain antimicrobial peptide-LKLHI and its application in hydrogels for wound healing, *International Journal of Biological Macromolecules*, 31 (23), **2023**, 1-15, <https://doi.org/10.1016/j.ijbiomac.2023.124056>
164. Pulat M., Oytun Akalin G., Preparation and characterization of gelatin hydrogel support for immobilization of *Candida Rugosa* lipase, *Artificial Cells, Nanomedicine, and Biotechnology*, 41 (3), **2013**, 145-151, <https://doi.org/10.3109/10731199.2012.696070>
165. Segura T., Anderson B., Chung P., Webber R., Shull K., Shea L., Crosslinked hyaluronic acid hydrogels: a strategy to functionalize and pattern, *Biomaterials*, **2005**, 26 (4), 359-371, <https://doi.org/10.1016/j.biomaterials.2004.02.067>
166. Haidari H., Kopecki Z., Sutton A., Garg S., Cowin A., Vasilev K., pH-Responsive “Smart” Hydrogel for Controlled Delivery of Silver Nanoparticles to Infected Wounds, *Antibiotics*, 10 (1), **2021**, 1-15, <https://doi.org/10.3390/antibiotics10010049>
167. Alavarse A., Frachini E., Silva R., Lima V., Shavandi A., Petri D., Crosslinkers for polysaccharides and proteins: Synthesis conditions, mechanisms, and crosslinking efficiency, a review, *International Journal of Biological Macromolecules*, 31 (2), **2022**, 558-596, <https://doi.org/10.1016/j.ijbiomac.2022.01.029>
168. Lee H., Hwang C., Kim H., Jeong S., Enhancement of bio-stability and mechanical properties of hyaluronic acid hydrogels by tannic acid treatment, *Carbohydrate Polymers*, 18 (6), **2018**, 290-298, <https://doi.org/10.1016/j.carbpol.2018.01.056>
169. Sahiner N., Soft and flexible hydrogel templates of different sizes and various functionalities for metal nanoparticle preparation and their use in catalysis, *Progress in Polymer Science*, 38 (9), **2013**, 1329-1356, <https://doi.org/10.1016/j.progpolymsci.2013.06.004>
170. Wang S., Hsieh P., Chen P., Chen Y., Jan J., Genipin-cross-linked poly(L-lysine)-based hydrogels: Synthesis, characterization, and drug encapsulation, *Colloids and Surfaces B: Biointerfaces*, 12 (8), **2013**, 423-431, <https://doi.org/10.1016/j.colsurfb.2013.06.028>

171. Slusarewicz P., Zhu K., Hedman T., Kinetic Analysis of Genipin Degradation in Aqueous Solution, *Natural Product Communications*, 5 (12), **2010**, 1853-1858, <https://dx.doi.org/10.1177/1934578X1000501202>
172. Øvrebø Ø., Giorgi Z., De Lauretis A., Vanoli V., Rossi F., Characterisation and biocompatibility of crosslinked hyaluronic acid with BDDE and PEGDE for clinical applications, *Reactive and Functional Polymers*, 200 (4), **2024**, 1-9, <https://doi.org/10.1016/j.reactfunctpolym.2024.105920>
173. Kahoush M., Cayla A., Behary N., Mutel B., Genipin-Mediated Immobilization of Glucose Oxidase Enzyme on Carbon Felt for Use as Heterogeneous Catalyst in Sustainable Wastewater Treatment, *Journal of Environmental Chemical Engineering*, 9 (4), **2021**, 1-12, <https://doi.org/10.1016/j.jece.2021.105633>
174. Strom A., Larsson A., Okay O., Preparation and physical properties of hyaluronic acid-based cryogels, *Journal of Applied Polymer Science*, 11 (2), **2015**, 1-11, <https://dx.doi.org/10.1002/app.42194>
175. Horkay F., Magda J., Alcoutlabi M., Atzet S., Zarembinski T., Structural, mechanical and osmotic properties of injectable hyaluronan-based composite hydrogels, *Polymer*, 51 (19), **2010**, 4424-4430, <https://dx.doi.org/10.1016/j.polymer.2010.06.027>
176. Shah C., Barnett S., Swelling Behavior of Hyaluronic Acid Gels, *Journal of Applied Polymer Science*, 15 (43), **1992**, 293-298, <https://doi.org/10.1002/app.1992.070450211>
177. Yabuuchi K., Katsumata T., Shimoboji T., Hashimoto Y., Kishida A., Variable swelling behavior of and drug encapsulation in a maleimide-modified hyaluronic acid nanogel-based hydrogel, *Polymer Journal*, 56 (5), **2024**, 505-515, <https://doi.org/10.1038/s41428-023-00881-7>
178. Tan H., Li H., Rubin J., Marra K., Controlled gelation and degradation rates of injectable hyaluronic acid-based hydrogels through a double crosslinking strategy, *Journal of Tissue Engineering and Regenerative Medicine*, 5 (10), **2011**, 790-797, <https://doi.org/10.1002/term.378>
179. Aswathy S., Narendrakumar U., Manjubala I., Commercial hydrogels for biomedical applications, *Heliyon*, 6 (4), **2020**, 1-13, <https://doi.org/10.1016/j.heliyon.2020.e03719>
180. Burdick J., Chung C., Jia X., Randolph M., Langer R., Controlled Degradation and Mechanical Behavior of Photopolymerized Hyaluronic Acid Networks, *Biomacromolecules*, 6 (1), **2005**, 1-15, <https://doi.org/10.1021/bm049508a>
181. Bulpitt P., Aeschlimann D., New strategy for chemical modification of hyaluronic acid: Preparation of functionalized derivatives and their use in the formation of novel biocompatible hydrogels, *Biomedical Materials Research*, 47 (2), **1999**, 152-169, [https://doi.org/10.1002/\(sici\)1097-4636\(199911\)47:2%3C152::aid-jbm5%3E3.0.co;2-i](https://doi.org/10.1002/(sici)1097-4636(199911)47:2%3C152::aid-jbm5%3E3.0.co;2-i)
182. Lee S., Park Y., Hwang S., Effect of bFGF and fibroblasts combined with hyaluronic acid-based hydrogels on soft tissue augmentation: an experimental study in rats, *Maxillofacial Plastic and Reconstructive Surgery*, 41 (1), **2019**, 41-47, <https://doi.org/10.1186/s40902-019-0234-0>
183. Song L., Qiu H., Chen Z., Wang J., Zhang X., Injectable hyaluronate/collagen hydrogel with enhanced safety and efficacy for facial rejuvenation, *Collagen and Leather*, 21 (1), **2024**, 6-21, <https://doi.org/10.1186/s42825-024-00165-7>
184. Kočí Z., Sridharan R., Hibbitts A., Kneafsey S., Kearney C., O'Brien F., The Use of Genipin as an Effective, Biocompatible, Anti-Inflammatory Cross-Linking Method for Nerve Guidance Conduits, *Advance Biosystems*, 4 (3), **2020**, 1-11, <https://doi.org/10.1002/adbi.201900212>

185. Wang C., Lau T., Loh W., Su K., Wang D., Cytocompatibility study of a natural biomaterial crosslinker—Genipin with therapeutic model cells, *Journal of Biomedical Materials Research Part B*, 97 (1), **2011**, 58-65, <https://dx.doi.org/10.1002/jbm.b.31786>
186. Vo N., Huang L., Lemos H., Mellor A., Novakovic K., Genipin-crosslinked chitosan hydrogels: Preliminary evaluation of the in vitro biocompatibility and biodegradation, *Journal of Applied Polymer Science*, 138 (34), **2021**, 1-11, <https://doi.org/10.1002/app.50848>
187. Pan N., Pereira H., Silva M., Vasconcelos A., Celligoi M., Improvement Production of Hyaluronic Acid by *Streptococcus zooepidemicus* in Sugarcane Molasses, *Applied Biochemistry and Biotechnology*, 182 (1), **2017**, 276-293, <https://doi.org/10.1007/s12010-016-2326-y>

## 6. ANNEXES

Table A1 - FTIR peak table of Genipin, HA, PEGDE, and EGDE standards.

Standards	Peaks (cm <sup>-1</sup> )	Assignment	References
Genipin	1680	C=O (carbonyl) stretching vibration	173
	1622	C=C stretching vibration	
	2800-3000	C-H stretching vibration	
	3000-3600	Aromatic C-H and O-H stretching vibration	
HA	3400-3449	O-H and N-H stretching vibration	187
	2822-2922	C-H stretching vibration	
	1622	C=O (carbonyl) stretching vibration	
	1418	C-O stretching vibration	
	1155	C-O-C stretching vibration	
PEGDE and EGDE	1050-1150	C-O-C stretching vibration	172

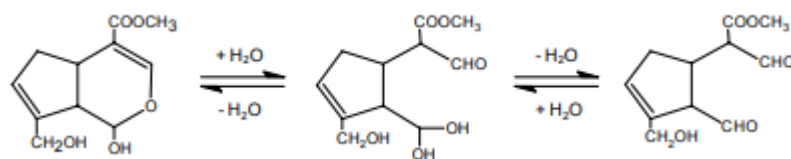


Figure A1 - The proposed reversible ring-opening reactions of genipin in aqueous solution. (Reaction that makes Genipin-HA-PEGDE turns brown)<sup>171</sup>.

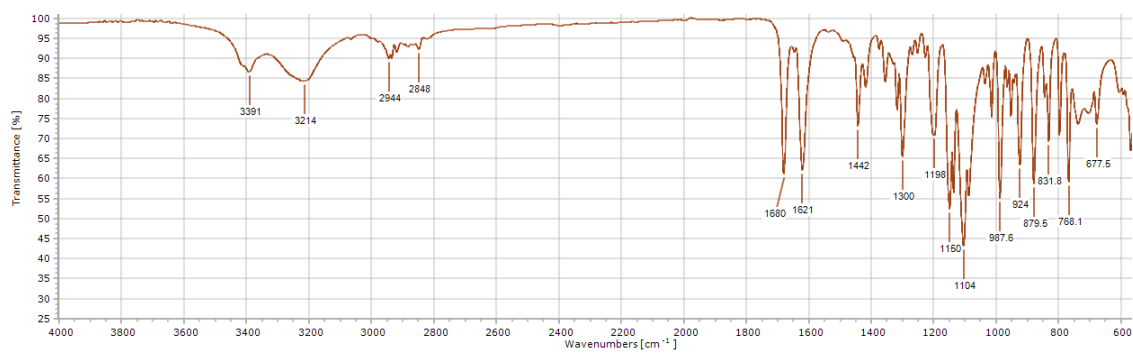


Figure A2 – ATR-FTIR spectrum of Gen powder.

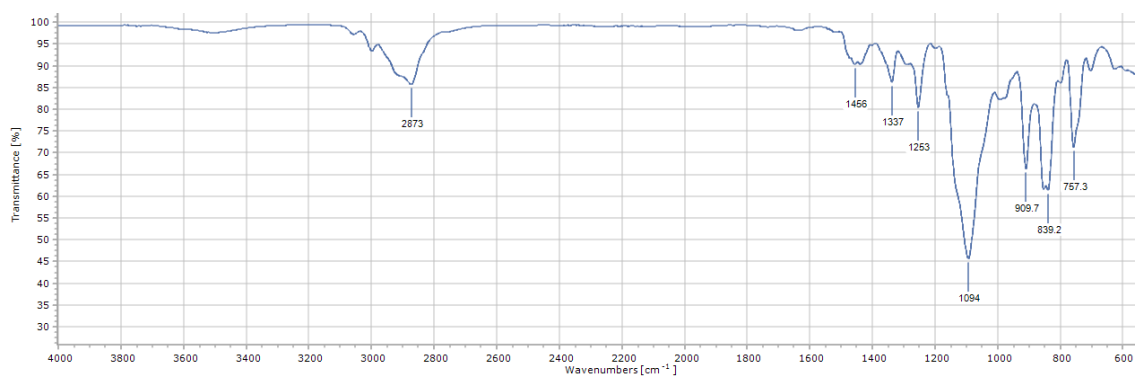


Figure A3 – ATR-FTIR spectrum of EGDE standard.

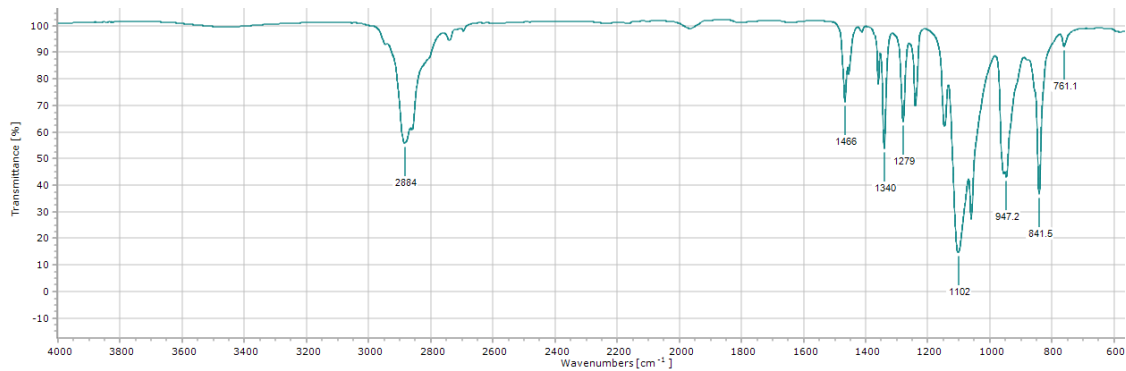


Figure A4 – ATR-FTIR spectrum of PEGDE powder.

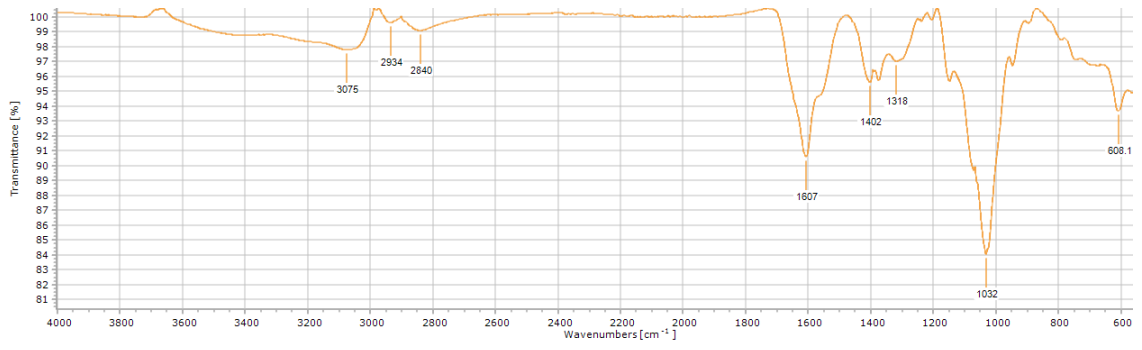


Figure A5 - ATR-FTIR spectrum of native HA (0.6-1.0 million Da).

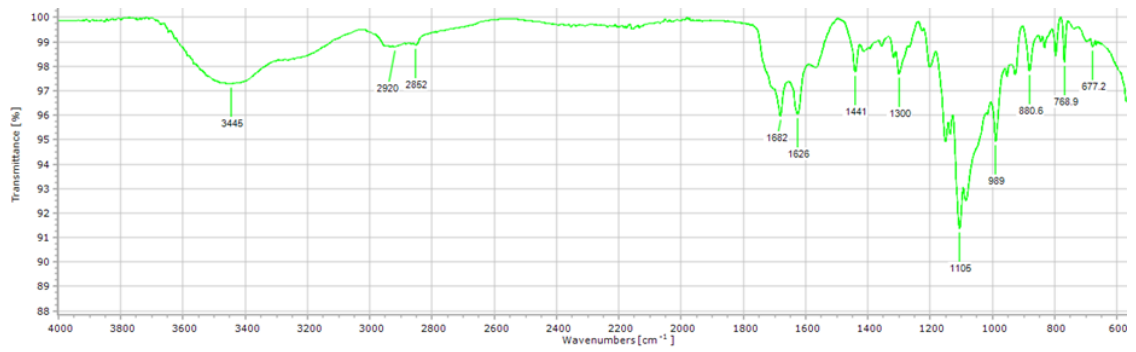


Figure A6 - ATR-FTIR spectrum of acidic Gen solution (pH = 6).

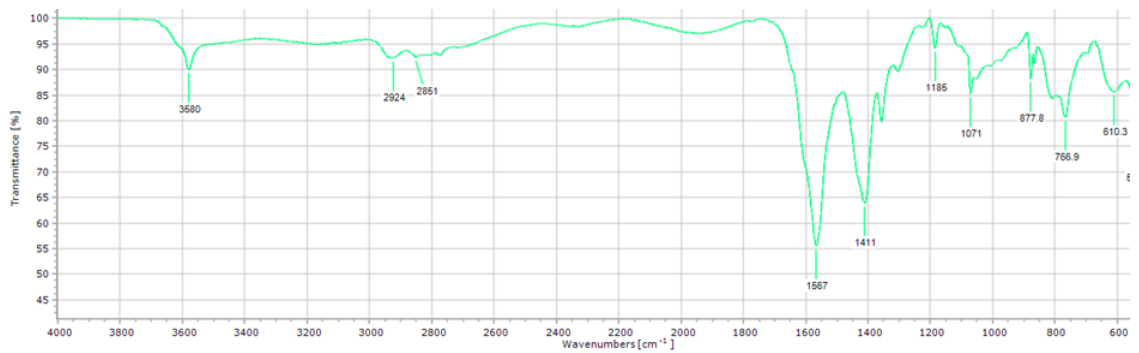


Figure A7 - ATR-FTIR spectrum of alkaline Gen solution (pH = 12).

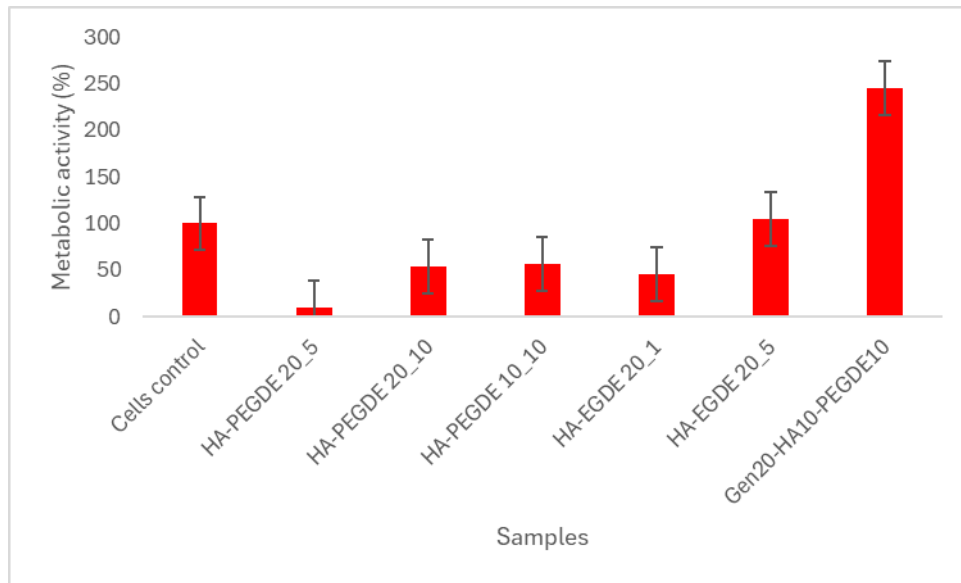


Figure A8 - Metabolic activity of embryo mouse fibroblasts (NIH 3T3) in direct contact with HA-PEGDE, HA-EGDE, and Gen-HA-PEGDE hydrogels as measured by the resazurin reduction assay.



Cofinanciado por:

